University of Messina

Department of Chemical, Biological, Pharmaceutical and Environmental Sciences, University of Messina

PhD in Chemical Sciences – XXIX Cycle
(SSD CHIM/08)

DESIGN, SYNTHESIS AND PRELIMINARY BIOLOGICAL EVALUATION OF GLUTAMATE IONOTROPIC RECEPTOR LIGANDS

Dr. Milad Espahbodinia

Supervisor:
Prof. Maria Zappalà

Coordinator:
Prof. Sebastiano Campagna

2014-2016

Table of contents

Chapter 4. Experimental section

Chapter 1. Aim of the research project

1.1 Development of novel 2,3-benzodiazepines as noncompetitive AMPAR antagonists

AMPA receptors, like NMDA and kainate receptors, belong to the glutamate ion channel receptor family (Dingledine et al., 1999; Traynelis et al., 2010; Palmer et al., 2005). As ligand-gated ion channels, AMPA receptors are composed of domains that span the membrane to form a pore or channel, and the channel is gated by glutamate. Upon glutamate binding, the receptor rapidly opens its channel pore to allow flow of small cations such as Na^+ and K^+, which causes an increase in the postsynaptic membrane potential. AMPA receptors mediate the majority of fast excitatory neurotransmission in the CNS, and play crucial roles during neuronal development and synaptic plasticity (Dingledine et al., 1999; Traynelis et al., 2010; Palmer et al., 2005). Each of the AMPA receptor subunits, GluA1-4 (Collingridge et al., 2009), can form homomeric channels by itself or assemble into heteromeric channels (Sobolevsky et al., 2009).

AMPA receptors are subject to RNA alternative splicing (Sommer et al., 1990) and editing (Sommer et al., 1991). RNA splicing and editing are developmentally regulated, and generate additional, functionally different receptors (Dingledine et al., 1999; Palmer et al., 2005; Sommer et al., 1991). All AMPA receptor subunits exist as two splice variants, flip and flop. The alternative splice cassette is found at the C-terminal end of the loop between TMIII and TMIV. Although the change in the receptor subunits is small (only a few amino acids are changed), the effect can be quite dramatic, resulting in altered desensitisation kinetics.

The calcium permeability of the GluA2 subunit is determined by the post-transcriptional editing of the GluA2 mRNA, which changes a single amino-acid in the

TMII region from glutamine (Q) to arginine (R). This is the so called Q/R editing site - GluA2Q is calcium permeable whilst GluA2R is not - positioned at the narrow constriction of the channel in the re-entry loop, exists exclusively in the GluA2 subunit (Figure 1) (Seeburg et al., 1996). Homomeric GluA2Q can form functional channels, which are Ca^{2+} permeable, whereas GluA2R, the edited R isoform (arginine), cannot form channels alone (Hume et al., 1991; Schiffer et al., 1997). In contrast, a glutamine Q remains at this equivalent position for GluA1, 3 and 4 (Sommer et al., 1991; Seeburg et al., 2003).

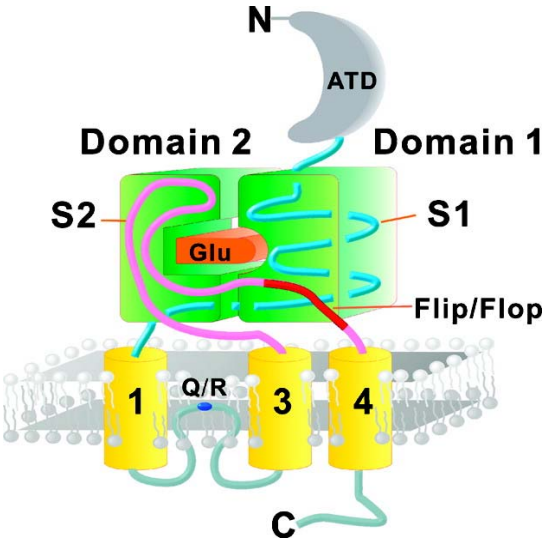

Figure 1. Schematic drawing of the topology of an AMPA receptor subunit showing the sequence location of the alternatively spliced flip/flop region (from Pei et al, 2009).

AMPA receptors are tetramers (Sobolevsky et al., 2009; Safferling et al., 2001; Armstrong et al., 2000; Mayer, 2005). AMPA receptors assembled from different subunits exhibit distinct gating, permeation, and rectification properties as well as Ca^{2+} permeability. GluA2 is a key subunit in controlling AMPA receptor assembly and function (Sans et al., 2003). This is because at the molecular level, GluA2R-containing channels are Ca^{2+}-impermeable, whereas those lacking GluA2R are permeable to Ca^{2+} (and Zn^{2+}) and exhibit distinctly fast kinetics (Geiger et al., 1995). The GluA2R-containing AMPA

receptors are found in most of the principal neurons in the neocortex, hippocampus, amygdala and cerebellum (Lambolez 1996; Sans et al., 2003).

Excessive AMPA receptor activity has been implicated in various neurological diseases, such as amyotrophic lateral sclerosis (ALS), ischemia and epilepsy (Dingledine et al., 1999; Liu et al., 2007), by a pathogenic mechanism known as excitotoxicity. Several studies demonstrate that excessive activity of Ca^{2+}-permeable AMPA receptors is involved in a wide range of neurological diseases. Thus, blocking excessive AMPA receptor activity would be a promising therapeutic approach for the treatment of these diseases. AMPA receptor antagonists show a broad range of neuroprotection and are better tolerated with lesser side effects as compared with NMDA receptor antagonists.

Various AMPA receptor antagonists have been synthesized; for example, NBQX (6-nitro-7-sulfamoylbenzo[*f*]quinoxaline-2,3-dione) is a potent, competitive antagonist of AMPA channels, but it also blocks kainate receptors (Honore et al., 1988).

Mechanistically, noncompetitive antagonists are considered better suited for a more selective blockade of AMPA receptors, because they bind to a regulatory site(s) distinct to the agonist site and their actions should not depend on the concentration of an agonist. Noncompetitive antagonists have also the theoretical advantage to counteract excitotoxicity even at high concentration of glutamate and to show less side-effects than competitive antagonists (Parsons et al, 1998). It should be pointed out that all of these small-molecules are typically drug-like and amenable to chemical optimization for oral bioavailability and favourable pharmacokinetic properties.

There are a number of pharmacological agents that affect AMPAR function through interactions outside of the agonist-binding domain (Kew et al., 2005). Perampanel, a selective noncompetitive AMPAR antagonist, has recently gained FDA approval for

clinical use in the treatment of partial-onset seizures and primary generalized tonic-clonic (PGTC) seizures (Rogawski et al., 2013). Radioligand-binding studies suggest that the blocking site coincides with that of GYKI 52466 (Figure 2), the prototype of 2,3-benzodiazepine noncompetitive AMPAR antagonists (Solyom et al., 2002).

The most promising group of noncompetitive antagonists of AMPA receptors are 2,3-benzodiazepine derivatives, whose prototype GYKI 52466, 1-(4-aminophenyl)-4-methyl-7,8-methylenedioxy-5*H*-2,3-benzodiazepine, demonstrated significant anticonvulsant and neuroprotective action (Solyom et al, 2002). These antagonists bind at the interface between the S1 and S2 glutamate binding core and channel transmembrane domains, specifically interacting with S1-M1 and S2-M4 linkers, thereby disrupting the transduction of agonist binding into channel opening (Balannik et al., 2005).

More recently, the crystal structures of the rat AMPA-subtype GluA2 receptor in complex with three noncompetitive inhibitors have been reported (Yelshanskaya, et al. 2016). The inhibitors bind to a binding site, completely conserved between rat and human, at the interface between the ion channel and linkers connecting it to the ligand-binding domains. The authors propose that the inhibitors stabilize the AMPAR closed state by acting as wedges between the transmembrane segments, thereby preventing gating rearrangements that are necessary for ion channel opening.

The research group with whom I worked during my PhD has been involved by many years in the synthesis of new 1-(4-aminophenyl)-3,5-dihydro-7,8-methylenedioxy-4*H*-2,3-benzodiazepin-4-ones (e.g. **1,** Figure 2) and in the characterization of their mechanism of action (Grasso et al., 1999; Grasso et al., 2003; Zappalà et al, 2006a). During the development of this research project, the Authors demonstrated that an improvement of AMPAR affinity of 2,3-benzodiazepin-4-ones has been reached by substituting the benzo-

fused dioxole nucleus with the dioxane homologue (i.e. **2,** Figure 2) (Zappalà et al, 2006b; Micale et al. 2008). Moreover, the Authors found that the addition of a methyl group at the 3' position (i.e. **2b**) enhanced the antagonist activity, whereas the introduction of another methyl group at the 5' position (i.e. **2c**), was not fruitful for the increase of the potency on GluA2Q receptors (Wang et al., 2015), according to the binding assays and functional tests already performed (Micale et al. 2008).

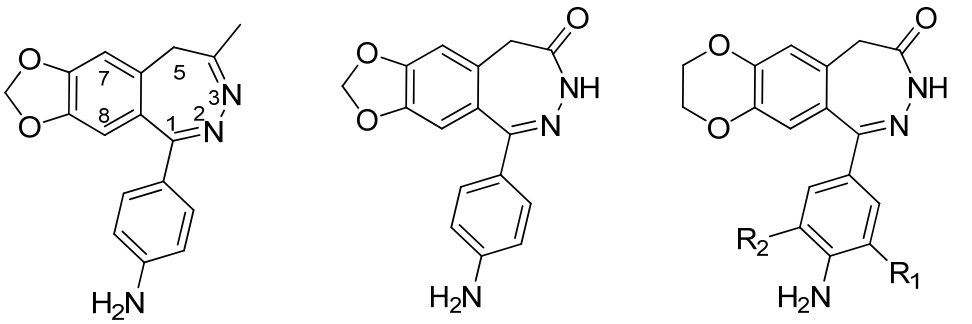

Figure 2. Model compounds GYKI 52466, **1** and **2a-c**.

Furthermore, in collaboration with Dr. Niu, using a laser-pulse photolysis technique, the mechanism of action of compounds **1** and **2** and their binding site on the AMPA receptors were further characterized in the microsecond-to-millisecond time domain (Ritz et al., 2008; Ritz et al., 2011, Qneibi et al., 2012, Wang et al., 2015).

Kinetic studies showed that compound **1** and **2** are noncompetitive antagonist of GluA2Q homomeric receptors. Noteworthy, compound **1** prefers to bind to the open-channel state whereas derivatives **2** show a higher affinity towards the closed-channel state of the GluA2Q receptors. By a double-inhibition experiment, it was demonstrated that compound **1** and derivatives **2** do not seem to bind to the same binding site on GluA2Q receptor, and there is no an apparent allosteric interaction between these putative binding sites on the same receptor (Qneibi et al., 2012, Wang et al., 2015).

It has been recently reported (Wang et al., 2014) that the introduction of a thiadiazole moiety at the *N*-3 position of the 2,3-benzodiazepine scaffold yields an enhancement in potency and selectivity on AMPA receptors. The two 2,3-benzodiazepines GYKI 47409 and GYKI 47654 (Figure 3) were found to be far more potent inhibitors of both the closed and open conformations of all four homomeric AMPA receptor channels than the unsubstituted 2,3-benzodiazepine GYKI 52466 as well as N-3 substituted derivatives Talampanel and GYKI 53784. The Authors proposed that the heterocycle at the N-3 position is able to well accommodate into a "side pocket", generating a strong interaction with residues surrounding this binding site, as predicted by a four-point pharmacophore model (Rezessy and Solyom, 2004) that suggests a role of the heteroatom of the thiadiazole moiety as H-bond acceptor.

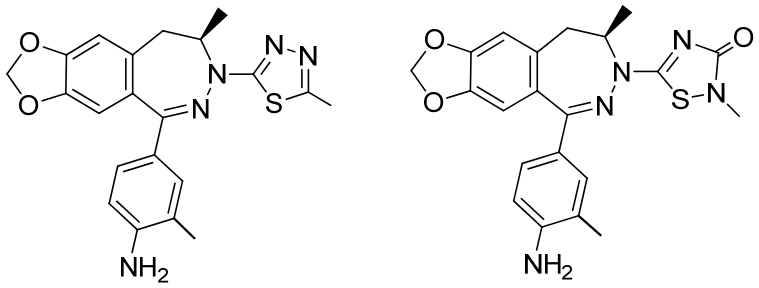

GYKI 47409 GYKI 47654

Figure 3. Structure of thiadiazole derivativesGYKI 47409 and GYKI 47654

To better define the structure–activity relationship (SAR) of this class of compounds, we planned to synthesize two groups of analogues of 2,3-benzodiazepines **2a-2c**.

The first group of these compounds (Figure 4) bears a methyl group on 7,8-ethylenedioxy moiety (**3a-3c**) in order to create additional hydrophobic interactions between the 7,8-ethylenedioxy portion and the receptor site.

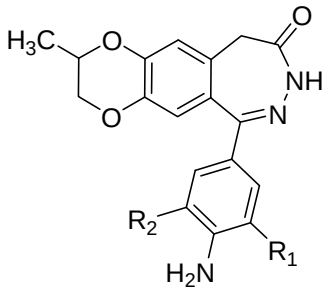

3a R_1=R_2=H
3b R_1= CH_3, R_2=H
3c R_1=R_2=CH_3

Figure 4. Structure of novel 2,3-benzodiazepines noncompetitive AMPAR antagonists **3a-3c**

The second group of 2,3-benzodiazepines has been designed starting from the above-mentioned thiadiazole derivatives GYKI 47409 and GYKI 47654. We decided to insert at the *N*-3 position a more flexible heterocycle that could better fit into the binding pocket and presumably maintain the same capability to interact with the receptor site via hydrogen bond as the thiadiazole nucleus does. In particular, I synthesized derivatives **4a-4c** in which a 3-bromoisoxazolin-5-yl has been linked to *N*-3 and derivatives **5a-5c** in which the same heterocycle was linked to *N*-3 by means of a methylene spacer (Figure 5). The choice of the 3-bromoisoxazolin-5-yl is in agreement with literature data (Solyom et al, 2007), in which the substituent at N-3 position could be represented by a substituted or unsubstituted 5-or 6-membered, aromatic, saturated or partially saturated heterocyclic ring containing at least two heteroatoms, with one of them being a nitrogen atom.

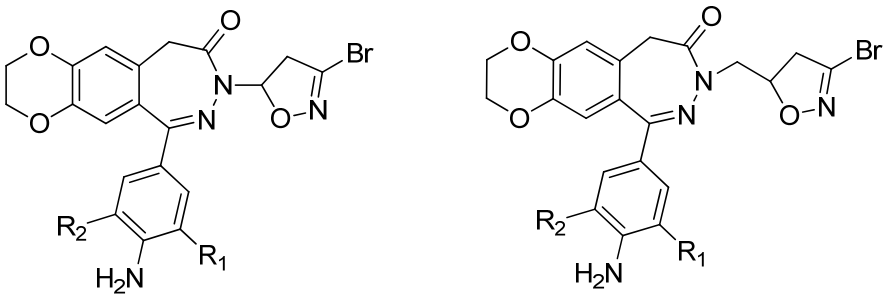

4a $R_1=R_2=H$
4b $R_1= CH_3$, $R_2=H$
4c $R_1=R_2=CH_3$

5a $R_1=R_2=H$
5b $R_1= CH_3$, $R_2=H$
5c $R_1=R_2=CH_3$

Figure 5. Structure of GYKI compounds and novel 2,3-benzodiazepines noncompetitive AMPAR antagonists **4a-4c** and **5a-5c**.

The synthesized compounds have been characterized for their inhibitory properties by a set of functional assays. Using human embryonic kidney cells, i.e. HEK-293 cells, to transiently express homomeric receptor channels, individually, and using whole-cell recording to monitor the receptor function, we have characterized the potency and selectivity of these compounds towards AMPARs.

1.2 Evaluation of novel 2,3-benzodiazepin-4-one noncompetitive AMPAR antagonist on leukemia Jurkat T cell growth, cell cycle and apoptosis

Over the past years several lines of evidences implicated glutamate in the development and proliferation of different types of cancers inside and outside of the central nervous system (Prickett et al. 2012; The et al. 2012). Beside to its excitatory role in the CNS, glutamate is involved in others cellular and biochemical functions such as proliferation, differentiation and survival of the neural cells (Luján et al., 2005). A number of findings revealed that the inhibition of AMPA receptor activity was able to inhibit migration and to induce apoptosis in human glioblastoma cells (Walczak et al, 2014), and to decrease cell growth in different non-neuronal cancer cell lines (Rzeski et al., 2001). Noteworthy was the evidence that different non-neuronal tumoral cell lines, such as human leukemia Jurkat T cell line, expressed AMPA receptor subunits GluA2-GluA4 (Stepulak et al., 2009), and glutamate might facilitate the spread and growth of leukemia T cells through interactions with GluA3 subunit AMPA receptor (Ganor et al., 2009). Despite these interesting and intriguing results, a deeper molecular and pharmacological characterization of putative AMPA antagonist has not yet been performed.

Recently, Stepulak et al. (2011) has shown that the AMPA antagonist GYKI 52466 reduced the viability of laryngeal cancer cell lines.

With the aim to elucidate the potential mechanism in cell cycle regulation elicited by 2,3-benzodiazepine derivatives, compound **2c**, based on primary screening on six different tumor cell lines, has been selected as the most active 2,3-benzodiazepine-4-one derivatives.

The ability of compound **2c** to modulate the cell cycle distribution and the molecular determinants involved in the cell cycle check points, together with its potential ability to modulated apoptotic pathways in human Jurkat T cell line has been evaluated.

1.3 Development of subtype-specific agonists for NMDA receptor glycine binding sites

The NMDA receptors are heterologous complexes consisting of several subunits assembled to form tetrameric arrangements. So far, seven different subunits have been identified, each with a specific modulatory influence on the receptor: one GluN1subunit, four GluN2 subunit (GluN2A-D) and two subunits GluN3 (GluN3A-B) (Paoletti, et al., 2007).

The most common NMDAR architecture consists of the coassembly of two GluN1 subunits and two GluN2 subunits organized as a dimer of dimers with a GluN1-GluN2-GluN1-GluN2 pattern with an overall axis of two-fold symmetry within the extracellular domains and with the ion channel domain exhibiting a four-fold symmetry.

NMDARs differ from other ligand-gated ion channels as they present the peculiarity to require two distinct ligands for their activation. Glu and Asp are the endogenous agonists for the receptor and bind to residues located in the GluN2 subunits that are the major determinants of the pharmacological and biophysical properties of these receptors. Glycine or D-serine acts as an essential coagonist and binds to residues located in the GluN1 and GluN3 subunits, increasing the frequency of channel opening channel (Yao et al, 2006: Madry et al, 2008).

The involvement of NMDARs in many neurological disorders and the crucial role of Glu as the major excitatory neurotransmitter in the mammalian CNS, triggered intense research plans aimed at the synthesis of new drug candidates characterized by a selective agonistic or antagonistic activity at these receptors.

During the past several decades, a great number of iGluR ligands have been developed, but few of them are specific for a single subtype. For the glycine site in the GluN1 subunit of NMDA receptors, a large number of antagonists exists, but relatively

few full and partial agonists have been reported (Bräuner-Osborne et al. 2000; Chen et al. 2008; Urwyler et al. 2009).

In recent years, a large number of structures of isolated iGluR agonist binding domains (ABDs) have disclosed important information on the molecular basis for orthosteric ligand recognition, and the mechanisms underlying activation, desensitization, and allosteric modulation (Furukawa and Gouaux, 2003; Inanobe et al., 2005; Yi et al., 2016; Hackos et al., 2016; Jespersen et al, 2014). These studies also show that structural differences exist in the dimer interface between ABDs of GluN1 and the different GluN2A-D subunits (Yi et al., 2016; Hackos et al., 2016).

On the basis of these structural differences, agonists capable of differentiating between the glycine binding site of GluN1 in a GluN2 subunit-dependent manner have been recently developed by the research group with whom I worked for a six month period (Maolanon et al. 2017). A series of Ser and Cys analogues have been designed and synthesized and displayed pronounced variation in activity among GluN1/2A-D NMDA receptor subtypes. In particular, *S*-benzyl substituted L-cysteine (*R*-form) **6a** showed extensive potentiation (169% response relative to glycine) of maximal current at GluN1/2C receptor subtype relative to the current induced by Gly. Thus, this compound may be considered a superagonist at the glycine site of the GluN1/2C receptor. These levels of superagonistic activity are unprecedented among all NMDA receptor agonists described to date (Bräuner-Osborne et al. 2000; Chen et al. 2008; Dravid et al., 2010). Although non-natural *R*-isomers generally are more active than *S*-isomers, it is notable that the cysteine analogue **6a** is the active enantiomer since this L-form has *R* absolute configuration.

In order to further evaluate the ability of L-Cys derivatives to differentiate between the glycine binding site of GluN1 in a GluN2 subunit-dependent manner, and to assess the effect of substituents with different electronic characteristics on the agonist properties of

the lead compound **6a**, I designed and synthesized new L-cysteine derivatives S-substituted **6b-6g** in which a chlorine atom or a methoxy group has been introduced in different positions of the benzyl moiety and compound **6h** in which the aromatic ring has been replaced by a 4-pyridyl nucleus. (Figure 6).

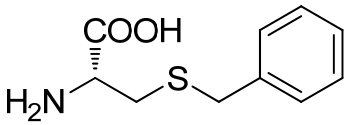

6a

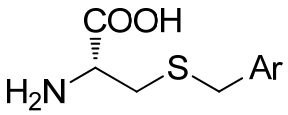

Comp.	Ar	Comp.	Ar
6b	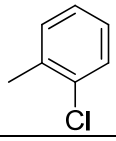	**6f**	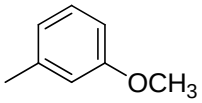
6c	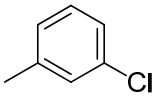	**6g**	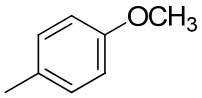
6d	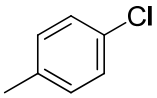	**6h**	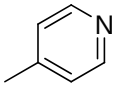
6e	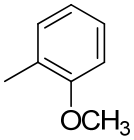		

Figure 6. Structure of the superagonist **6a** and of the designed analogues **6b-6h**

The synthesized compounds have been characterized by two-electrode voltage-clamp (TEVC) electrophysiology using *Xenopus* oocytes expressing recombinant NMDA receptor subtypes. Concentration–response data for the compounds have been generated in the continuous presence of a saturating concentration of Glu (100–300 μM) at the four GluN1/GluN2A-D NMDA receptor subtypes.

Chapter 2. Glutamate receptors

Currently,(*S*)-glutamic acid (Glu) is considered the main excitatory neurotransmitter in the mammalian central nervous system (CNS) and is implicated in key processes of brain development such as learning and memory (Riedel et al, 2003), and in several neuropathological conditions (Coyle et al., 2002).

An excessive glutamatergic stimulation can induce neuronal citotoxicity through at least two mechanisms:

• osmotic damage caused by the excessive influx of Na^+ in the cell through the ionic channels;

• damage induced by the alteration of the homeostasis of Ca^{2+}.

The effects of glutamate are mediated by its interaction with different receptor subtypes that, according to the mechanism of signal transduction, were grouped into two broad classes: ionotropic receptors (iGluRs) and metabotropic receptors (mGluRs).

The first mediate fast neurotransmission through the depolarization of the membrane potential directly by the opening of the pore-channel that increase the transmembrane flow of mono- and divalentcations.

The iGluRs are divided, on the basis of the name of the main exogenous agonists, in NMDA receptors (N-methyl-D-aspartic acid), AMPA [(RS)-2-amino-3-(3-hydroxy-5-methylisoxazol-4-yl)propionic acid] and KA (kainic acid)receptors (Traynelis et al., 2010).

The second family of receptors mediateslow modulatory responses and acts indirectly since the activation of the receptors by the ligand is transmitted from a protein G to the effector that is responsible for the increase in the intracellular second messengers.

Eight different subtypes of mGluRs have so far been identified. They are classified into three subgroups based on homologies in the peptide sequence, signal transduction mechanisms and pharmacology. The mGlu of group I (mGluR1, mGluR5) act by activating the phospholipase C; group II (mGluR2, mGluR3) and group III (mGluR4,6,7,8) acting through inhibition of adenylcyclase activity (Mayer, 2006; Traynelis et al., 2010).

2.1. Glutamate ionotropic receptors (iGluR)

Glutamate ionotropic receptors are a family of tetrameric receptors channel permeable to Na^+, K^+, and Ca^{2+}, whose opening and mediated by the interaction with the orthosteric ligand. Although they may be also located in the presynaptic terminal, they have localization predominantly post-synaptic, where they are involved in the fast excitatory neurotransmission and various forms of synaptic plasticity. The glutamate released from the presynaptic terminal interact with their receptors evoking an excitatory current post-synaptic (EPSC) whose profile shows a biphasic pattern. After an initial massive influx of cations (a few ms) mediated by the sudden activation of AMPAR, these receptors desensitize and simultaneously activate the NMDAR argue that the slow component of the EPSC. After 50-60ms, NMDAR the close and the charge flow terminates.

The AMPA receptors are generally co-expressed with the NMDA receptors at the level of the glutamatergic synapses where jointly contribute to the processes of synaptic plasticity that are involved in the phenomena of learning and memory, excitotoxicity and neuroprotection. These receptors typically differ in their kinetics of the response to the presynaptic release of glutamate. The AMPA receptors mediate fast postsynaptic answers even to potential very negative or in the absence of action potentials. Rapid desensitization

of these receptors is responsible of the EPSCs; the NMDA receptors, instead, are characterized by a slower kineticand a weak or nodesensitization.

From the structural point of view the receptor channel is a tetramer, composed of identical subunits (homotetramer) or different (heterotetramer), that are assembled in two subsequent steps. Initially two subunits interact to form a dimer, and then two dimers are organized delimiting the central pore and giving rise to the mature receptor.A recent study aimed to clarify the mechanism assembly, has highlighted that the heterotetramers assemble from heterodimers (Riou et al., 2012).

The different subunits have a shared modular structure that consists of:

- a large N-terminal domain (NTD extracellular) that in addition to being involved in the assembly and in the modulation of different subtypes, has the binding site for the allosteric modulators;
- an extracellular domain of binding to the agonist (ABD) also known as the S1-S2 domain;
- a transmembrane domain (TMD) composed by three transmembraneα-helices (M1, M3 e M4) and by a short loop (M2) which constitutes the filter of ionic selectivity; this re-entrant loop is a peculiar structural feature that distinguishes iGluR subunits from other neurotransmitter-gated ion channels.
- a C-terminal domain (CTD) of variable size that has several phosphorylation sites and is involved in the modulation, in traffic and in the localization of the receptor (Madden, 2002).

The recent crystallization of subtype homomeric GluA2 of AMPAR has represented a turning point for the resolution of the structure of the ionotropic receptors, in particular the data obtained show that the region of the pore has a much more compact structure and

symmetrical with respect to the extracellular domains. Moreover, the interactions between the NTD of different subunits are relatively small compared to what previously hypothesized (Sobolevsky et al., 2009).

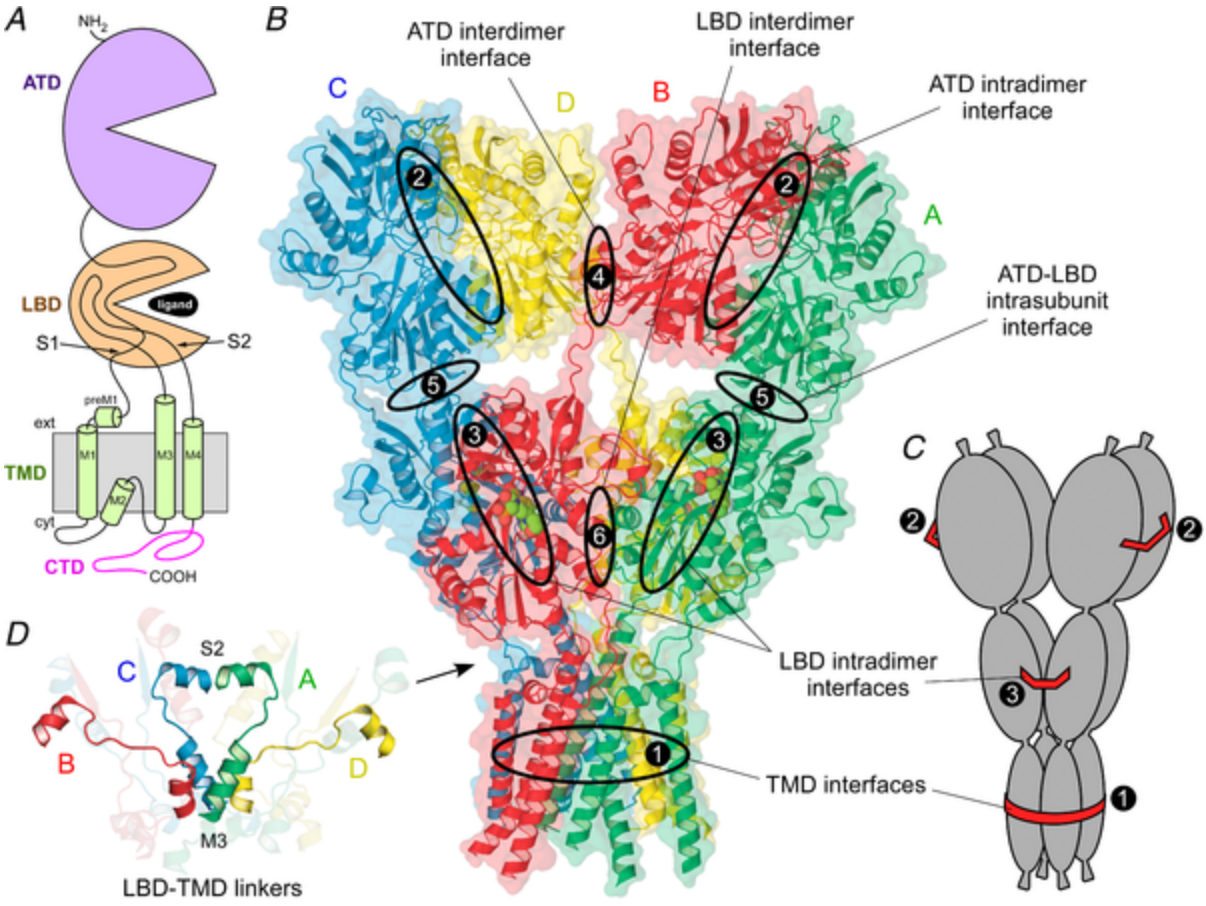

Figure 7. Structure of iGluR. *A*, topology of iGluR subunit. *B*, structure of AMPA subtype rat GluA2 receptor in the closed antagonist bound state (3KG2). Strong and weak interfaces are shown as large and small ovals, respectively. *C*, model of the assembly of four three-compartmental sausages with strong interactions holding together (1) all four bottom compartments, (2) left and right pairs of the top compartments and (3) front and back pairs of the middle compartments. *D*, LBD–TMD linkers – the iGluR gating transmission domain – include S1–M1, M3–S2 and S2–M4, of which S1–M1 and S2–M4 are shown transparent. The M3–S2 linkers, the central element of the gating machinery, have different conformations and secondary structures for the two diagonal pairs of subunits, A/C and B/D (from Sobolevsky, 2015).

The large structural and functional diversity of the different receptor subtypes is supported both by the large number of subunits, and from translational and post-transcriptional modifications. For example the pre-mRNA of some subunits may undergo a process of nucleotide editing that produces the incorporation of an arginine (R) in the mature receptor while the genomic DNA in that site code for a glutamine (Q). The point at which occurs the nucleotide editing takes the name of Q/R site and appears to be involved in regulation of neuronal development and in ionic selectivity of receptors containing the subunit GluA2 (Seeburg et al., 1998).

From a pharmacological point of view, in the absence of ligand the channel is closed and the receptor is in a rest state (R), following the binding of the agonist the receptor passes in an activated state (A) and the channel opens allowing the ion flow. After an interval of 1-100 ms in function of the receptor subtype, the channel closes while the binding site is still busy, preventing the binding with another molecule of agonist. In this condition the receptor is in a desensitized state (D) (Talukder et al., 2010)

2.2 AMPA receptors

AMPA receptors are the most abundant ionotropic glutamate receptors in the mammalian brain.

The AMPAR are a heterogeneous family of homo- or heterotetrameric assembly of four different subunits of about 100 kDa identified as GluA1-2-3-4. As previously mentioned, these receptors show a rapid kinetics of activation and desensitization that justifies the fast component of the glutamatergic EPSP.

The pharmacological characteristics of the AMPAR differ greatly in function of the subtypes taken into consideration and the post-transcriptional modifications of the different

subunits. For example, the length of CTD of some subunits is determined by variations in the splicing of the primary transcript. It has been demonstrated that the length of the CTD influence the turnover of AMPAR, in detail the longer CTD reduces the receptor turnover. This mechanism may explain some forms of LTP, mediated by the expression in the synapses of receptors composed of subunits with the longer CTD (Seeburg et al., 1998).

It is well known that as a result of alternative splicing of exons 14 and 15, the isoforms "Flip" and "flop" of the subunits of AMPAR are respectively expressed. The incorporation in the tetramer of variant "Flip" confers a quicker kinetics of activation of the receptor and a slower desensitization (Coleman et al., 2006). During the development, the "Flip" isoform is more expressed with respect to the isoform "flop", while in the adult, the expression levels of the two splice variants are relatively similar. This observation has been confirmed by experimental evidence that suggest the involvement of receptors that contain subunits "Flip" in the growth and maturation of neocortical neurons during the prenatal period.

A further level of heterogeneity of AMPAR is related to the nucleotide editing of primary transcripts of the subunit GluA2.The deamination of an adenosine to inosine, catalyzed by adenosine deaminase, leads to the expression of an arginine (R) in M2 reentrant loop of mature receptor, while the genomic DNA in that position code for a glutamine (Q). The AMPAR incorporating the edited subunits are impermeable to Ca^{2+} and consequently not mediate the metabolic responses related to the homeostasis of Ca^{2+} itself. . However, since nearly all GluA2 subunits are edited and the majority of AMPA receptors contain the GluA2 subunit, most AMPA receptors do not flux calcium. However, GluA2-lacking AMPA receptors are common in interneurons and some cortical neurons where their rapid kinetics allows particularly fast synaptic signaling and their calcium permeability mediates novel forms of synaptic plasticity (Isaac et al., 2007).

2.2.1 AMPA receptor subunits

It is now well established that there are four AMPA receptor subunits designated GluA1–GluA4 (formerly GluR1–GluR4), each encoded by a separate gene (Lodge, 2009). AMPA subunit shared the modular structure as the other iGluR subunits.

The large extracellular ATD is involved in receptor assembly, trafficking and modulation. A ligand-binding domain LBD serves as the recognition site for agonists (including the natural agonist glutamate) and also represents the binding site for competitive antagonists. The transmembrane domain forms the ion channel and consists of three membrane-spanning hydrophobic domains and one intramembranous reentrant loop.

A short cytoplasmic carboxy-terminal domain is involved in targeting the receptor to synapses. The peptide segments connecting the ligand-binding domain to the transmembrane domain transmit conformational changes elicited by agonist binding to the transmembrane ion channel domain, allowing agonist binding to gate the channel to the open state; these segments can be considered the "transducing domain" (Szenasi et al., 2008). This region of the channel is critical to binding of noncompetitive antagonists, which prevent channel gating (Balannik et al., 2005).

Each subunit consists of approximately 900 amino acids and exhibits 65–75% sequence homology to other subunits. All AMPA receptors are tetrameric combinations of the four subunits. While homomeric receptors are functional, native AMPA receptors are believed to be heteromers. For example, in hippocampal pyramidal cells of mature rats, the most common subunit configurations are GluA1/GluA2 and GluA2/GluA3 (Wenthold et al., 1996).

The near-full-length crystal structure of GluA2 (Fig. 7 and fig. 8B) revealed a number of interesting features about AMPARs. For example, the ATD and LBD each

possess a 2-fold rotational symmetry, where subunits of like conformation are positioned opposite to each other (Fig. 8*A* right panels) (Sobolevsky *et al.* 2009). In contrast, the TMD displays 4-fold symmetry. Further, there is a mismatch in subunit arrangement between the ATD and LBD. In the fully assembled receptor (Fig. 8*A*, right panels), subunits that are proximal to each other (B and D) at the ATD level are located distally at the LBD level, and vice versa (Gan et al., 2015).

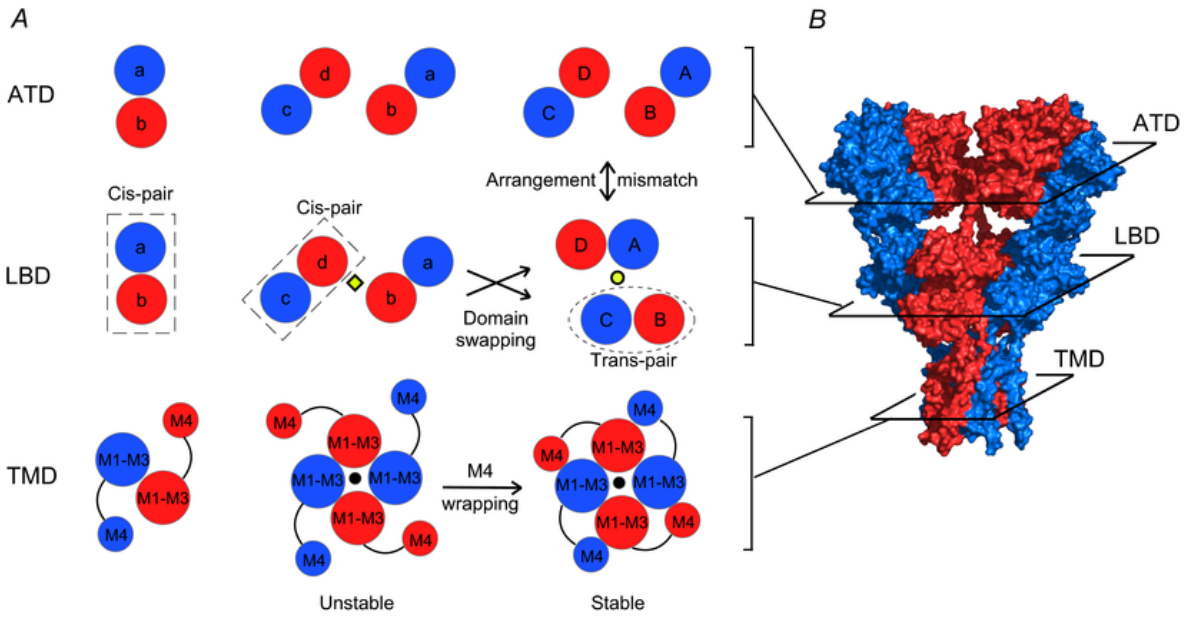

Figure 8. *A* Model of AMPAR assembly; *B*, crystal structure of GluA2 receptor (3KG2) (from Gan et al., 2015).

Figure 8*A* illustrates a hypothetical model of AMPAR assembly highlighting the intrinsic interactions among subunits at levels of the ATD, the LBD, and the TMD. In this model, the ATD facilitates the formation of dimers (left panels). At the dimer stage, the LBDs of the two participating subunits might associate to form an LBD pair (dubbed '*cis*-LBD pair'). Dimers then associate with each other via interactions within the ion channel core to form an unstable intermediate termed a 'proto-tetramer' (central panels). *Cis*-LBD pairs persist into the proto-tetramer stage leading to an arrangement at the level of the LBD

matching that of the ATD. The M4 transmembrane segment of each subunit then wraps around the ion channel core (M1–M3) of an adjacent subunit – a process we term 'M4 wrapping' – and stabilizes the tetramer. At some point during this process, the LBDs separate and exchange their interacting partners to form '*trans*-LBD pairs' leading to the subunit arrangement mismatch between the ATD and the LBD observed in the fully assembled tetrameric complex (Sobolevsky et al. 2009). We refer to this process as 'domain swapping'. M4 wrapping in the TMD, along with domain swapping, presumably contributes to the overall intrinsic energetics of tetramerization. Additionally extrinsic factors such as ER chaperones and glycosylation could also have important, albeit undefined, modulatory effects on these subunit interactions facilitating tetramerization.

Recently, the crystal structures of the rat AMPA-subtype GluA2 receptor in complex with three noncompetitive inhibitors have been reported (Yelshanskaya, et al. 2016). The inhibitors bind to a novel binding site, completely conserved between rat and human, at the interface between the ion channel and linkers connecting it to the ligand-binding domains. The authors propose that the inhibitors stabilize the AMPA receptor closed state by acting as wedges between the transmembrane segments, thereby preventing gating rearrangements that are necessary for ion channel opening.

AMPA receptors are associated with a variety of transmembrane proteins that function as auxiliary subunits, including TARPs (transmembrane AMPA receptor regulatory proteins), such as stargazin; cornichon proteins (CNIH-2, CNIH-3); and SynDIG1 (synapse differentially induced gene 1) (Diaz, 2010). The auxiliary subunits regulate channel gating and are involved in subunit folding, assembly, surface expression and the clustering of AMPA receptors at synapses. In addition, the subunits modulate the sensitivity of AMPA receptors to pharmacological agents, including antagonists (Cokić and Stein, 2008).

Binding studies with ^{3}H-AMPA showed that this class of receptors is widely distributed in the CNS and that the expression levels vary in function of the brain regions analyzed. The highest expression levels were observed in the hippocampus, in the cerebral cortex and in the cerebellum. In particular, the subtype prevalent in hippocampus is the heterotetramerGluA1/GluA2, whereas the GluA3receptors are expressed at high levels in the encephalic nuclei. The GluA4 subunit is especially expressed in the early stages of neuronal development and is replaced by the GluA1 in SNC adult, thus suggesting a role in the development of SNC. As regards the cerebral cortex, high levels of expression of the subtypes GluA1 and GluA2/3 were reportedin GABAergic interneurons and in excitatory interneurons.

2.2.2 Post-translational modifications of AMPA receptors

Properties and function of AMPARs may also be modulated by post-translational modifications such as glycosylation, palmitoylation and phosphorylation.

Glycosylation is a protective modification that can occur at 4-6 different sites located in the extracellular domains of each AMPAR subunit. This N-glycosylation may facilitate the maturation of AMPARs and protect them from proteolytic degradation (Jiang *et al.*, 2006).

Palmitoylation is a reversible fatty acetylation that regulates protein trafficking and cellular localization. All AMPAR subunits can be palmitoylated on two cysteine residues in their transmembrane domain TM2 and in their intracellular C-terminal region. The first palmitoylation in TM2 leads to an accumulation of AMPAR in the Golgi apparatus, resulting in a decreased expression of the receptor in the cell surface. On the other hand, palmitoylation at the C-terminal domain contributes to receptor internalization by

disrupting its interaction with the 4.1N protein, known to stabilize AMPAR expression on the surface (Hayashi *et al.*, 2005).

Four and two phosphorylation sites have been reported for the GluA1 and GluA2 subunits, respectively (Lee *et al.*, 2010), all residing in the intracellular C-terminal. Phosphorylation of these Ser e Tyr residues is involved in the mechanisms of synaptic plasticity: hippocampal NMDA-dependent Long-Term Potentiation (LTP) and Depression (LTD).

2.3 NMDA receptors

Expressed in ubiquitous manner in the CNS, NMDA receptors mediate fast gluammatergic neurotransmission in CNS and play important roles in neuronal functions such as the processing of information, learning and memory formation, synaptic plasticity and neuronal development. The NMDA receptors also play an important role in nociception: many antagonists of the receptor have been shown capable of effectively attenuate the pain in both acute and chronic (Bräuner-Osborne et al., 2000; Petrenko et al, 2003).

An abnormal activation of NMDA receptors may lead to an increase in the levels of Ca^{2+} intracellular up to cytotoxic levels, thus promoting the neuronal death (excitotoxicity). The permeability to calcium represents a peculiarity for NMDA receptors with respect to the other two classes of ionotropic receptors, AMPA and KA, that show instead a predominant permeability to Na^{+} and K^{+} ions (Liu et al., 2007). Excitotoxicity mediated by NMDA receptors was observed in many conditions both acute, as ischemia or trauma,and chronic as in many neurodegenerative diseases including Parkinson's, Alzheimer's, Huntington's disease and amyotrophic lateral sclerosis. A hypofunction of

NMDA receptors is involved in the pathophysiology of schizophrenia (Lynch et al., 2002; Vrajováet al., 2010)

The architecture of the NMDA receptors allows them to exist in multiple isoforms, each with specific characteristics of molecular composition, expression spatial and temporal, intracellular localization, functional properties, pharmacological and kinetics (Laube et al. 1998).

The NMDA receptors are heterologous complexes consisting of several subunits assembled to form tetrameric arrangements. So far, seven different subunits have been identified, each with a specific modulatory influence on the receptor: one GluN1subunit, four GluN2 subunit (GluN2A-D) and two subunits GluN3 (GluN3A-B) (Paoletti, et al., 2007).

Eight subunits GluN1 are generated by alternative splicing of a single gene, while the GluN2 and GluN3 subunits are encoded by six different genes. The subunits GluN1 and GluN2 are essential for the functions of the receptor and therefore are always present in the complex. A splice variant of the subunit GluN1 combines with at least one subunit GluN2A-D and less frequently with a modulatory subunit GluN3A-B. The most common architecture of the NMDA receptor consists in a co-assembly of two GluN1 subunits and two GluN2 subunits organized as a dimer of dimers with an arrangement GluN1- GluN1-GluN2-GluN2 disposed around the ion channel (Fig. 9). In the receptor subtypes that express a GluN3modulatory subunit, the most common co-assembly consists in a ternary GluN1-GluN2-GluN3tetramericcomplex. (Paoletti, et al.,2007; Cull-Candy et al., 2001; Schorge et al., 2003).

NMDA receptors differ from other ligand-gated ion channels because they have the peculiarity of requiring two separate ligands for its activation. Glutamate is the endogenous

agonist and binds to residues located in GluN2 subunit that are the main determinants of the pharmacological properties and biophysical of these receptors. The glycine acts as a co-agonist and binds to residues of the GluN1 subunits and probably also of the GluN3subunits, increasing the affinity of the receptor for the glutamate and the frequency of opening of the channel (Yao et al, 2006: Madry et al, 2008).

Moreover, GluN2 subunits have: (i) binding sites for allosteric regulators (e.g. extracellular Zn^{+2}); (ii) binding sites for non-competitive antagonists such as feniletanolammine (e.g. ifenprodil)located at the interface with GluN1 subunits; (iii) two or three sites for polyamines (voltage-dependent and voltage-independent); (iv) a site for channel blockers (e.g. phencyclidine) (Fig. 9) (Gielen et al., 2009).

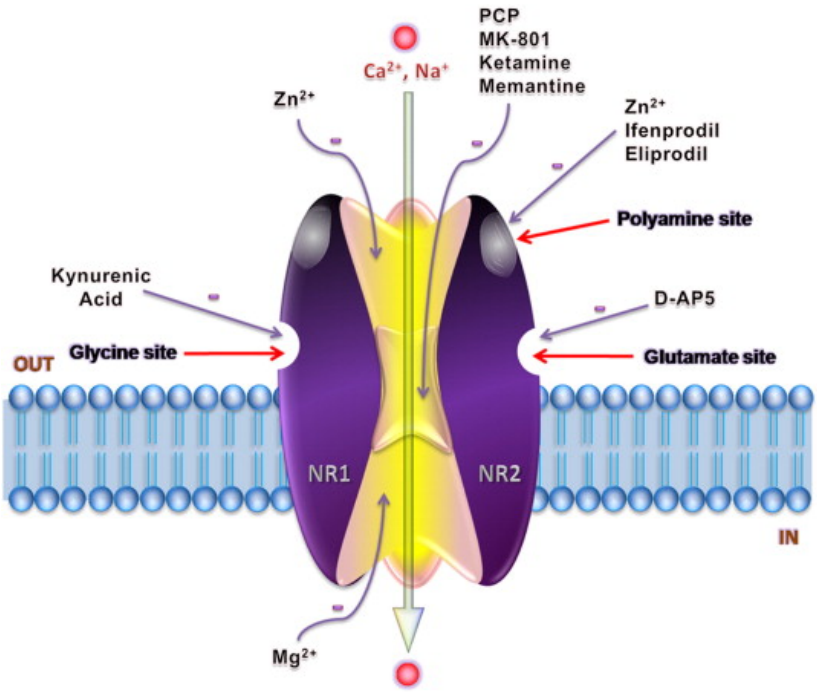

Figure 9. Heterotetramer GluN1/GluN2 NMDA receptor and its modulatory sites (from Ghasemi et al., 2011).

2.3.1 NMDA receptor subunits

The GluN1 and GluN2 subunits share a common basic topology with other iGluRs (AMPA and KA receptors), characterized by four hydrophobic domains (M1-M4) within the central portion of the sequence: M1, M3 and M4 are membrane-spanning segments, whereas M2 domain forms a re-entrant loop in the membrane and lines the pore of the ion channel.

NMDAR subunits also have a cytoplasmic carboxylic terminal domain (CTD), a large extracellular amino-terminal domain (ATD), and an extracellular loop between M3 and M4. The size of CTD is different in the various subunits and contains several sites of interaction with numerous intracellular proteins such as protein kinases and protein phosphatases.

The ATD has a key role in subunit assembly and it also contains the binding sites of the negative allosteric modulators Zn^{2+} and ifenprodil-like compounds (Paoletti, 2007; Huggins and Grant, 2005). Endogenous Zn^{2+} binds at the GluN2A subunit with nanomolar affinity and at the GluN2B subunit with a >100-fold lower affinity, while it does not affect GluN2C and GluN2D subunits (Paoletti et al. 2000; Rachline et al., 2005). Ifenprodil-like compounds bind selectively at the GluN1-GluN2B interface (Karakas, et al. 2011).

The large extracellular loop shared by M3 and M4 domains (S2 region) forms with the extracellular N-terminus (S1 region) the ligand binding domain (LBD). The S1 region is a highly conserved domain involved in the crucial interaction with the γ-carboxylate of the ligand by means of an arginine residue. Conversely, the S2 region is less conserved among different subtypes; this peculiarly allows the generation of subtype selective ligands. The LBD is a clamshell-like motif in which the two lobes (referred to as D1 and

D2 according to the regions that form them) can adopt different conformational states depending on NMDAR subunit and/or the feature of the ligand.

X-ray studies demonstrated that LBD of isolated GluN1 subunits adopt "closed" conformations in complex with full agonists (i.e. glycine or D-serine) and partial agonists (e.g. D-cycloserine) leading to receptor activation, and that the degree of the domain closure is essentially the same (Furukawa and Gouaux, 2003; Inanobe et al., 2005).

Conversely, site-directed mutagenesis studies performed on Glu binding site of GluN2B subunits co-expressed with GluN1 indicated that partial agonists might induce "half-open" conformations of the LBD (Hansen, et al, 2005).

Finally, the LBD adopts open conformations in the "apo" (ligand-free) form and in complexes with antagonists (Furukawa and Gouaux, 2003). The M2 domain of GluN2 and GluN1 subunits contains an asparagine residue in the so-called QRN site. The name of this site arose from the fact that it is occupied by an asparagine (N) residue in NMDARs and by a glutamine (Q) or an arginine (R) in non- NMDARs, which is critical for high-calcium permeability and voltage-dependent magnesium block (O'Leary et al., 2009; Chaffey and Chazot, 2008).

Several studies revealed that in NMDAR subtypes incorporating a GluN3 subunit, the ion channel conductance, Ca^{2+} permeability and Mg^{2+} block are markedly reduced. These functional differences are due to the structure of the channel-lining M2 domain that differs from that of other subunits around the QRN site (Sasaki et al., 2002). In particular, in the GluN3 subunits, an Asn residue is replaced with Gly followed by Arg at the N+1 site, generating at this locus a sequence that is Gly-Arg, whereas in GluN1 the sequence is Asn-Ser and Asn-Asn in GluN2. The presence of the protonated Arg residue in GluN3 is

likely responsible for the specific permeation properties and magnesium sensitivity of the GluN3-containing NMDA receptors (Matsuda et al., 2002).

The four GluN2 subunits have different distributions throughout the CNS. GluN2B and GluN2D are already expressed during embryonic stages, while GluN2A and GluN2C expression begins after birth. GluN2A subunit is ubiquitously expressed in the adult brain and it is particularly abundant in hippocampus and cerebellum. GluN2B predominate in the forebrain especially in the cerebral cortex, hippocampus and thalamic regions (Loftis and Janowsky, 2003).

The expression of GluN2C subunits is nearly entirely confined to the cerebellum, mostly in Purkinje and granule cells with almost no expression in the forebrain. The presence of GluN2D subunit in the adult brain is restricted to a few areas such as the globuspallidus, thalamus, subthalamic nuclei, and superior colliculus (Wenzel et al., 1996) Moreover, there is evidence that triheteromeric GluN1/GluN2A/ GluN2B receptors are present in the cortex and hippocampus and GluN1/GluN2A/GluN2C and GluN1/GluN2B/GluN2D in the cerebellum (Cull-Candy and Leszkiewics, 2004). GluN3A and GluN3B subunits also showed distinct expression in different regions of the CNS. GluN3A is particularly expressed in the cortex, midbrain and hippocampus, whereas GluN3B is predominant in somatic motor neurons in the brain, brainstem and spinal cord (Nishi et al., 2001; Eriksson et al, 2002).

2.3.2 NMDA receptor channel activation

The binding of Glu and glycine to their sites on the NMDAR complex determines the opening of a cation permeable pore, responsible for the postsynaptic depolarization. The NMDARs, as well as other members of the iGluR family, when activated, allow the

passage of Na+ ions into the cell and K+ ions out of the cell, to generate a short-lived depolarization called excitatory postsynaptic potential (EPSP).

Unlike the other two subtypes of iGluRs, the NMDARs ion channels also enable intracellular passage of Ca^{2+} ions, which can produce strong biochemical signals in the postsynaptic cell, affecting numerous intracellular signaling and processing systems (Popescu, 2005). Ca^{2+} influx through NMDARs can induce the long-term potentiation (LTP), a long-lasting enhancement in signal transmission that is thought to play a critical role in regulating synaptic plasticity, a cellular mechanism that underlies learning and memory. Ca^{2+} influx is also required for synapse formation, synaptic maintenance and physiological pruning during development (Cooke and Bliss, 2006).

However, an excessive entry of Ca^{2+} may cause neuronal cell death through activation of a variety of Ca^{2+}- dependent proteolytic enzymes such as calpains and endonucleases. All this mechanism triggers off excitotoxicity that leads to pathologic neurodegeneration (Arundine and Tymianski, 2003).

Another peculiarity of NMDARs with respect to the other iGluRs is their gating kinetics, which determines the time course of synaptic currents. NMDARs show much slower deactivation kinetics based on their subunit composition and a weak or no desensitization. This has been proven for GluN1/GluN2A receptors, which deactivate more rapidly (ms) than those containing GluN2B or GluN2C, which in turn deactivate at least 10 times more rapidly (s) than NR2D containing receptors (Erreger et al, 2004).

The prolonged deactivation time course of NR2D containing receptors has been recently explained by means of crystallographic studies performed on isolated GluN2D LBD in complex with various agonists and by electrophysiological experiments. These studies revealed unique features for this subunit: the Glu-bound form induces

conformational changes in a region located at the backside of the ligand binding site (called 'hinge loop') which are not present in other ligand-bound forms. This Glu-induced conformational variability of GluN2D LBD influences both deactivation kinetics and receptor activity (Vance et al, 2011).

2.3.3 NMDA receptor modulatory binding sites

At resting membrane potential, the NMDARs ion channel is blocked by micromolar concentrations of extracellular Mg^{2+} ions. This voltage-dependent block can be relieved by a membrane depolarization beyond ~40mV and it is considered a protective mechanism by which the NMDARs avoid the massive influx of Ca^{2+} into neurons and the consequential neuronal damage.

The asparagine residue following the QRN site of the GluN2 subunits seems to be responsible for the high sensitivity towards magnesium blockade, especially in NMDARs that express GluN2A and GluN2B subunits in comparison to those ones containing GluN2C and GluN2D subunits (Cull-Candy et al, 2001).

Beyond extracellular Mg^{2+}, other endogenous and exogenous ions/compounds may modulate the responsivity of the NMDAR complex. The divalent cation Zn^{2+} is packaged into synaptic vesicles of axons and when it is coreleased with Glu can modulate neuronal excitability mediated by NMDARs through a reversible and voltage-dependent block, depending of its synaptic concentration. At nanomolar concentrations (IC_{50} = 10-30 nM) , Zn^{2+} exerts a high-affinity voltage-independent inhibition on GluN2A-containing NMDARs while at micromolar concentrations (IC_{50} = 20-100 μM) a low-affinity voltage-dependent channel block has been recorded. However, the inhibition is complete only when the voltage-dependent block occurs.

The high-affinity voltage independent binding site of Zn^{2+} resides within the cleft of the ATD and stabilizes at a closed conformation within the ATD by means of coordination bonds with His residues (Low et al. 2000). The low-affinity voltage-dependent binding site of Zn^{2+} instead, is located within the re-entrant M2 pore loop (Paoletti et al., 2000).

A similar interaction model has been proposed for the voltage-dependent GluN2B-containing NMDARs where residues His127 and Glu284 of the ATD come into direct contact with the cation Zn^{2+}, and residues Glu47 and Asp265 coordinate water molecules that increase Zn^{2+} sensitivity (Karakas et al, 2009). Cu^{2+} may directly interact with the NMDARs recognition site, acting as a non-competitive antagonist, and high concentrations of Cu^{2+} were shown to reduce specific glutamate binding (Liu and Zhang, 2000). Polyamines (e.g. extracellular spermine) enable to potentiate or inhibit glutamate-mediated responses of NMDARs. The potentiating effects of polyamines include an increased affinity of the receptor for subsaturating concentrations of glycine, an increase of glutamate-induced currents in the presence of saturating concentrations of glycine and a decrease in NMDAR desensitization. The inhibitory effects of polyamines on NMDARs include a voltage-dependent blockade and a reduced affinity for Glu.

NMDARs are also very sensitive to changes in H+ concentration. They are partially inhibited under physiological conditions and blocked in hypoxic/ischemic conditions, wherein the overproduction and extracellular accumulation of lactic acid cause a decrease of pH. In such pathological conditions H+ ions provide another important protective mechanism against Ca^{2+}-mediated excitotoxicity.

Protein phosphorylation/dephosphorylation represents another mechanism of NMDARs modulation, with the balance between activity of *Src* family kinases and tyrosine phosphatases representing the major device. Phosphorylation is a posttranslational modification that occurs at the intracellular C-terminal domains of NMDARs and regulates

important functions such as excitability, trafficking and synaptic plasticity (Salter and Kalia, 2004).

Generally, it is a subunit-preferring reaction that involves the esterification of the hydroxyl groups of specific amino acids. For instance, GluN1 subunit is phosphorylated at Ser890 and Ser896 by two distinct PKC (PKCγand PKCα, respectively) modulating the NMDAR function and/or intracellular localization (Sanchez-Pérez and Felipe, 2005), while the concurrent PKC-PKA phosphorylation of two adjacent serine residues (Ser896 and Ser897) promotes subunit trafficking from the endoplasmic reticulum to the surface membrane (Scott et al., 2003). Also, GluN2A and GluN2B subunits contain several serine and tyrosine residues as phosphorylation sites. In regards to GluN2A subunit, phosphorylation of Ser1232 by CDK5 has been related with increased NMDA-evoked currents and excitotoxicity (Li et al 2001, Wang et al., 2003), and the action of a *Src* kinase on Tyr1387 with a reduced high-affinity voltage-independent zinc inhibition.

In GluN2B subunits, *Src* activity may influence endocytosis in some conditions (Snyder et al 2005), whereas a casein kinase (CKII) activity is involved in surface expression (Chung et al., 2007). Moreover, the activity of these subunits can be modulated by *Src*family tyrosine kinases and Ca^{2+}/calmodulin-dependent protein kinase II (CaMKII) promoting LTP (Barria and Malinow, 2005). GluN2C subunits contain two important serine residues for modulatory activity: Ser1230 (phosphorylated by PKC and PKA) that is located near the extreme of the C terminus and, unlike other GluN2 subunits, does not affect trafficking but instead channel sensitivity (Chen et al., 2006); Ser1096 (phosphorylated by PKB/Akt) that is involved in trafficking to the surface membrane (Chen and Roche, 2009). Three serine residues have been identified as possible targets for kinases in GluN2D subunits, but their function is still unknown. Phosphorylation of GluN3A and GluN3B subunits instead, has not been reported yet.

Other post-translation modifications of NMDARs that can affect their localization or activity include: *i) N*-glycosylation at the ATD and LBD (Standley and Baudry, 2000); *ii*) palmitoylation at two different clusters of cysteine residues of the C termini of GluN2A and GluN2B subunits that regulates NMDAR trafficking (Hayashi et al. 2009); *iii*) *S*-nitrosylation at both GluN1 and GluN2 subunits that reduces agonist-evoked currents (Choi, et al., 2000); *iv*) extracellular redox modulation involving disulfide bonds of specific cysteine residue within the ATD and/or LBD of GluN1 and GluN2 subunits and affecting Zn^{2+} high-affinity voltageindependent binding sites (Choi, et al., 2001).

2.4 Synaptic plasticity

The mechanisms through which the various environmental stimuli and physiological alter the functionality of the synapses and modulate the reorganization of the connections in the CNS, are defined mechanisms of synaptic plasticity. On the basis of the time course of these adjustments, the plasticity is defined in the short term or long term. It is known that the neuronal adaptations in the long term are responsible for many forms of conditional learning, memory and various behavioral aspects of dependencies from substances of abuse. The two main forms of synaptic plasticity long term are the LTP (Long-Term Potentiation) and LTD (Long-Term Depression), which induce respectively a strengthening or a decrease of the synaptic transmission after repeated stimuli over- or under-threshold.

Learning and memory as well as other processes involved in all human behaviour are possible due to the ability of the mammalian brain to undergo experience-based adaptations. Such plasticity is exquisitely regulated by highly intricate molecular mechanisms (Fleming and England, 2010; Shepherd and Huganir, 2007) and it occurs at

the level of synapses that become stronger or weaker in response to specific patterns of activity. These changes mediate the efficiency of synaptic transmission and, consequently, the activity of neuronal networks, ultimately representing the cellular correlate of learning and memory.

Despite being the most thoroughly studied forms of synaptic plasticity, the molecular mechanisms mediating LTP and LTD are still unclear. In general, two molecular mechanisms seem to underlie the changes in synaptic strength: either changes in the amount of neurotransmitters released by presynaptic neurons into the synaptic cleft or changes in the number and function of receptors on the postsynaptic neuron that respond to those neurotransmitters (Fleming and England, 2010). This second mechanism has gained particular support in the last decade, even though Lynch and Baudry had already proposed an increase in the number of synaptic GluRs during LTP more than twenty years ago (Lynch and Baudry, 1984). This idea came back to light after electrophysiological experiments suggested the existence of 'silent synapses' (Isaac *et al.*, 1995). These synapses, lacking AMPARs but with NMDARs, upon induction of LTP are converted to 'functional' synapses by delivery of AMPARs to the synaptic membrane.

AMPARs in the adult hippocampus contain GluA1/2 or GluA2/3 heteromers, but several lines of evidence point to a central role for the GluA1 subunit in hippocampal LTP, since knockout mice for GluA1 subunit were reported to be deficient in LTP (Zamanillo *et al.*, 1999). Accordingly, studies in organotypic hippocampal cultures transiently expressing GFP-tagged AMPARs showed a rapid translocation of GluA1-GFP to dendritic spines following LTP (Shi *et al.*, 1999). Moreover, the rapid translocation of this central subunit to the synaptic membrane requires a high-frequency stimulation and is highly dependent on the activation of NMDARs (Shi *et al*., 1999), which is consistent with what was described earlier, suggesting the activity-dependent insertion of GluA1-containing AMPARs in the

synaptic membrane. Furthermore, it was shown that the re-insertion of GluA1-containing AMPARs into the plasma membrane from recycling endosomes is enhanced in response to LTP-inducing stimuli, contributing not only to enhance synaptic efficacy but also to supply lipid membrane for the extension of dendritic spines during this phenomenon (Park *et al.*, 2004). Thus, these results seem to suggest the need of a stable pool of GluA1- containing AMPARs in close proximity to synaptic sites for the rapid modulation of the synaptic membrane upon LTP induction. Recent data suggest that GluA1 homomers are the first channels to be inserted during LTP, contributing to the early remodelling of synapses that occurs in the initial phases of this phenomenon, with a subsequent switch to GluA2-containing heteromers, thought to contribute to the consolidation of LTP (Plant *et al.*, 2006) although this finding remains controversial (Adesnik and Nicoll, 2007). Also, the changes in synaptic activity, based on the cycling of AMPARs in and out of synapses, are highly dependent on the phosphorylation of receptors and many studies support a critical role for CaMKII- and PKA-dependent phosphorylation of GluA1 at Ser831 and Ser845, respectively, in LTP. Particularly, while phosphorylation of Ser831 by CaMKII seems to be crucial for the induction of LTP (Lee *et al.*, 2000) but not required for the synaptic delivery of receptors (Hayashi *et al.*, 2000), PKA-mediated phosphorylation of Ser845 is necessary, although not sufficient, for this event (Malinow, 2003).

Regarding LTD, many studies show that this phenomenon results from the endocytosis of AMPARs (Beattie *et al.*, 2000). Indeed, the activation of NMDARs or insulin receptors can cause a loss of synaptically expressed AMPARs (Man *et al.*, 2000). Particularly, NMDAR-dependent LTD is known to require a moderate increase in postsynaptic calcium influx and activation of the calcium-dependent phosphatase calcineurin (Beattie *et al.*, 2000). The activation of this phosphatase mediates the regulation of the phosphorylation of AMPAR subunits, which is also important for LTD

expression. Thus, LTD further requires the dephosphorylation of the GluA1 subunit in Ser831 and 845 (Lee *et al.*, 2000). The mechanisms by which these dephosphorylation states of the GluA1 subunit mediate the internalization of AMPARs are still unclear but may involve differential regulation of AMPAR binding partners (Shepherd andHuganir, 2007). Furthermore, the regulated endocytosis of AMPARs is also dependent of the GluA2 subunit. Interaction between the GluA2 subunit and the clathrin adaptor protein AP2 is required to AMPAR internalization, and also, phosphorylation of this subunit mediates the disruption of the stabilizer GluA2-GRIP interaction, resulting in the removal of synaptic AMPARs, by facilitation of the GluA2-PICK1 interaction (Perez *et al.*, 2001).

The LTP and LTD mediated by NMDAR, are induced by specific patterns of synaptic activation (Malenka and Bear, 2004). As regards the LTP, it is necessary the synchronized activities of neurons pre- and postsynaptic. When the release of glutamate from presynaptic terminals and the depolarization of the post-synaptic cell occur at the same time, the maximal activation of NMDAR receptor takes places. In particular, the GluN1/GluN2B subtype seems to have a central role in the LTP (Malinow and Miller, 1986). These receptors allow the massive influx of Ca^{2+} and activation of intracellular signal which are ultimately responsible for the increase in synaptic functionality (MacDermott et al., 1986). On the contrary, a low frequency stimulation of the postsynaptic terminal does not cause the depolarization of the post-synaptic cell and then the passage of Ca^{2+} through the NMDAR is very reduced. This stimulus induces in the neurone a series of metabolic adaptations targeted to reduce the functionality of the synapses.

A fundamental characteristic of the synaptic plasticity phenomena mediated by NMDAR is that they are synapses-specific. In vitro experiments have shown that it is possible to induce LTP in a specific synapses without causing alterations in the synapses

adjacent. However, it has been demonstrated that the intradendritic diffusion of active form of Ras from an activated synapse to the adjacent ones, is able to favor the induction of LTP (Harvey et al., 2008).

Recent studies suggest that the synchronization of the pre- and postsynapsis can generate an potential of action that propagates to the terminals presynaptic, causing a further release of neurotransmitter and then a further depolarization of postsynapsis. If the activation of presynapsis is repeatedly evoked before (5ms) the depolarization of the postsynaptic neuron ("pre-post"), LTP is induced. On the contrary, when the depolarization of the postsynapsis precedes repeatedly the activation of the presynapsis, LTD is induced. For this mechanism of induction of plasticity, the time profiles of activation of the synaptic compartments are therefore fundamental (Dan and Poo, 2006; Caporale and Dan, 2008).

As previously mentioned, the flow of Ca^{2+} ions through the NMDAR is the main responsible of the LTP and LTD mediated by NMDAR. The increase in the concentration of synaptic Ca^{2+} activates the CaMKII, that in turn mediates the phosphorylation of several proteins including the AMPAR, increasing the conductance and translocation to the membrane (Malenka and Bear, 2004). The molecular mechanisms that regulate the induction of LTP however, prove to be very complex and involve other protein kinase as the PKA, PKC, tyrosine kinase and MAPK.

The ultrastructural alterations induced during the LTP involve new protein synthesis, which is promoted by the activation of protein kinase (PKA, CaMKIV, PKM-z, ERK), transcription factors (CREB, BDNF) and "immediate early gene" (ARC) (Sacktor, 2008). Many of the described effects have also been observed in the GABAergic inhibitory synapses, suggesting that the NMDAR receptors are involved in the long term modulation of both excitatory and inhibitory neurotransmission in the CNS (Castillo et al., 2011).

Chapter 3. Results and discussion

3.1 Development of novel 2,3-benzodiazepines as noncompetitive AMPAR antagonists

3.1.1 Synthesis of compounds 3a-c

The synthesis of compounds **3a-3c** is showed in Scheme 1. The synthesis was performed starting from the 2-(3,4-dihydroxyphenyl)acetic acid **7**, commercially available, which has been initially converted to the methyl ester **8**. Compound **8** reacted then with 1,2-dibromopropane, in the presence of potassium carbonate, to afford compound **9**. Ketoesters **10a-10c** have been prepared by a Friedel-Crafts acylation of the derivative **9** with the appropriate *p*-nitrobenzoic acid in the presence of phosphorous pentoxide. The subsequent treatment of **10a-10c** with hydrazine gave the 2,3-benzodiazepine **11a-11c,** which have been converted into the corresponding amino derivatives **3a-3c** by reduction at the nitro group with Raney-Ni/ammonium formate.

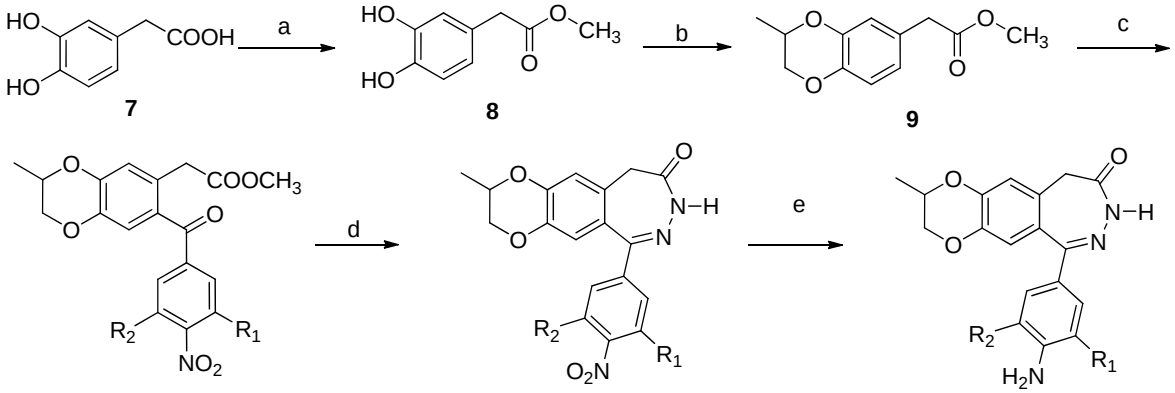

10a R_1,R_2=H
10b R_1=CH_3,R_2=H
10c R_1R_2=CH_3

11a R_1,R_2=H
11b R_1=CH_3,R_2=H
11c R_1R_2=CH_3

3a R_1,R_2=H
3b R_1=CH_3,R_2=H
3c R_1R_2=CH_3

Scheme 1: a) MeOH, HCl, r.t. 12h; b) 1,2-dibromopropane, K_2CO_3, acetone, Δ, 42h; c) ArCOOH, P_2O_5, CH_2Cl_2, r.t. 16h; d) NH_2NH_2 H_2O, n-butanol, Δ, 20h; e) Ni-Raney, $HCOONH_4$, EtOH, Δ, 2h.

3.1.2 Synthesis of compounds 4a-4c and 5a-5c

The synthetic procedure to achieve compounds **4a-4c** and **5a-5c** is showed in Schemes 2-4. The synthesis was performed starting from the intermediate **8** which was made to reacted with 1,2-dibromoethane, in the presence of potassium carbonate, to afford compound **12**. Compounds **13a-13c** have been synthesized, as above described for derivatives **10**, through the acylation of compound **12** with the appropriate *p*-nitrobenzoic acid. The subsequent treatment of derivatives **13a-13c** with hydrazine afford the 2,3-benzodiazepin-4-one **14a-14c** (Scheme 2).

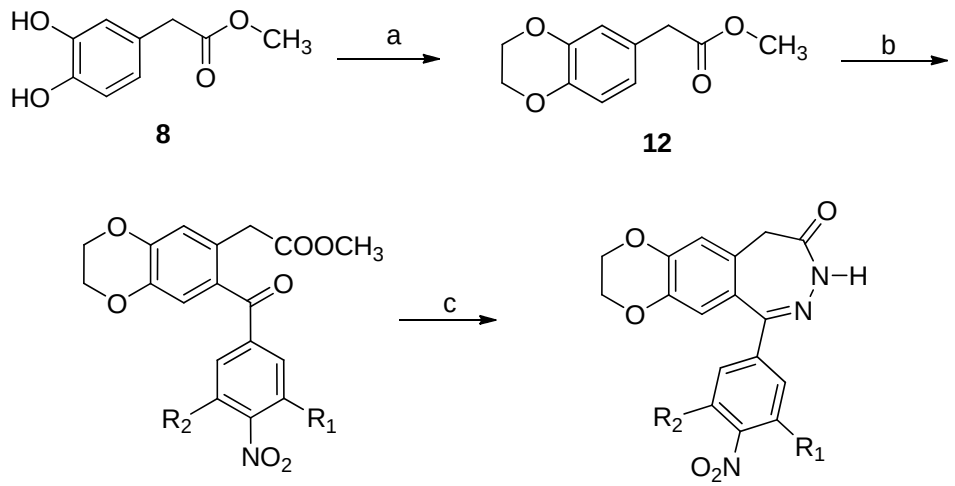

Scheme 2. a) $BrCH_2CH_2Br$, K_2CO_3, acetone, Δ, 42h; b) ArCOOH, P_2O_5, CH_2Cl_2, r.t. 16h; c) $NH_2NH_2\,H_2O$, ethanol, Δ, 20h;

To achieve the synthesis of compounds **4a-4c**, in which the 3-bromoisoxazoline nucleus is directly bound to the N3 of the 2,3-benzodiazepine, the intermediates **14a-14c** were treated with vinyl bromide in the presence of K_2CO_3 as base, CuI as catalyst and

N,N′-dimethylethylenediamine (DMEDA) as a ligand. The resulting mixture was heated in a microwave reactor at 100°C for 3 h to afford the corresponding products of *N*-alkylation **15a-15c**. The nucleus 3-bromo-isoxazoline was built *via* 1,3-dipolar cycloaddition between dipolarophiles **15a-15c** and bromonitrile oxide, generated *in situ* by dehydrohalogenation of the stable precursor dibromoformaldoxime (DBF) to affords compounds **16a-16c**. Finally, the reduction of the nitro group gave the desired amino derivatives **4a-4c** in good yields (Scheme 3).

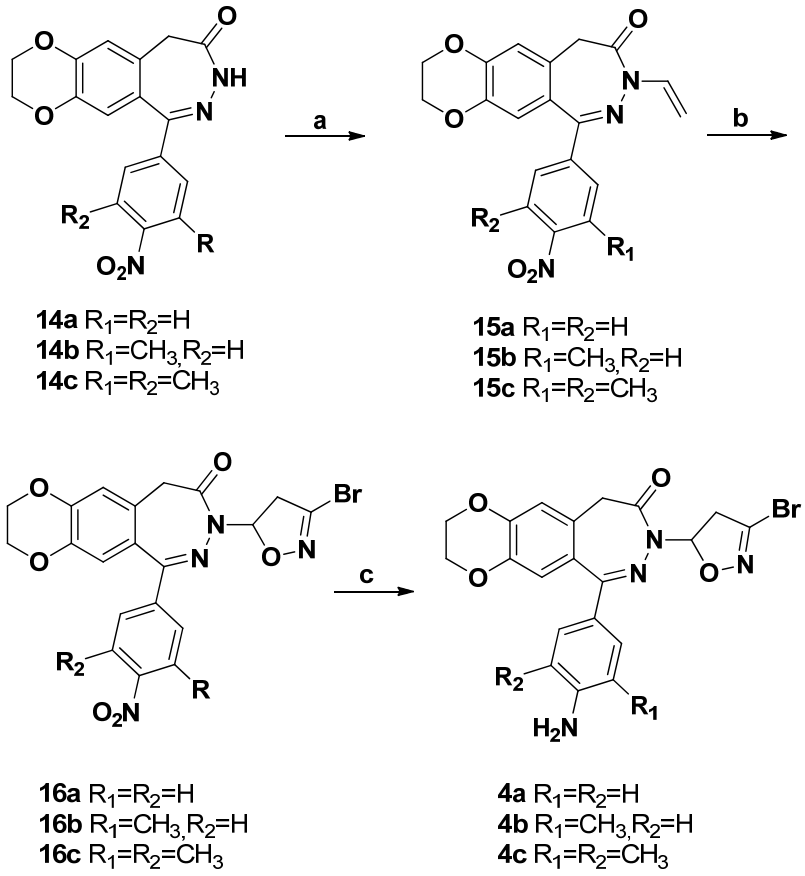

Scheme 3. a) Vinyl bromide, CuI, K_2CO_3 DMF, MW, 3h; b) DBF, $NaHCO_3$, EtOAc, r.t. 72h c) AcOH, Zn, 1h, 0°C-rt.

With a similar approach, derivatives **5a-5c**, in which the 3-bromo isoxazoline heterocycle is linked to N3 by means of a methylene spacer, were synthesized. 2,3-

Benzodiazepines **14a-14c** were N-alkylated with allyl bromide, in the presence of NaH, to give the intermediate on which the 3-bromo-isoxazoline nucleus was built *via* 1,3-dipolar cycloaddition. To obtain the 4'-amino derivatives, a reduction with Zn powder and acetic acid has been performed, which gave the final compounds **5a-5c** in good yields.

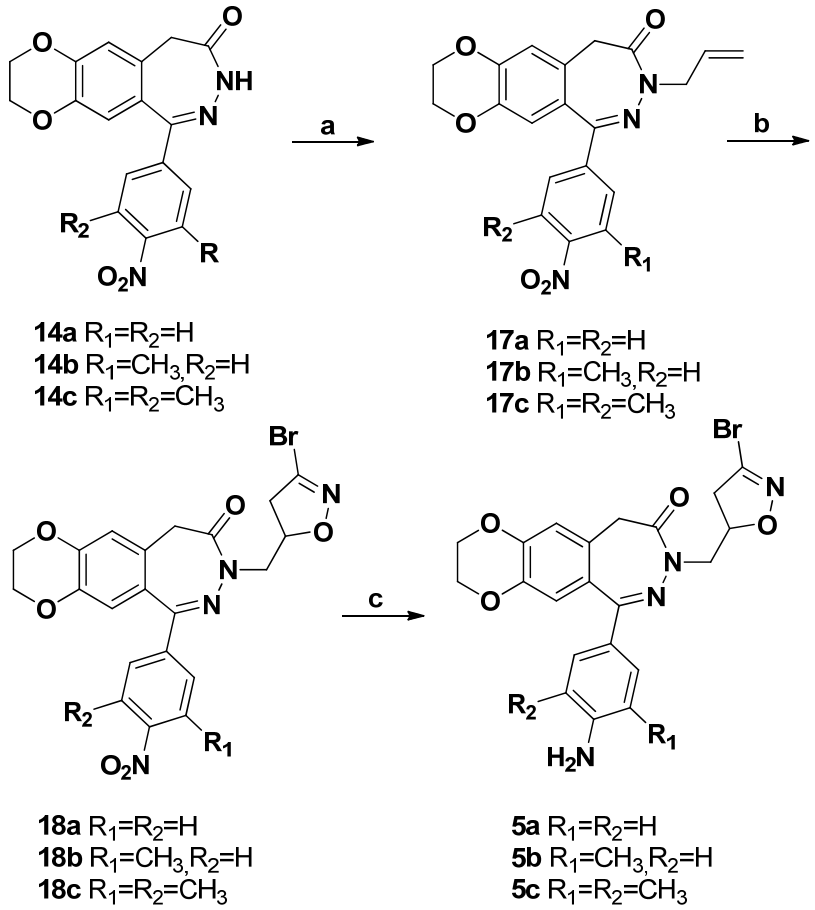

Scheme 4. a) allyl bromide, NaH, DMF, 0°C-rt; b) DBF, $NaHCO_3$, EtOAc, r.t. 72h c) AcOH, Zn, 1h, 0°C-rt.

3.1.3 Inhibition of the glutamate-evoked current of AMPA receptors

The synthesized compounds **3a-3c**, **4a-4c** and **5a-5c** have been characterized for their antagonistic effects against homomeric $GluA2Q_{flip}$ receptors, transiently expressed in human embryonic kidney HEK-293 cells. Using whole-cell recording, we measured the glutamate-evoked current amplitude in the absence (control or *A*) and presence of a compound (A_I); a pair of representative whole-cell current response is shown in Figure 10. Specifically, a saturating glutamate concentration (i.e. 3 mM glutamate) was used to measure the potency of a compound for the open form of the channel, since essentially all the channels (~96%) would be in the open state at this concentration. In contrast, a low glutamate concentration (0.1 mM) was used to measure the potency of the compound for the closed-channel form. At a low glutamate concentration, the majority of the receptors would be in the closed-channel state (Wu, et al., 2014). The ratio of the whole-cell current amplitude in the absence and presence of an inhibitor (i.e. A/A_I) as a function of inhibitor concentration is reported in Table 1. As in can be seen from the graphic in Figure 11, compounds **5a** and **5c** showed a higher affinity towards the closed state of the $GluA2Q_{flip}$ receptor channel, in agreement with Balannik studies (Balannik et al., 2005). It should be noted that compound **4a** is a strong inhibitor, judged by the A/A_I value, although the *t*-test showed p=0.051 for the inhibition of the closed- and the open-channel state.

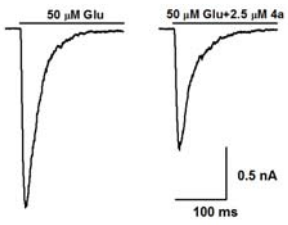

Figure 10. A pair of representative whole-cell traces obtained in 2.5 μM **4a** assay on the closed conformation of GluK2 channel.

Table 1. Activity of compounds **3b-3c, 4a-4c** and **5a-5c** on homomeric receptors GluA2

Compound	Conc. (μM)	Receptor State	A/A_I
3b	20	Closed	1.36±0.01
		Open	
3c	20	Closed	1.45±0.02
		Open	
4a	2.5	Closed	1.75±0.41
		Open	1.18±0.18
4b	1	Closed	1.01±0.06
		Open	1.16±0.19
4c	1	Closed	1.21±.012
		Open	1.24±0.08
5a	1	Closed	1.44±0.15
		Open	1.09±0.10
5b	10	Closed	1.23±0.15
		Open	1.20±0.12
5c	2.5	Closed	1.46±0.25
		Open	0.95±0.04

The closed- and the open-channel conformations were determined at the 0.1 mM and 3 mM Glu concentrations, respectively (Wu, et al., 2014).

Next, we measured A/A_I values at different inhibitor concentrations and two different glutamate concentrations. Using these values, we estimated K_I for both the closed- and the open-channel states for an AMPA receptor. As seen in the table 1, almost all compounds showed a ratio $A/A_I > 1$, with the most active compounds being represented by the 2,3-benzodiazepines **4a**, **5a** and **5c**. Among them, **5a** and **5c** showed a higher potency for the closed-channel than the open-channel state of AMPA receptors.

Thus, considering as selection criteria the ratio $A/A_I > 1$ and appropriate physico-chemical parameters (e.g. sufficient water solubility), which allowed us to perform assays

using high concentrations of these compounds, we selected compounds **4a**, **5b** and **5c** for further characterization.

An analysis of the calculated inhibition constants reported in Table 2 put in evidence that, with exception of compound **5b**, the introduction of the 3-bromoisoxazolin-5-yl substituent at the *N*-3 position of the 2,3-benzodiazepine nucleus gave an overall increase of binding affinity towards $GluA2Q_{flip}$ homomeric channels.

Furthermore, the obtained data clearly confirmed an increased affinity for the closed-channel state of GluA2 receptor, with the most selective compound being represented by compound **5c**, which did not inhibit at all the open-channel state.

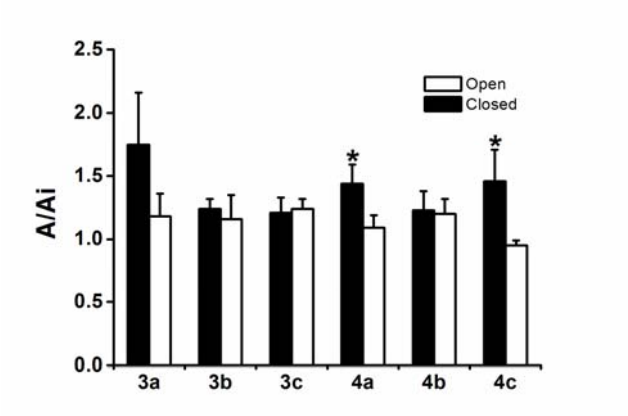

Figure 11. Inhibition assays of compounds **4a-c** and **5a-c** on $GluA2Q_{flip}$ AMPAR. Error bars represent standard deviation from mean. The concentration tested was 2.5 μM for **4a** and **5c**, 1 μM for **5a**, **4b** and **4c** and 10 μM for **5b**. $A/A_I = 1$ represents no inhibition (see Experimental Section). The *t*-test was used for the comparison between the A/A_I values obtained in closed and open channel states. $*p \leq 0.05$.

Thus, compound **5c** was additionally characterized for its effect on the GluA1, GluA3 or GluA4 homomeric channels (Table 3). Statistical analysis (see legend in Figure 12) showed that only the A/A_I value of $GluA2Q_{flip}$ for the closed state is significantly different from one (one being no inhibition). For the open state, GluA1, 3, and 4 AMPARs

exhibited significant inhibition while GluA2 did not. Compound **5c** also showed a significantly higher inhibition on GluA1 than GluA3 (but not GluA4).

Table 2. Inhibition constants for the closed-channel and open-channel conformation of $GluA2Q_{flip}$ homomeric channels by the three selected compounds.

Compound	Receptor State	K_I (μM)
4a	Closed	3±1
	Open	14±6
5b	Closed	50±21
	Open	50±15
5c	Closed	5±1
	Open	No inhibition
2a[a]	Closed	21±1
	Open	33±1
2b[a]	Closed	4±1
	Open	9± 1
2c[a]	Closed	94±15
	Open	164±8
GYKI 52466[a]	Closed	4±1
	Open	5±1

[a]From Qneibi et al, 2012.

Table 3. Activity of compound **5c** on homomeric receptors GluA1, GluA3 and GluA4

Comp.	Receptor	Receptor State	A/A_I	K_I
5c	GluA1[a]	Closed	1.19±0.13	13.2±0.2
		Open	1.39±0.08	6.4±0.1
	GluA3[b]	Closed	1.09±0.19	27. 8±0.9
		Open	1.18±0.10	13.9±0.1
	GluA4[b]	Closed	1.34±0.13	7.4±0.1
		Open	1.22±0.07	11.4±0.1

[a]For GluA1 assay, the K_I value for the closed-channel conformation was tested at 40-50 μM glutamate concentration. For the open-channel value, we used 2 mM (Wu, et al., 2014).

[b]For GluA3 and GluA4 receptor assays, the corresponding K_I value for the closed-channel conformation was determined at 100 μM glutamate. For the K_I value for the open-channel conformation, we used a saturating glutamate concentration (i.e., 3 mM) (Wu, et al., 2014).

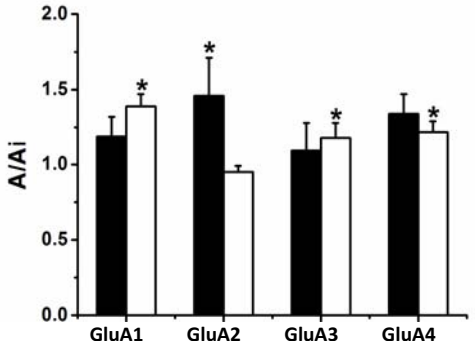

Figure 12. A/A_I values of compound **4c** on different AMPAR. Error bars represent the standard deviation from the mean. Hollow column represents open-channel state and the solid column represents the closed-channel state. A/A_I = 1 represents no inhibition (see Experimental Section).). One-way ANOVA followed by Tukey's HSD tests were used for multiple comparison (closed state: $F_{4,10} = 5.217$, $p = 0.017$, HSD = 0.381; open state: $F_{4,10} = 21.631$, p = 6.5E-5, HSD = 0.177). *$p \leq 0.05$

In conclusion, in the present study (Espahbodinia et al., 2017), I designed and synthesized a series of novel *N*-3-bromoisoxazolin-5-yl substituted 2,3-benzodiazepines as noncompetitive AMPAR antagonists, with the idea that this flexible heterocycle could establish interactions with an additional binding pocket of the receptor, like the thiadiazole nucleus of GYKI 47409 does. Although some *N*-3-substituted 2,3-benzodiazepines have been previously reported, this is our initial attempt to couple a heterocycle (i.e., a 3-bromoisoxazoline ring) to the *N*-3 position. Within this investigation, we identified some interesting new molecules, and among these, the 2,3-benzodiazepine **5c** showed antagonist properties against the homomeric AMPARs GluA1, GluA2Q, GluA3 and GluA4. Compound **5c** has also shown a slightly higher potency against GluA2Q, whose abnormal expression and activation mediates Ca^{2+}-induced toxicity and neurodegeneration in several neurological disorders, such as ischemic injury or ALS (Weiss, 2011). Coupling a 3-bromoisoxazoline moiety with a methylene linker to the 2,3-benzodiazepin-4-one scaffold, the potency of the resulting compounds has improved. As compared with the unsubstituted compound, i.e. **2a**, which has a K_I value of 21 μM and 33 μM for the closed-channel and the open-channel conformations, respectively (Qneibi et al., 2012), compound **5c** has shown a K_I of 5 μM for the closed-channel conformation, while it does not inhibit the open-channel form, and it is even more potent than the strictly-related analog **2c**, which shows K_I values of 94 μM and 164 μM for the closed-channel and the open-channel conformation, respectively (Wang et al., 2015). Thus, these results clearly show that the *N*-3 coupling of a 3-bromoisoxazoline ring to the 1-(4-aminophenyl)-3,5-dihydro-7,8-ethylenedioxy-4*H*-2,3-benzodiazepin-4-one scaffold is desirable in making more potent AMPAR antagonists, presumably binding to the same noncompetitive site (Wang et al., 2015). Future efforts will be devoted to further modify the isoxazoline ring in order to generate new analogs with higher potency and selectivity towards AMPARs.

3.2 Evaluation of compound 2c on leukemia Jurkat T cell growth, cell cycle and apoptosis

Several researches focused on the ability of glutamate antagonists to limit the growth of different human cancers (Rzeski et al., 2001). Recently, Stepulak et al. (2011) has shown that the AMPA antagonist GYKI 52466 reduced the viability of laryngeal cancer cell lines. In the present study, we identify one over seven tested 2,3-benzodiazepine-4-ones non-competitive AMPA antagonists compounds, able to markedly inhibit, the cell viability (< 75%) of different cancerous cell lines, and in particular the growth of human leukemia Jurkat T cells (Parenti et al., 2016).

Indeed all the tested compounds were essentially inactive at 10^{-5} M concentration. Instead, compound **2c** obtained a remarkable inhibition of cell viability and growth, reaching a GI_{50} value in the micromolar range. This result together with the finding that the human leukemia Jurkat T cells possess the GluA2–4, AMPA receptor subunits (Stepulak, 2009) led us to adopt this cellular model in order to understand the possible molecular mechanism exerted by **2c** compound.

Table 4 showed that compound **2c** was able to reduce the growth of the leukemia Jurkat T cells in a dose and time dependent manner. In particular the inhibition of cell growth was present already detectable after 24 h of incubation, with a GI_{50} of 3.5 ± 0.61 μM, and increased over time with the lasting of incubation time reaching a GI_{50} of 2.2 ± 0.46 μM at 72 h of incubation. However, the treatment of leukemia Jurkat T cells with compound **2c** for 72 h did not change significantly the GI_{50}, when compared to that one obtained after 48 h of incubation. Interesting the extent of cell growth inhibition was similar higher to those obtained with 5-fluoruracil (5-FU) used as reference drug. Once the compound was removed, the cells restart to proliferate, suggest that the molecule might act mainly on cell cycle modulation rather than through direct induction of cytotoxicity.

Table 4. Effect of compounds **2c** and 5-FU on the Growth of leukemia Jurkat T cells.

	2c (μM)			**5-FU (μM)**		
	GI_{50}	**TGI**	**LC_{50}**	**GI_{50}**	**TGI**	**LC_{50}**
24 h	3.5 ± 0.61	5.1 ± 0.25	> 100	1.8 ± 0.41	> 100	> 100
48 h	2.2 ± 0.31	3.7 ± 0.42	> 100	4.3 ± 0.28	11 ± 0.38	> 100
72 h	2.2 ± 0.46	6.4 ± 0.53	> 100	4.7 ± 0.22	10.3 ± 0.42	> 100

Human leukemia Jurkat T cells were cultured at three different time points (24, 48, 72 h) and treated with different concentrations of **2c** or 5-FU. The respective $GI_{50,}$ TGI and LC_{50} values were calculated as described in the Materials and Methods section. The data shown represent the mean of 4 independent experiments done in quintuplicate.

However, it must be underlined that this was the case at GI_{50} concentration used, while at TGI concentration the cells did not proliferate even after 72 h of recovery time.

Interestingly, data obtained from cell cycle analysis indicated that **2c** was able to accumulate the treated cell in the G_2/M phase, and in parallel to reduce the G_0/G_1 phase in a time-dependent manner. In particular, already after 12 h of incubation time we assisted at a maximal arrest in G_2/M, which lasted over time. It is well known that CDK1/Cyclin B1 complex is involved in the G_2/M phase checkpoint by regulating the process of M phase (Smits et al, 2001). An intricate balance maintains the activity of the complex, where the inhibiting kinases Myt-1- and Wee-1 play a pivotal role.

Table 5. Effect of different concentration of compound **2c** on leukemia Jurkat T cells cell cycle distribution at different time point.

	12 h			24 h		
	% G_0/G_1	**% S**	**% G_2/M**	**% G_0/G_1**	**% S**	**% G_2/M**
Control	61.3 ± 6.5	18.7 ± 5.1	6.67 ± 3.67	62.5 ± 1.9	16.7 ± 2.3	16,5 ± 1,5
1.5 µM 2c	51.9 ± 6.5	11.2 ± 1.2	13.9 ± 2.0*	54.2 ± 8.4	13.6 ± 3.4	24.7 ± 0.8**
2.5 µM 2c	14.2 ± 4.6***	10.4 ± 0.8*	73.24 ± 4.6***	17.8 ± 0.2***	3.9 ± 0.5***	70.5 ± 1.6***
5 µM 2c	4.08 ± 1.1***	5.5 ± 0.8***	81,5 ± 4.3***	6 ± 0.5***	6.8 ± 1.8***	78.5 ± 5***

Leukemia Jurkat T cells were incubated with different concentrations of compound **2c** a two different time points as indicated and the cell cycle phase distribution was assessed by flow cytometry. The values are mean ± SD of two independent experiments with three determination each. * $p < 0.05$, ** $p < 0.01$ and *** $p < 0.001$ compared to the corresponding control (unpaired *t*-test).

The results of immunoblot analysis (Figure 13) pointed out that **2c** was capable to alter the complex CyclinB1/Cdc2 by increasing significantly Cyclin B1 and *p*-Cdc2$^{(Tyr15)}$ levels through the induction of Myt-1 and not presumably by *p*-Wee-1$^{(Ser642)}$, whose level increased only very modestly, in particular after 12 and 18 h of incubation time. In addition, since we were unable to detect p21 protein in both control and treated samples, as logical consequence we could state that the arrest of the G_2/M transition occurred independently from p21 expression, at least in our system.

To get more insights on cell death in leukemia Jurkat T cells, the expression and activity of apoptosis-related proteins such as Bcl-2, Bcl-xl, p53, were evaluated using 2.5 and 5 µM concentrations of the compound at different time points. As shown in Figure 14A, the protein expression of Bcl-2 and Bcl-xl were markedly down-regulated by the compound **2c** in a dose and time dependent manner, reaching the maximal effect after 24 h

of incubation with 5 μM concentration of **2c** (Figure 14B). In particular, while the inhibition of Bcl-2 protein expression is sustained at 18 and 24 h of treatment at the higher concentration tested, the immunoreactivity of Bcl-xl began to decline already at the former time point at 5 μM **2c** exposure. In addition after 24 h of incubation time both the concentrations tested were able to decrease the expression of Bcl-xl.

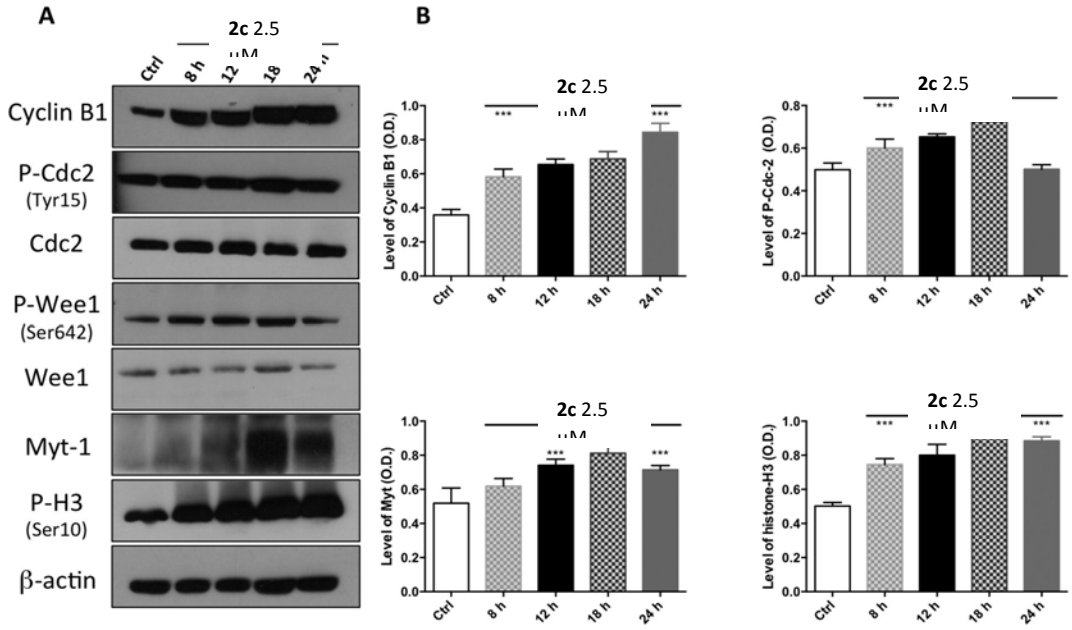

Figure 13. **2c** *modulated G_2/M phase checkpoint protein expression in leukemia Jurkat T cells.* (A) Representative western blots at different time points of human Jurkat T cells treated with 2.5 μM of ***1 g***. (B) Densitometric analyses of protein levels of Cyclin B1, phpspho-Cdc2, Myt-1 and phpspho-histone-*H*3 of Jurkat T whole cell lysate after incubation with 2.5 μM of ***1 g***. Densitometry values were normalized to the protein loading control beta-actin. The values are expressed as the mean ± SD of three independent experiments ($n = 3$ per group). ** $p < 0.01$ and *** $p < 0.001$ vs untreated cells (Ctrl), using One-way ANOVA with Dunnett's as post test.

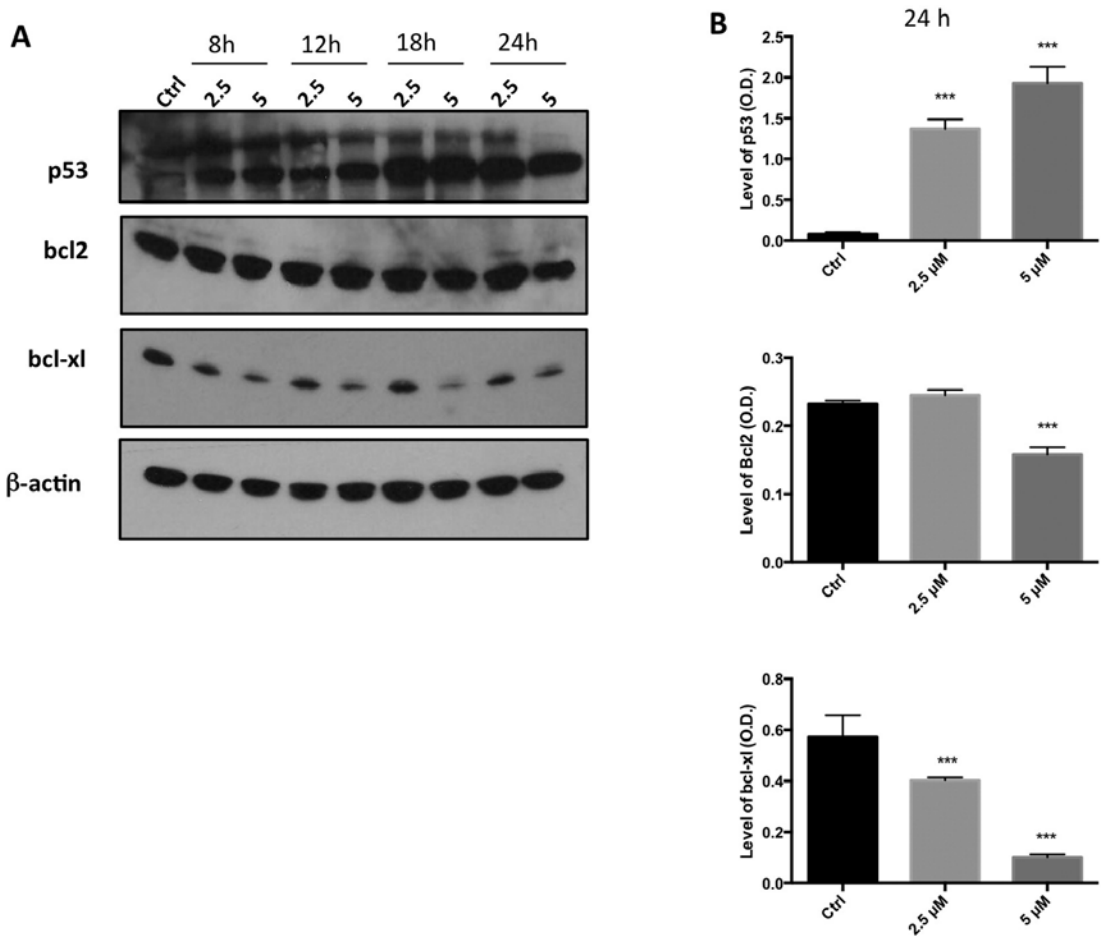

Figure 14. *Effect of* ***2c*** *on p53*, *bcl2*, *bcl-xl protein expression in leukemia Jurkat T cells.* (A) Representative western blots at different time points and (B) densitometric analyses of protein levels of p53, bcl2 and bcl-xl of Jurkat T cell lysate after incubation with 2.5 and 5 µM of ***2c*** for 24 h. Densitometry values were normalized to the protein loading control, beta-actin or lamin B1 as far as regarded p53 protein. The values are expressed as the mean ± SD of three independent experiments ($n = 4$ per group). *** $p < 0.001$ vs untreated cells (Ctrl), using One-way ANOVA with Dunnett's as post test.

Moreover, leukemia Jurkat T cells treated with compound **2c** at 2.5 and 5 µM concentrations for 24 and 48 h, exhibited a significant increase in peptide cleavage activity compared to the untreated cells. In particular the activity elicited by a 2.5 µM concentration of **2c**, already detectable at 24 h, significantly increased ($p < 0.05$) at 48 h (Figure 15), confirming the previous results. The most interesting results were obtained

with the highest concentration used; indeed after 24 h of incubation we assisted to a dramatic increase af caspase-3 activity, which decreased after 48 h of incubation although it remained significantly greater in comparison with untreated cells. We surmise that the observed cleavage of DEVD was mostly due to the activation of caspase-3 pathway, since pre-treating the Jurkat T cells with the pan-caspase inhibitor *Z*-VAD-FMK showed a complete block of this effect (Figure 15).

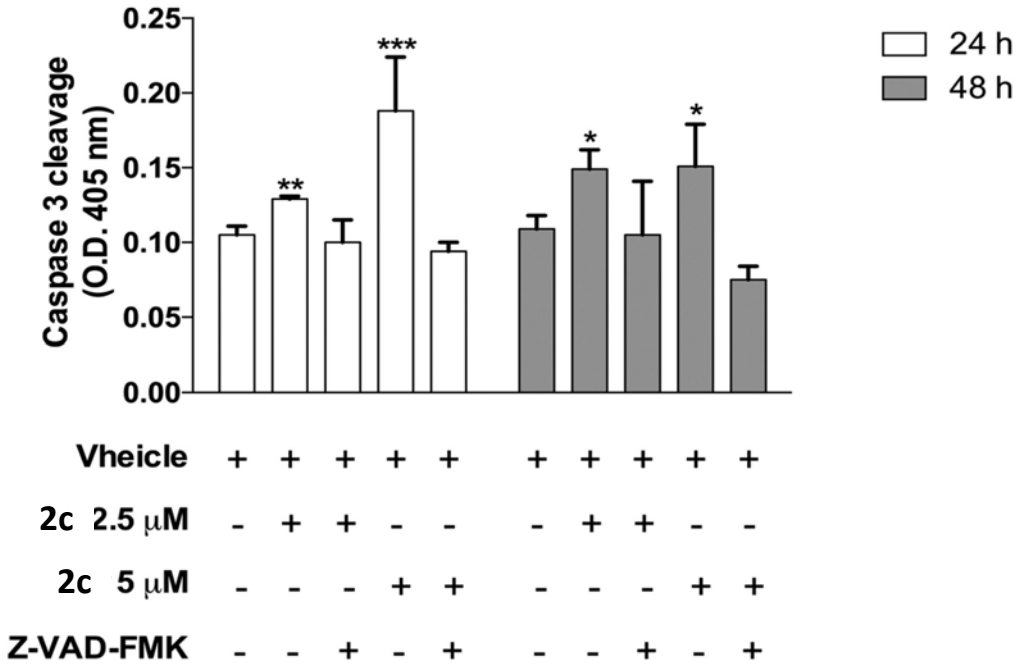

Figure 15. *Measurement of caspase-3 activity in* ***2c*** *treated leukemia Jurkat T cell line.* Leukemia Jurkat T cells were treated with 2.5 or 5 μM of **2c**, in presence or not of *Z*-VAD-FMK inhibitor, or vehicle alone either for 24 and 48 h. Data represent the mean ± SD of three independent experiments carried out in quadruplicate. * $p < 0.05$, ** $p < 0.01$ and ***$p < 0.001$ vs. control cells exposed to vehicle only. One-way ANOVA and Dunnett's as post test.

The molecule also induced apoptosis through the enhanced expression of the pro-apoptotic p53, and the inhibition of Bcl-2, and Bcl-xl, followed by the activation of caspase-3 (for details see Parenti et al. 2016).

Overall, the results obtained suggested that compound **2c** might act mostly as a cytostatic rather than cytotoxic compound. Although further studies are necessary, in order to identify others specific pathways involved in the activity of the compound **2c**, the presented results identified a novel molecule acting on specific G_2/M checkpoint regulation pathway that might be a good molecule for future development in the cancer research.

3.3 Development of subtype-specific agonists for NMDA receptor glycine binding sites

3.3.1 Synthesis of L-cysteine derivatives 6b-h and evaluation of their agonist properties

Compounds **6b-6h** were synthesized from Boc-protected L-cysteine (**19**) by deprotonation with C_2H_5ONa, alkylation with the respective alkyl halides, followed by Boc-deprotection under acidic conditions of the obtained intermediates **20b-20h**, as depicted in Scheme 5.

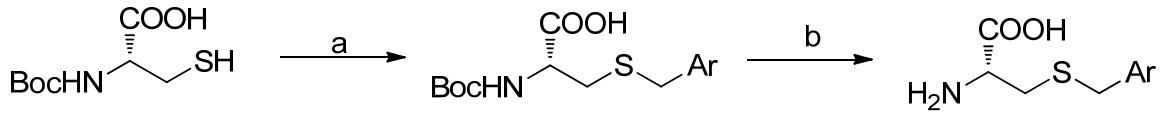

19 **20b-20h** **6b-6h**

Comp.	Ar	Comp.	Ar
b	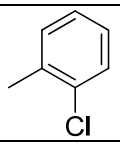	**f**	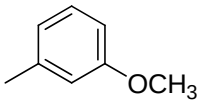
c	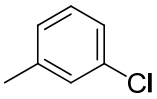	**g**	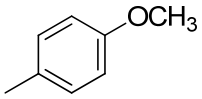
d	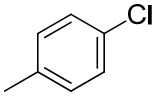	**h**	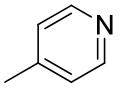
e	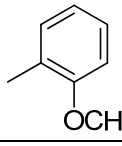		

Scheme 5. a) C_2H_5ONa, $ArCH_2Br$, dry EtOH, 1h rt, then 4-12 h 80°C. b) 2M HCl,Et_2O, overnight.

The synthesized compounds **6b-6h** were characterized by two-electrode voltage-clamp (TEVC) electrophysiology using *Xenopus* oocytes expressing recombinant NMDA receptor subtypes. We generated concentration–response data for the compounds in the continuous presence of a saturating concentration of Glu (100–300 μM) at the four GluN1/GluN2A-D NMDA receptor subtypes.

As reported in Table 6, none of the synthesized compounds show agonist activity at NMDA receptor subtype GluN1/GluN2A and GluN1/GluN2B, whereas show weak partial agonist properties at GluN1/GluN2C and GluN1/GluN2D (max 30% of the response elicited by glycine).

Table 6. Agonist potencies of compounds **6a-6h** at recombinant GluN1/GluN2A-D receptors measured using TEVC electro-physiology.[a]

	R_{max} %			
	GluN1/GluN2A	GluN1/GluN2B	GluN1/GluN2C	GluN1/GluN2D
6a	NR	NR	169	NR
6b	NR	NR	21	18
6c	NR	NR	23	32
6d	NR	NR	29	11
6e	NR	NR	11.6	6.7
6f	NR	NR	7	10
6g	NR	NR	23	15
6h	NR	NR	8	21

[a] The relative maximal currents (R_{max}) are the maximal responses to the indicated agonists obtained by fitting the full concentration-response data normalized to the maximal response activated by glycine in the same recording. NR indicates responses <5 % at 300 μM of the compound

Chapter 4. Experimental section

4.1 Chemistry

All reagents and solvents were obtained from commercial suppliers and were used without further purification. Reactions under microwave irradiation were performed on a CEM Discover apparatus. Elemental analyses were carried out on a C. Erba Model 1106 (Elemental Analyzer for C, H and N) and the obtained results are within ±0.4% of the theoretical values. Merck Silica Gel 60 F_{254} plates were used as analytical TLC; flash column chromatography was performed on Merck Silica Gel (200–400 mesh). ^{1}H and ^{13}C NMR spectra were recorded on Varian Gemini 300 MHz or 400 MHz Bruker Avance III or 600 MHz Bruker Avance III spectrometers, as reported below, using the residual signal of the deuterated solvent as internal standard. Splitting patterns are described as singlet (s), doublet (d), doublet of doublet (dd), triplet (t), quartet (q), multiplet (m) and broad singlet (bs). ^{1}H chemical shifts are expressed in δ (ppm) and coupling constants (J) in hertz (Hz).

4.1.1. Synthesis of 2,3-benzodiazepine derivatives 3-5

Methyl 2-(3,4-dihydroxyphenyl)acetate (8)

To a solution of 2-(3,4-dihydroxyphenyl)acetic acid **7** (2 g, 12 mmol) in MeOH (50 mL), at room temperature, HCl was added and the reaction mixture was stirred for 24 h. Solvent was removed under reduced pressure, the residue was diluted with H_2O and was neutralized till pH=7.Then the organic layer was extract with ethyl acetate (2 x 150 mL) and dried over Na_2SO_4. The solvent was removed under reduced pressure and the residue was purified by column chromatography using dichloromethane/MeOH (9:1) as eluent to

afford compound **8**. Yield=1,4 g, 69%; R_f = 0.60 (dichloromethane/MeOH 9:1); ^{1}H-NMR (300 MHz, $CDCl_3$): δ = 3.47 (s, 2H), 3.64 (s, 3H), 6.60 (d, *J*=8.1 Hz, 1H), 6.71-6.79 (m, 2H), 6.96 (bs, 2H).

(3-Methyl-2,3-dihydro-benzo[1,4]dioxin-6-yl)-acetic acid methyl ester (9)

To a solution of compound **8** (3 g, 16 mmol) in acetone (100 mL) was added potassium carbonate (11.05 g, 80 mmol) and 1,2-dibromopropane (16.15 g, 80 mmol). The reaction mixture was stirred for 96 hours at 56 °C. Solvent was removed under reduced pressure, the residue was diluted with H_2O and then the organic layer was extracted with ethyl acetate (3 x 150 mL) and dried over Na_2SO_4. The solvent was removed under reduced pressure and the residue was purified by column chromatography using petroleum ether/ethyl acetate (8:2) as eluent to give compound **9**. (200 mg, 5.6%); R_f = 0.57 (petroleum ether/ethyl acetate 8:2); ^{1}H NMR (300 MHz, $CDCl_3$): δ = 1.37 (d, *J*=6.4 Hz, 3H), 3.53 (s, 2H), 3.70 (s, 3H), 3.83 (m, 1H), 4.16-4.35 (m, 2H), 6.71-6.78 (m, 1H), 6.79-6.86 (dd, *J*=8.1, 2.8 Hz, 2H).

[3-Methyl-7-(4-nitrobenzoyl)-2,3-dihydro-benzo[1,4]dioxin-6-yl]-acetic acid methyl ester (10a)

4-nitrobenzoic acid (48.5 mg, 0.29 mmol) and phosphorus pentoxide (218.6 mg, 1.54 mmol) were added to a stirred solution of compound **9** (50 mg, 0.22 mmol) in dichloromethane (50 mL). The mixture was stirred overnight at room temperature, then it was diluted with H_2O and the organic layer was extract with chloroform (2 x 50 mL). The organic layer was treated with 10% NaOH, then it was washed with brine and finally it was dried over Na_2SO_4. The solvent was removed under reduced pressure and the residue was

purified by column chromatography using petroleum ether/ethyl acetate (8:2) as eluent. Yield =70 mg, 85.6%;^{1}H NMR (300 MHz, $CDCl_3$): δ = 1.37-1.43 (m, 3H), 3.64 (s, 3H), 3.89 (s, 2H), 4.11 (dd, *J*=13.2, 6.1 Hz, 1H), 4.17-4.43 (m, 2H), 6.56 (s, 1H), 6.98 (d, *J*=2.4 Hz, 1H), 7.90-7.96 (m, 2H), 8.00-8.29 (m, 2H).

[3-Methyl-7-(3-methyl-4-nitrobenzoyl)-2,3-dihydro-benzo[1,4]dioxin-6-yl]-acetic acid methyl ester (10b)

Compound **10b** has been synthesized, according to the synthetic procedure previously described, starting from compound **9** (50 mg, 0.22 mmol), phosphorus pentoxide (223 mg, 1.5 mmol) and 3-methyl-4-nitrobenzoic acid (52 mg, 0.29 mmol) Yield =70 mg, 77%; R_f= 0.37 (petroleum ether/ethyl acetate 8:2); ^{1}H NMR (300 MHz, $CDCl_3$): δ = 1.37-1.43 (m, 3H), 2.64 (s, 3H), 3.64 (s, 3H), 3.89 (s, 2H), 4.11 (dd, *J*=13.2, 6.1 Hz, 1H), 4.17-4.43 (m, 2H), 6.87 (d, *J*=3.4 Hz, 1H), 6.93 (d, *J*=2.4 Hz, 1H), 6.64-6.80 (m, 2H), 8.00 (d, *J*=8.3 Hz, 1H,).

[7-(3,5-Dimethyl-4-nitrobenzoyl)-3-methyl-2,3-dihydro-benzo[1,4]dioxin-6-yl]-acetic acid methyl ester (10c)

Compound **10c** has been synthesized, according to the synthetic procedure previously described, starting from compound **9** (50 mg, 0.22 mmol), phosphorus pentoxide (223 mg, 1.5 mmol) and 3,5-dimethyl-4-nitrobenzoic acid (57 mg, 0.29 mmol). Yield= 70 mg, 77%; R_f = 0.45 (petroleum ether/ethyl acetate 8:2); ^{1}H NMR (300 MHz, $CDCl_3$): δ = 1.39 (dd, *J*=9.9, 6.4 Hz, 3H,), 2.36 (s, 6H), 3.64 (s, 3H), 3.86 (d, *J*=2.6 Hz, 2H), 3,88-3.93 (m, 1H), 4.14-4.43 (m, 2H), 6.86 (d, *J*=3.3 Hz, 1H), 6.93 (d, *J*=3.1 Hz, 1H), 7.52 (s, 2H).

9H-2-Methyl-6-(4-nitrophenyl)-2,3,8,10-tetrahydro-1,4-dioxyn[2,3-h][2,3]benzodiazepin-9-one (11a)

Hydrazine hydrate (0.05 mL, 0.99 mmol) and HCl 6N (0.38 mL) were added to a solution of compound **10a** (70 mg, 0.20 mmol) in ethanol (100 mL) then the mixture was heated at reflux and stirred for 20 h. After cooling at room temperature, the formed precipitate was filtered and purified through an ethanol treatment. Yield=35 mg, 49.5%; ^{1}H NMR (300 MHz, $CDCl_3$): δ = 1.43 (d, *J*=6.4 Hz, 3H), 3.86 (m, 3H), 4.29 (m, 2H), 6.5 (s, 1H), 6.9 (d, *J*=2.4 Hz, 1H), 7.00 (s, 1H), 7.66-7.77 (m, 2H), 8.00 (m, 2H). ($C_{18}H_{15}N_3O_5$)

9H-2-Methyl-6-(3-methyl-4-nitrophenyl)-2,3,8,10-tetrahydro-1,4-dioxyn[2,3-h][2,3]benzodiazepin-9-one (11b)

Compound **11b** has been prepared, according to the procedure previously described, starting from compound **10b** (70 mg, 0.17 mmol), hydrazine hydrate (0.027 mL, 0.5 mmol) and HCl 6N (0.38 mL). Yield=35 mg, 51%; R_f = 0,64 (petroleum ether/ethyl acetate 8:2); ^{1}H NMR (300 MHz, $CDCl_3$): δ = 1.41 (d, *J*=6.4 Hz, 3H), 2.65 (s, 3H), 3.87 (t, 3H), 4.29 (m, 2H), 6.87 (d, *J*=3.6 Hz, 1H), 6.93 (d, *J*=2.4 Hz, 1H), 7.00 (s, 1H), 7.66-7.77 (m, 2H), 8.00 (d, *J*=8.3 Hz, 1H). ($C_{19}H_{17}N_3O_5$)

9H-2-Methyl-6-(3,5-dimethyl-4-nitrophenyl)-2,3,8,10-tetrahydro-1,4-dioxyn[2,3-h][2,3]benzodiazepin-9-one (11c)

Compound **11c** has been prepared, according to the procedure previously described, starting from compound **10c** (57 mg, 0.17 mmol), hydrazine hydrate (0.027 mL, 0.5 mmol) and HCl 6N (0.38 mL). Yield = 30 mg, 44%; R_f = 0.64 (petroleum ether/ethyl acetate 7:3);^{1}H NMR (300 MHz, $CDCl_3$): δ= 1.39 (dd, *J*=8.9, 6.4, Hz, 3H), 2.35 (s, 6H), 3.86 (m,

3H), 4.28 (m, 2H), 6.86 (d, *J*=3.4 Hz, 1H), 6.94 (d, *J*=3.1 Hz, 1H), 7.00 (s, 1H), 7.52 (s, 2H). ($C_{20}H_{19}N_3O_5$)

9H-6-(4-Aminophenyl)-2-methyl-2,3,8,10-tetrahydro-1,4-dioxyn[2,3-h][2,3]benzodiazepin-9-one (3a)

A suspension of nitroderivative **11a** (100 mg, 0.28 mmol) with Ni-Raney (60 mg) and ammonium formate (68 mg, 1 mmol) in EtOH (40 mL) was stirred under reflux for 2 h and then filtered through Celite. The organic layer was evaporated under reduced pressure and the residue, dissolved in $CHCl_3$, was washed with saturated NaCl to remove ammonium formate. The organic layer, dried over Na_2SO_4, was evaporated under reduced pressure and the residue was crystallized from acetone and petroleum ether. Yield= 40 mg, 44%; ^{1}H NMR (300 MHz, $CDCl_3$): δ = 1.41 (d, *J*=6.4 Hz, 3H), 3.73 (s, 2H), 3.90 (m, 1H), 4.04 (bs, 2H), 4.29 (m, 2H), 6.87 (m, 1H), 6.93 (d, *J*=2.4 Hz, 1H), 7.00 (s, 1H), 7.72 (m, 2H), 8.00 (m, 2H). ^{13}C NMR (75 MHz, $CDCl_3$): δ = 18.2, 45.0, 72.0, 76.8, 114.4, 114.7, 116.2, 122.8, 126.5, 129.3, 129.9, 145.5, 149.2, 151.0, 155.4, 172.8 Anal. ($C_{18}H_{17}N_3O_3$)

9H-6-(4-Amino-3-methylphenyl)-2-methyl-2,3,8,10-tetrahydro-1,4-dioxyn-[2,3-h][2,3]benzodiazepin-9-one (3b)

With the same procedure compound **3b** has been prepared starting from the nitroderivative **11b** (100 mg, 0.27 mmol), Ni-Raney (60 mg) and ammonium formate (68 mg, 1 mmol). Yield= 33 mg, 36%; R_f = 0,43 (petroleum ether/ethyl acetate 7:3); ^{1}H NMR (300 MHz, $CDCl_3$): δ = 1.41 (d, *J*=6.4 Hz, 3H), 2.20 (s, 3H), 3.73 (s, 2H), 3.90 (t, 1H), 4.04 (bs, 2H), 4.29 (m, 2H), 6.87 (d, *J*=3.6 Hz, 1H), 6.93 (d, *J*=2.4 Hz, 1H), 7.00 (s, 1H), 7.72 (m, 2H),

8.00 (d , *J*=8.3 Hz, 1H). ^{13}C NMR (75 MHz, $CDCl_3$): δ = 15.2, 18.3, 44.7, 71.8, 77.0, 114.3, 116.2, 122.7, 126.5, 127.2, 129.0, 129.5, 130.2, 144.7, 145.5, 148.2, 155.7, 173.1; Anal. ($C_{19}H_{19}N_3O_3$) C, H, N. calc.% C, 67.64; H, 5.68; N, 12.46; found. % , 67.82; H, 5.51; N, 12.76.

9H-6-(4-Amino-3,5-dimethylphenyl)-2-methyl-2,3,8,10-tetrahydro-1,4-dioxyn-[2,3-h][2,3]benzodiazepin-9-one (3c)

With the same procedure compound **3c** has been prepared starting from the nitroderivative **11c** (30 mg, 0.07 mmol), Ni-Raney (60 mg) and ammonium formate (19 mg, 0.3 mmol). Yield = 10 mg, 36%; R_f = 0.48 (petroleum ether/ethyl acetate 7:3); ^{1}H NMR (300 MHz, $CDCl_3$): *δ* = 1.39 (s, 3H), 2.20 (s, 6H), 3.73 (s, 2H), 4.04 (bs, 2H), 4.29 (d, *J*=10.7 Hz, 3H), 6.86 (d, *J*=3.0 Hz, 1H), 6.97 (d, *J*=3.9 Hz, 1H), 7.00 (s, 1H), 7.48 (s, 2H). ^{13}C NMR (75 MHz, $CDCl_3$): δ = 15.5, 18.4, 44.9, 71.9, 76.9, 114.5, 116.3, 122.8, 126.6, 127.0, 129.1, 129.4, 130.3, 144.6, 145.7, 148.3, 155.6, 173.0; Anal. ($C_{20}H_{21}N_3O_3$) C, H, N. calc.% C, 68.36; H, 6.02; N, 11.96; found. % , 69.85; H, 5.88; N, 12.27.

Methyl (3,4-ethylenedioxyphenyl)acetate (12)

To a solution of compound **8** (3 g, 16 mmol) in acetone (100 mL) was added potassium carbonate (11.05 g, 80 mmol) and 1,2-dibromoethane (16.15 g, 80 mmol), the reaction mixture was stirred then for 96 h at 56 °C. The solvent was removed *in vacuo,* the residue was diluted in water and then the organic layer was extract with ethyl acetate (3 x 150 mL) and dried over Na_2SO_4. The solvent was removed under reduced pressure and the residue was purified by column chromatography using petroleum ether/ethyl acetate (8:2) as eluent to afford compound **12**. (200 mg, 5.6%); R_f = 0.57 (petroleum ether/ethyl acetate 8:2); ^{1}H NMR (300 MHz, $CDCl_3$): δ = 3.51 (s, 2H), 3.68 (s, 3H), 4.22 (s, 4H), 6.72-6.81 (m, 3H).

Methyl 4,5-ethylenedioxy-2-(4-nitrobenzoyl)phenylacetate (13a)

Compound **13a** was prepared with the same procedure employed for compounds **10a**, starting from a solution of compound **12** (337 mg, 1.6 mmol), 4-nitrobenzoic acid (350 mg, 2.1 mmol) and phosphorus pentoxide (3.2 g, 110 mmol) in dichloromethane (50 mL). Yield =208 mg, 36%; R_f = 0.63 (petroleum ether/ethyl acetate 5:5); ^{1}H NMR (300 MHz, $CDCl_3$): δ = 3.61 (s, 3H), 3.87 (s, 2H), 4.24-4.32 (m, 4H), 6.85 (s, 1H), 6.89 (s, 1H,), 7.91 (d, 2H, *J*=8.6 Hz), 8.29 (d, 2H, *J*=8.6 Hz).

Methyl 4,5-ethylenedioxy-2-(3-methyl-4-nitrobenzoyl)phenylacetate (13b)

With a similar procedure, compound **13b** has been synthesized from a solution of compound **12** (337 mg, 1.6 mmol), 3-methyl-4-nitrobenzoic acid (380 mg, 2.1 mmol) and phosphorus pentoxide (3.2 g, 110 mmol) in dichloromethane (50 mL). Yield = 280 mg, 46%; R_f = 0.56 (petroleum ether/ethyl acetate5:5); ^{1}H NMR (300 MHz, $CDCl_3$): δ = 2.58 (s, 3H), 3.57 (s, 3H), 3.82 (s, 2H), 4.20-4.31 (m, 4H), 6.81 (s, 1H), 6.87 (s, 1H,), 7.55-7.75 (m, 2H,), 7.94 (d, *J* = 8.4 Hz, 1H).

Methyl 4,5-ethylenedioxy-2-(3,5-dimethyl-4-nitrobenzoyl)phenylacetate (13c)

With a similar procedure,compound **13c** has been synthesized from a solution of compound **12** (1.0 g, 4.8 mmol), phosphorus pentoxide(4.8 g, 3.3 mmol) and 3,5-dimethyl-4-nitrobenzoic acid (1.2 g, 6.2 mmol). Yield = 850 mg, 45%; R_f = 0.34 (petroleum ether/ethyl acetate7:3); H NMR (300 MHz, $CDCl_3$): δ = 2.31 (s, 6H), 3.59 (s, 3H), 3.81 (s, 2H), 4.24-4.31 (m, 4H), 6.82 (s, 1H), 6.91 (s, 1H,), 7.49 (s, 2H).

3,5-Dihydro-7,8-ethylenedioxy-1-(4-nitrophenyl)-4H-2,3-benzodiazepin-4-one (14a)

Compound **14a** has been prepared starting from a solution of compound **13a** (208 mg, 0.5 mmol), hydrazine hydrate (0.090 mL, 1.8 mmol) and HCl 6N in ethanol (100 mL). The reaction mixture was stirred at reflux for 20h. The solvent was evaporated under reduced pressure and the residue was diluted with water and then extracted with ethyl acetate. The compound was purified by column chromatography (ethyl acetate/petroleum ether 7:3). Yield = 115 mg, 56%; R_f = 0,67 (ethyl acetate/petroleum ether 7:3); ^{1}H NMR (300 MHz, $CDCl_3$): δ = 3.44 (s, 2H), 4.24-4.30 (m, 4H), 6.58 (s, 1H), 7.03 (s, 1H), 7.78 (d, *J*=8.9 Hz, 2H), 8.30 (d, *J*=8.9Hz, 2H), 8.51 (bs, 1H, NH).

3,5-Dihydro-7,8-ethylenedioxy-1-(3-methyl-4-nitrophenyl)-4H-2,3-benzodiazepin-4-one (14b)

Compound **14b** has been synthesized with the same procedure previously described, stirring a solution of compound **13b** (280 mg, 0.75 mmol), hydrazine hydrate (0.12 mL, 2 mmol) and HCl 6N in ethanol (100 mL). Yield =75 mg, 28%; R_f = 0.67 (ethyl acetate/petroleum ether 7:3); ^{1}H NMR (300 MHz, DMSO-d6): δ = 2.55 (s, 3H), 3.43 (s, 2H), 4.15-4.43 (m, 4H), 6.58 (s, 1H), 7.03 (s, 1H), 7.55 (dd, *J*=8.5, 1.6 Hz, 1H), 7.63 (s, 1H), 8.06 (d, *J*=8.5 Hz, 1H).

3,5-Dihydro-1-(3,5-dimethyl-4-nitrophenyl)-7,8-ethylenedioxy-4*H*-2,3-benzodiazepin-4-one (14c)

Compound **14c** has been synthesized with the same procedure previously described, stirring a solution of compound **13c** (747 mg, 1.9 mmol), hydrazine hydrate (0.3 mL, 6.2 mmol) and HCl 6N (0.04 ml) in ethanol (100 mL). Yield = 283 mg, 39%; R_f =

0,61(EtOAc/petroleum ether 7:3). ^{1}H NMR (300 MHz, $CDCl_3$): δ = 2.33 (s, 6H), 3.46 (s, 2H), 4.24-4.34 (m, 4H), 6.66 (s, 1H), 6.88 (s, 1H), 7.36 (s, 2H), 8.67 (s,1H).

3,5-Dihydro-7,8-ethylenedioxy-1-(4-nitrophenyl)-3-vinyl-5H-2,3-benzodiazepin-4-one (15a).

Compound **14a** (126 mg, 0.37 mmol), vinyl bromide (42 μL, 0.37 mmol), potassium carbonate (152 mg, 1.1 mmol), CuI (3.5 mg, 0.018 mmol) and DMEDA (4 μL, 0.037 mmol) were dissolved in toluene (5 mL). The resulting mixture was heated in a microwave reactor at 100°C for 3 h. The solvent was removed *in vacuo* and the residue was diluted with water. The organic layer was extracted with EtOAc (3 x 150 mL), dried over Na_2SO_4, filtered and concentrated. The residue was purified by chromatography using petroleum ether/EtOAc (7:3) as eluent to give compound **15a**. Yield= 82.5 mg, 61%; R_f = 0.57 (petroleum ether/ EtOAc 7:3); ^{1}H NMR (300 MHz, $CDCl_3$) δ = 3.52 (bs, 2H). 4.17-4.35 (m, 4H), 4.70 (dd, *J* = 8.9, 0.6 Hz, 1H), 5.18 (dd, *J* = 15.6, 0.6 Hz, 1H), 6.67 (s, 1H), 6.93 (s, 1H), 7.51 (dd, *J* = 15.6, 8.9 Hz, 1H), 7.88 (d, *J* = 8.2 Hz, 2H), 8.28 (d, *J* = 8.2 Hz, 2H).

3,5-Dihydro-7,8-ethylenedioxy-1-(3-methyl-4-nitrophenyl)-3-vinyl-5*H*-2,3-benzodiazepin-4-one (15b).

With the same procedure described for compound **15a**, compound **15b** has been prepared from a solution of compound **14b** (80 mg, 0.224 mmol), vinyl bromide (20 μL, 0.16 mmol), potassium carbonate (48 mg, 0.36 mmol), CuI (1.6 mg, 0.008 mmol) and DMEDA (2.4 μL, 0.022 mmol). Yield = 58.4 mg, 68%; R_f = 0.54 (EtOAc/ petroleum ether 7:3); ^{1}H NMR (300 MHz, $CDCl_3$) δ 2.64 (s, 3H), 3.50 (bs, 2H), 4.17–4.40 (m, 4H), 4.69 (d, *J* = 8.9

Hz, 1H), 5.17 (d, *J* = 15.6 Hz, 1H), 6.69 (s, 1H), 6.92 (s, 1H), 7.50 (dd, *J* = 15.5, 8.9 Hz, 1H), 7.64 (d, 8.5 Hz, 1H), 7,68 (s, 1H), 8.01 (d, *J* = 8.5 Hz, 1H).

3,5-Dihydro-1-(3,5-dimethyl-4-nitrophenyl)-7,8-ethylenedioxy-3-vinyl-5*H*-2,3-benzodiazepin-4-one (15c).

With the same procedure described for compound **15a**, compound **15c** has been prepared from a solution of compound **23c** (120 mg, 0.327 mmol), vinyl bromide (30 μL, 0.27 mmol), potassium carbonate (75 mg, 0.54 mmol), CuI (2.4 mg, 0.012 mmol) and DMEDA (3,5 μL, 0.033 mmol). Yield = 78.9 mg, 61% ;R_f = 0,63 (ethyl acetate/ petroleum ether 7:3); ^{1}HNMR (300 MHz, $CDCl_3$) δ 2.36 (s, 6H), 3.51 (bs, 2H), 4.18-4.35 (m, 4H), 4.68 (d, *J* = 8.9 Hz, 1H), 5.17 (d, *J* = 15.5 Hz, 1H), 6.71 (s, 1H), 6.93 (s, 1H), 7.45 (s, 2H), 7.48 (dd, *J* =15.5, 8.9 Hz 1H).

3-(3-Bromoisoxazol-5-yl)-3,5-diidro-7,8-ethylenedioxy-1-(4-nitrophenyl)-5*H*-2,3-benzodiazepin-4-one (16a)

To a solution of compound **15a** (80 mg, 0.219 mmol) in EtOAc (5 mL) was added DBF (89 mg, 0.43 mmol) and $NaHCO_3$ (73 mg, 0.87 mmol). The reaction mixture was stirred at room temperature for 72 h. The mix was diluted then with EtOAc (40 mL) and washed with water (2 x 100 mL). The organic layer was separated, dried over Na_2SO_4, filtered and concentrated. The residue was purified by chromatography using ethyl acetate/petroleum ether (5:5) as eluent to afford compound **16a**.Yield = 52.3 mg, 49%; R_f = 0.42 (EtOAc /petroleum ether 5:5); ^{1}H NMR (300 MHz, CDCl3) δ = 3.20-3.71 (m, 4H), 4.19-4.44 (m, 4H), 6.67 (s, 1H), 6.92 (s, 1H), 7.07 (mc, 1H), 7.75 (d, *J* = 8.9 Hz, 2H), 8.29 (d, *J* = 8.9 Hz,

2H); ^{13}C NMR (75 MHz, $CDCl_3$): δ = 26.7, 43.0, 64.3, 71.6, 114.5, 114.6, 121.2, 126.6, 129.4, 130.1, 139.0, 145.7, 149.5, 150.7, 155.6, 164.0, 171.0; Anal. ($C_{20}H_{15}BrN_4O_6$); C, H, N. calc. % C, 49.30; H, 3.10; N, 11.50; found. % C, 49.55; H, 2.87; N, 11.88.

3-(3-Bromoisoxazol-5-yl)-3,5-dihydro-7,8-ethylenedioxy-1-(3-methyl-4-nitrophenyl)-5H-2,3-benzodiazepin-4-one (16b)

With a similar procedure, compound **16b** was prepared starting from **15b** (55 mg, 0.145 mmol) DBF (59 mg, 0.29 mmol) and $NaHCO_3$ (48 mg, 0.58 mmol). Yield = 37 mg, 51%. R_f= 0.58 (EtOAc/petroleum ether 5:5); ^{1}H NMR (300 MHz, $CDCl_3$) δ = 2.65 (s, 3H), 3.18-3.74 (m, 4H), 4.14-4.42 (m, 4H), 6.66 (s, 1H), 6.89 (s, 1H), 7.04 (mc, 1H), 7.41 (d, *J* = 8.4 Hz, 1H), 7.62 (s, 1H), 7.98 (d, *J* = 8.4 Hz, 1H); ^{13}C NMR (75 MHz, $CDCl_3$): δ = 15.6, 26.5, 42.6, 64.2, 71.5, 115.4, 115.6, 122.6, 127.7, 129.3, 130.0, 138.9, 145.5, 149.3, 150.8, 157.7, 163.9, 173.9; Anal. ($C_{21}H_{17}BrN_4O_6$); C, H, N. calc. % C, 50.32; H, 3.42; N, 11.18; found. % , C, 50.64; H, 3.34; N, 11.36.

3-(3-Bromoisoxazol-5-yl)-3,5-dihydro-1-(3,5-dimethyl-4-nitrophenyl)-7,8-ethylenedioxy-5H-2,3-benzodiazepin-4-one (16c)

With a similar procedure, compound **16c** was prepared starting from **15c** (68 mg, 0.17 mmol), DBF (70 mg, 0.34 mmol) and $NaHCO_3$ (58 mg, 0.69 mmol). Yield=67 mg, 75%; R_f= 0.58 (EtOAc/petroleum ether 5:5);^{1}HNMR δ = 2.35 (s, 6H), 3.18-3.68 (m, 4H), 4.21-4.37 (m, 4H), 6.69 (s, 1H), 6.89 (s, 1H), 7.05 (mc, 1H), 7.30 (s, 2H); ^{13}C NMR (75 MHz, $CDCl_3$): δ = 16.2 26.5, 43.5, 64.0, 71.5, 114.6, 114.7, 126.5, 127.2, 129.2, 136.6 139.0,

145.2, 150.0, 152.1, 156.0, 163.9, 173.8; Anal. ($C_{22}H_{19}BrN_4O_6$); C, H, N.calc. % C, 51.28; H, 3.72; N, 10.87; found. % , C, 51.59; H, 3.49; N, 11.06.

1-(4-Aminophenyl)-3-(3-bromoisoxazol-5-yl)-3,5-diidro-7,8-ethylenedioxy-5H-2,3-benzodiazepin-4-one (4a)

A solution of compound **16a** (47 mg, 0.096 mmol), at 0 °C, in AcOH (5.6 mL) was treated with Zn powder (50 mg, 0.77 mmol). The reaction mixture was stirred for 1 h at room temperature, then the solid was filtered and the solvent was removed *in vacuo*. The residue was diluted with EtOAc (2 x 100 mL) and washed two times with a saturated solution of $NaHCO_3$. The organic layer was dried over Na_2SO_4 and the solvent was removed under reduced pressure. The residue was purified by chromatography using ethyl acetate/petroleum ether (5:5) as eluent to afford compound **4a**. Yield = 9.5 mg, 22%. R_f = 0.60 (EtOAc/petroleum ether 8:2);^{1}H NMR (300 MHz, $CDCl_3$) δ 3.25-3.42 (m, 1H), 3.45-3.68 (m, 3H), 3.92 (bs, 2H), 4.17-4.36 (m, 4H), 6.66 (d, *J* = 8.3 Hz, 2H), 6.80 (s, 1H), 6.84 (s, 1H), 7.06 (mc, 1H), 7.36 (d, *J* = 8.3 Hz, 2H); ^{13}C NMR (75 MHz, $CDCl_3$): δ = 26.2, 42.9, 64.0, 71.4, 114.3, 114.5, 116.2, 126.9, 129.2, 129.9 139.2, 145.6, 149.3, 150.5, 155.4, 163.9, 169.8; Anal. ($C_{20}H_{17}BrN_4O_4$); C, H, N. calc.% C, 52.53; H, 3.75; N, 12.25; found. % , C, 52.76; H, 3.37; N, 12.62.

1-(4-Amino-3-methylphenyl)-3-(3-bromoisoxazol-5-yl)-3,5-diidro-7,8-ethylenedioxy-5H-2,3-benzodiazepin-4-one (4b)

With a similar procedure, compound **4b** was prepared starting from **16b** (30 mg, 0.06 mmol), Zn powder (32 mg, 0.48 mmol). Yield = 13 mg, 45%; R_f = 0.54 (ethyl

acetate/petroleum ether 5:5); ^{1}H NMR (300 MHz, $CDCl_3$) 2.20 (s, 3H), 3.22-3.33 (m, 1H), 3.39-3.58 (m, 3H), 3.88 (bs, 2H), 4.19-4.36 (m, 4H), 6.63 (d, *J* = 8.4 Hz, 1H), 6.81 (s, 1H), 6.85 (s, 1H), 7.01 (dd, *J* = 9.5 and 2.5 Hz, 1H), 7.12 (d, *J* = 8.4 Hz, 1H), 7.39 (s, 1H); ^{13}C NMR (75 MHz, $CDCl_3$): δ = 14.9, 26.5, 43.2, 64.4, 71.8, 114.5, 114.6, 116.2, 122.9, 126.7, 126.9, 129.0, 129.3, 129.9, 145.8, 149.0, 149.4, 155.5, 164.2, 171.2; Anal. ($C_{21}H_{19}BrN_4O_4$); C, H, N. calc. % C, 53.52; H, 4.06; N, 11.89; found. % , C, 53.67; H, 3.92; N, 11.98.

1-(4-Amino-3,5-dimethylphenyl)-3-(3-bromoisoxazol-5-yl)-3,5-diidro-7,8-ethylenedioxy-5H-2,3-benzodiazepin-4-one (4c)

With a similar procedure, compound **4c** was prepared starting from **16c** (40 mg, 0.077 mmol), Zn powder (40 mg, 0.66 mmol). Yield = 21.5 mg, 57%; R_f = 0.54 (EtOAc/petroleum ether 5:5); ^{1}H NMR (300 MHz, $CDCl_3$): δ = 2.19 (s, 6H), 3.21-3.32 (m, 1H), 3.40-3.55 (m, 3H), 3.87 (bs, 2H), 4.18-4.37 (m, 4H), 6.81 (s, 1H), 6.85 (s, 1H), 7.03 (dd, *J* = 9.5 and 2.5 Hz, 1H), 7.15 (s, 2H); ^{13}C NMR (75 MHz, $CDCl_3$): δ = 15.3, 26.5, 42.9, 64.4, 71.5, 114.3, 114.5, 123.0, 126.2, 127.5, 128.9, 129.3, 145.5, 147.0, 149.3, 155.4, 163.9, 170.9; Anal. ($C_{22}H_{21}BrN_4O_4$); C, H, N. calc.% C, 54.44; H, 4.36; N, 11.54; found. % , C, 54.72; H, 4.10; N, 11.82.

3-Allyl-3,5-dihydro-7,8-ethylenedioxy-1-(4-nitrophenyl)-5*H*-2,3-benzodiazepin-4-one (17a)

A solution of compound **14a** (100 mg, 0.294 mmol) in anhydrous DMF (5 mL) was added to a suspension of NaH (8 mg, 0.34 mmol) in 5 mL of the same solvent, at 0 ºC under N_2;

the reaction mixture was brought slowly to room temperature and stirred for 1 h. Then, allyl bromide (0.40 mL, 0.44 mmol) was added and the mixture was further stirred overnight. The reaction mixture was quenched with sat. NH_4Cl solution and extracted with EtOAc. The organic layer was washed with water, dried over Na_2SO_4 and concentrated under reduced pressure. Compound **17a** was obtained after purification by flash chromatography using ethyl acetate/petroleum ether (7:3) as eluent. Yield = 70 mg, 62.5%; R_f = 0.73 (ethyl acetate/petroleum ether 7:3); ^{1}H NMR (300 MHz, $CDCl_3$): δ = 3.46 (bs, 2H), 4.23-4.38 (m, 4H), 4.52 (bs, 2H), 5.04-5.20 (m, 2H), 5.78-5.95 (m, 1H), 6.64 (s, 1H), 6.92 (s, 1H), 7.80 (d, *J*=8.9 Hz, 2H), 8.25 (d, *J*=8.9 Hz, 2H).

3-Allyl-3,5-dihydro-7,8-ethylenedioxy-1-(3-methyl-4-nitrophenyl)-5*H*-2,3-benzodiazepin-4-one (17b)

Compound **17b** has been prepared with a similar procedure described for compound **17a**, starting from a solution of compound **14b** (100 mg, 0.282 mmol)**,** NaH (8 mg, 0.34 mmol) and allyl bromide (0.42 mL, 0.42 mmol). Yield = 72 mg, 68%; R_f = 0.78 (ethyl acetate/petroleum ether 7:3); ^{1}H NMR (300 MHz, $CDCl_3$): δ = 2.64 (s, 3H), 3.53 (bs, 2H), 4.20-4.38 (m, 4H), 4.69 (d, *J*=8.9 Hz*,* 1H), 5.17 (d, *J*=15.6 Hz*,* 1H), 6.68 (s, 1H), 6.92 (s, 1H), 7.50 (dd, *J*=8.9 and 15.6 Hz*,* 1H), 7.64 (dd, *J*=8.5, 1.6 Hz, 1H), 7.68 (s, 1H), 8.01 (d, *J*=8.5 Hz*,* 1H).

3-Allyl-3,5-dihydro-1-(3,5-dimethyl-4-nitrophenyl)-7,8-ethylenedioxy-5*H*-2,3-benzodiazepin-4-one (17c)

Compound **17c** has been prepared with a similar procedure described for compound **17a**, starting from a solution of compound **14c** (120 mg, 0.327 mmol), NaH (9.4 mg, 0,39

mmol) and allyl bromide (45 μL; 0.88 mmol). Yield = 91.5 mg, 68.5%; R_f = 0.57 (EtOAc /petroleum ether 4:6); ^{1}H NMR (300 MHz, $CDCl_3$): δ = 2.34 (s, 6H), 3.43 (bs, 2H), 4.12-4.35 (m, 4H), 4.35-4.75 (m, 2H), 4.94-5.18 (m, 2H), 5.70-5.98 (m, 1H), 6.66 (s, 1H), 6.90 (s, 1H), 7.34 (s, 2H).

3-[(3-Bromoisoxazol-5-yl)-methyl]-3,5-dihydro-7,8-ethylenedioxy-1-(4-nitrophenyl)-5*H*-2,3-benzodiazepin-4-one (18a)

To a solution of compound **17a** (60 mg, 0.158 mmol) in EtOAc (5 mL) was added DBF (64 mg, 0.3 mmol) and $NaHCO_3$ (53 mg, 0.63 mmol). The reaction mixture was stirred at room temperature for 72 h. The reaction mixture was diluted then with EtOAc (40 mL) and washed with water (2 x 100 mL). The organic layer was separated, dried over Na_2SO_4, filtered and concentrated. The residue was purified by chromatography using ethyl acetate/petroleum ether (5:5) as eluent to afford compound **18a**. Yield = 50 mg, 59%; R_f= 0.58 (EtOAc /petroleum ether 5:5); ^{1}H NMR (300 MHz, $CDCl_3$): δ = 2.71-2.96 (m, 1H), 3.04-3.23 (m, 1H), 3.46 (bs, 2H), 3.91-4.09 (m, 1H), 4.16-4.38 (m, 4H), 4.48-4.70 (m, 1H), 4.84-5.01 (m, 1H), 6.66 (s, 1H), 6.91 (s, 1H), 7.84 (d, *J*=8.5 Hz, 2H), 8.25 (d, *J*=8.5 Hz, 2H); ^{13}C NMR (75 MHz, $CDCl_3$): δ = 27.1, 42.6, 57.1, 62.3, 64.2, 114.5, 114.6, 121.2, 126.6, 129.4, 130.1, 139.0, 145.7, 149.5, 150.7, 155.6, 164.0, 171.0; Anal. ($C_{21}H_{17}BrN_4O_6$) C, H, N. calc.% C, 53.71; H, 3.92; N, 8.17; found. % , C, 53.87; H, 3.7; N, 8.34.

3-[(3-Bromoisoxazol-5-yl)-methyl]-3,5-dihydro-7,8-ethylenedioxy-1-(3-methyl-4-nitrophenyl)-5H-2,3-benzodiazepin-4-one (18b)

With a similar procedure, compound **18b** has been prepared starting from compound **17b** (49 mg, 0.125 mmol)**,** DBF (51 mg, 0.25 mmol) and $NaHCO_3$ (42 mg, 0.5 mmol). Yield = 30 mg, 46%; R_f = 0.52 (EtOAc /petroleum ether 5:5); ^{1}H NMR (300 MHz, $CDCl_3$): δ = 2.63 (s, 3H), 2.74-2.99 (m, 1H), 3.02-3.22 (m, 1H), 3.45 (bs, 2H), 3.89-4.70 (m, 6H), 4.82-5.00 (m, 1H), 6.67 (s, 1H), 6.90 (s, 1H), 7.57 (d, *J*=8.1 Hz*,* 1H), 7.65 (s*,* 1H), 7.98 (d, *J*=8.1 Hz*,* 1H); ^{13}C NMR (75 MHz, $CDCl_3$): δ = 15.2, 27.2, 42.5, 57.1, 62.2, 64.4, 114.4, 114.6, 121.3, 126.8, 129.6, 130.3, 139.2, 145.5, 149.3, 150.5, 155.4, 163.9, 170.9; Anal. ($C_{22}H_{19}BrN_4O_6$) C, H, N. calc.% C, 52.82; H, 3.63; N, 8.40; found. % , C, 52.98; H, 3.41; N, 8.56.

3-[(3-Bromoisoxazol-5-yl)-methyl]-3,5-dihydro-1-(3,5-dimethyl-4-nitrophenyl)-7,8-ethylenedioxy-5H-2,3-benzodiazepin-4-one (18c)

With a similar procedure, compound **18c** has been prepared starting from compound **17c** (90 mg, 0.22 mmol), DBF (89 mg, 0.44 mmol) and $NaHCO_3$ (74 mg, 0.88 mmol). Yield = 82 mg, 70%; R_f = 0.42 (EtOAc /petroleum ether 5:5).^{1}H NMR (300 MHz, $CDCl_3$): δ = 2.32 (s, 6H), 2.67-2.94 (m, 1H), 3.11 (mc, 1H), 3.42 (bs, 2H), 3.85-4.04 (m, 1H), 4.13-4.38 (m, 4H), 4.42-4.66 (m, 1H), 4-79-4.99 (m, 1H), 6.66 (s, 1H), 6.88 (s, 1H), 7.37 (s, 2H); ^{13}C NMR (75 MHz, $CDCl_3$): δ = 16.0, 27.1, 42.6, 57.2, 62.3, 64.3, 114.5, 114.7, 126.7, 127.3, 129.2, 136.2, 138.9, 145.6, 150.0, 152.2, 155.7, 164.1, 171.1; Anal. ($C_{23}H_{21}BrN_4O_6$); C, H, N. calc.% C, 52.19; H, 4.00; N, 10.58; found. % C, 52.35; H, 3.88; N, 10.75.

1-(4-Aminophenyl)-3-[(3-bromoisoxazol-5-yl)-methyl]-3,5-dihydro-7,8-ethylenedioxy-5H-2,3-benzodiazepin-4-one (5a)

A solution of compound **18a** (30 mg, 0.056 mmol), at 0 °C, in AcOH (3.5 mL) was treated with Zn powder (31 mg, 0.5 mmol). The reaction mixture was stirred for 1 h at room temperature, then the solid was filtered and the solvent was removed *in vacuo*. The residue was diluted with EtOAc (40 mL) and washed two times with a saturated solution of $NaHCO_3$ (2 x 100 mL). The organic phase was dried over Na_2SO_4 and the solvent was removed under reduced pressure. The residue was purified by chromatography using ethyl acetate/petroleum ether (8:2) as eluent to afford compound **5a.** Yield = 13 mg, 48%; R_f = 0.54 (ethyl acetate/petroleum ether 8:2); ^{1}H NMR (300 MHz, $CDCl_3$): δ = 2.71-2.87 (m, 1H), 3.06 (mc, 1H), 3.42 (bs, 2H), 3.80-4.03 (m, 3H), 4.15-4.37 (m, 4H), 4.42-4.58 (m, 1H), 4.86-5.02 (m, 1H), 6.68 (d, *J*=8.5 Hz, 2H), 6.80 (s, 1H), 6.87 (s, 1H), 7.45 (d, *J*=8.5 Hz, 2H); ^{13}C NMR (75 MHz, $CDCl_3$): δ = 26.9, 43.0, 57.1, 62.5, 64.2, 114.6, 114.8, 116.2, 123.0, 126.7, 127.2, 129.2, 129.3, 130.2, 145.5, 148.6, 149.4, 155.5, 164.2, 170.9; Anal. ($C_{21}H_{19}BrN_4O_4$) C, H, N. calc.% C, 53.52; H, 4.06; N, 11.89; found. % , C, 53.70; H, 3.92; N, 12.06.

1-(4-Amino-3-methylphenyl)-3-[(3-bromoisoxazol-5-yl)-methyl]-3,5-dihydro-7,8-ethylenedioxy-5H-2,3-benzodiazepin-4-one (5b)

With a similar procedure, compound **5b** was prepared from **18a** (21 mg, 0.04 mmol), Zn powder (21 mg, 0.3 mmol), and AcOH (2.3 mL). Yield = 9.4 mg, 46 %; R_f = 0.60 (ethyl acetate/petroleum ether 8:2); ^{1}H NMR (300 MHz, $CDCl_3$): δ = 2.19 (s, 3H), 2.72-2.94 (m, 1H), 2.98-3.18 (m, 1H), 3.42 (bs, 2H), 3.82-4.04 (m, 3H), 4.17-4.38 (m, 4H), 4.42-4.63 (m,

1H), 4.76-5.01 (m, 1H), 6.65 (d, *J* = 8.4 Hz, 1H), 6.80 (s, 1H). 6.86 (s, 1H, H-9), 7.25 (d, *J* = 8.4 Hz, 1H), 7.38 (s, 1H); ^{13}C NMR (75 MHz, $CDCl_3$): δ = 15.5, 26.8, 42.5, 57.2, 62.3, 64.4, 114.3, 114.5, 116.2, 122.7, 126.8, 126.9, 129.0, 129.3, 130.2, 145.5, 148.7, 149.4, 155.4, 163.9, 170.9; Anal. ($C_{22}H_{21}BrN_4O_4$) C, H, N. calc.% C, 54.44; H, 4.36; N, 11.54; found. % , C, 54.60; H, 4.14; N, 11.71.

1-(4-Amino-3,5-dimethylphenyl)-3-[(3-bromoisoxazol-5-yl)-methyl]-3,5-dihydro-7,8-ethylenedioxy-5H-2,3-benzodiazepin-4-one (5c)

With a similar procedure, compound **5c** was prepared from **18c** (80 mg, 0.15 mmol), Zn powder (79 mg, 1.2 mmol) and AcOH (8.8 mL). Yield = 44 mg, 58%; R_f = 0.54 (ethyl acetate/petroleum ether 5:5). ^{1}H NMR (300 MHz, $CDCl_3$) δ = 2.18 (s, 6H), 2.72-2.90 (m, 1H), 3.05 (mc, 1H), 3.40 (bs, 2H), 3.68-4.02 (m, 3H), 4.15-4.35 (m, 4H), 4.40-4.56 (m, 1H), 4.92 (mc, 1H), 6.80 (s, 1H), 6.85 (s, 1H), 7.20 (s, 2H); ^{13}C NMR (75 MHz, $CDCl_3$): δ = 15.9, 26.8, 43.0, 56.8, 62.2, 64.4, 114.4, 114.5, 122.6, 126.7, 127.2, 128.9, 129.3, 145.6, 147.0, 149.4, 155.5, 163.9, 171.2; Anal. ($C_{23}H_{23}BrN_4O_4$) C, H, N. calc. % C, 55.32; H, 4.64; N, 11.22; found. % C, 55.45; H, 4.52; N, 11.43.

4.1.2. Synthesis of L-Cys derivatives 6b-6h

(*R*)-*S*-(2-Chlorobenzyl)-*N*-Boc-cysteine 20b

To a solution of *N*-Boc-cysteine **19** (100 mg, 0.45 mmol) in anhydrous ethanol (50 ml) under nitrogen sodium ethoxide (0,334 ml, 0.90 mmol) was added. The reaction mixture was stirred for 1h in the room temperature and 2-chlorobenzylbromide (0.065 mL, 0.5 mmol) was then added. The reaction mixture was stirred at 80°C for 4h, then quenched by adding a little amount of water and then the organic phase was dried under vacuum. The pH of the mixture was brought to 3 with $KHSO_4$. The aqueous phase was extracted with Et_2O (3 x 50ml), dried ($MgSO_4$), concentrated and purified by column chromatography (EtOAc/*n*-Hep/AcOH 92.5/5/2.5). Yield = 120 mg, 77%; R_f = 0.35 (EtOAc/nHep/AcOH 6/3.5/5); ^{1}H NMR (400 MHz, $CDCl_3$) δ 9.37 (s, 1H), 7.40 – 7.29 (m, 2H), 7.24 – 7.14 (m, 2H), 5.38 (m, 1H), 4.58 (s, 1H), 3.86 (s, 2H), 2.97 (m, 2H), 1.45 (s, 9H).

(*R*)-*S*-(3-Chlorobenzyl)-*N*-Boc-cysteine 20c

With a similar procedure, compound **20c** was synthesized from *N*-Boc-cysteine **19** (100 mg, 0.45 mmol), 3-chlorobenzyl bromide (65µl, 0.50 mmol) and sodium ethoxide (334µl, 0.90 mmol). Yield = 121 mg, 78%; R_f = 0.32 (EtOAc/ nHep /AcOH 6/3.5/5); ^{1}H NMR (600 MHz, $CDCl_3$) δ 9.37 (s, 1H), 7.32 (s, 1H), 7.25 – 7.21 (m, 2H), 7.21 – 7.17 (m, 1H), 5.28 (m, 1H), 4.52 (s, 1H), 3.72 (s, 2H), 2.89 (m, 2H), 1.46 (s, 9H).

(*R*)-*S*-(4-Chlorobenzyl)-*N*-Boc-cysteine 20d

With a similar procedure, compound **20d** was synthesized from *N*-Boc-cysteine **19** (100 mg, 0.45 mmol), 4-chlorobenzyl bromide (0,065 ml, 0.50 mmol) and sodium ethoxide (0,334 ml, 0.90 mmol). Yield = 139 mg, 89%; R_f = 0.33 (EtOAc/ nHep /AcOH 6/3.5/5); ^{1}H

NMR (600 MHz, $CDCl_3$) δ 9.37 (s, 1H), 7.28 (d, *J* = 8.4 Hz, 2H), 7.24 (d, *J* = 8.4 Hz, 2H), 5.28 (m, 1H), 4.53 (s, 1H), 3.70 (s, 2H), 2.87 (m, 2H), 1.45 (s, 9H).

(*R*)-*S*-(2-Methoxybenzyl)-*N*-Boc-cysteine 20e

With a similar procedure, compound **20e** was synthesized from *N*-Boc-cysteine **19** (100 mg, 0.45 mmol), 2-methoxybenzyl bromide (98 mg, 0.50 mmol) and sodium ethoxide (0,334 ml, 0.90 mmol). Yield = 136 mg, 88%; R_f = 0.38 (EtOAc/ nHep /AcOH 6/3.5/5); ^1H NMR (400 MHz, $CDCl_3$) δ 8.13 (s, 1H), 7.18-7.24 (m, 2H), 6.90 (d, *J* = 7.5 Hz, 1H), 6.86 (dd, *J* = 8.6 Hz, 1H), 5.47 (m, 1H), 4.55 (s, 1H), 3.84 (s, 3H), 3.77 (s, 2H), 2.92 (m, 2H), 1.45 (s, 9H).

(*R*)-*S*-(3-Methoxybenzyl)-*N*-Boc-cysteine 20f

With a similar procedure, compound **20f** was synthesized from *N*-Boc-cysteine **19** (100 mg, 0.45 mmol), 3-methoxybenzyl bromide (98 mg, 0.50 mmol) and sodium ethoxide (0,334 ml, 0.90 mmol). Yield = 136 mg, 88%; R_f = 0.37 (EtOAc/ nHep /AcOH 6/3.5/5); ^1H NMR (400 MHz, $CDCl_3$) δ 7.73 (s, 1H), 7.20 (t, *J* = 7.8 Hz, 1H), 6.88 (m, 2H), 6.78 (dd, *J* = 8.2, 2.0 Hz, 1H), 5.39 (m, 1H), 4.51 (s, 1H), 3.79 (s, 3H), 3.70 (s, 2H), 2.88 (m, 2H), 1.44 (s, 9H).

(*R*)-*S*-(4-Methoxybenzyl)-*N*-Boc-cysteine 20f

With a similar procedure, compound **20f** was synthesized from *N*-Boc-cysteine **19** (100 mg, 0.45 mmol), 4-methoxybenzyl chloride (0,067 ml, 0.50 mmol) and sodium ethoxide (0,334 ml, 0.90 mmol). Yield = 134 mg, 87%; R_f = 0.46 (EtOAc/ nHep /AcOH 6/3.5/5); ^1H NMR (400 MHz, $CDCl_3$) δ 7.88 (s, 1H), 7.21 (d, *J* = 8.4 Hz, 2H), 6.83 (d, *J* = 8.4 Hz, 2H), 5.37 (m, 1H), 4.52 (s, 1H), 3.77 (s, 3H), 3.69 (s, 2H), 2.87 (m, 2H), 1.44 (s, 9H).

(*R*)-*S*-(Pyrid-4-ylmethyl)-*N*-Boc-cysteine 20h

With a similar procedure, compound **20h** was synthesized from *N*-Boc-cysteine **19** (100 mg, 0.45 mmol), 4-(chloromethyl)pyridine hydrochloride (81 mg, 0.50 mmol) and sodium ethoxide (0,334 ml, 0.90 mmol). Yield = 94 mg, 67%; R_f = 0.54 (EtOAc/ nHep /AcOH 6/3.5/5); ^{1}H NMR (600 MHz, DMSO) δ 8.47 (d, *J* = 4.2 Hz, 2H), 7.32 (d, *J* = 4.4 Hz, 2H), 6.17 (d, *J* = 5.5 Hz, 1H), 3.81 – 3.60 (m, 2H), 2.85 – 2.79 (m, 1H), 2.71 (dd, *J* = 13.1, 5.8 Hz, 1H), 1.38 (s, 9H).

(*R*)-*S*-(2-Chlorobenzyl)cysteine hydrochloride 6b

Compound **20b** (90 mg, 0.26 mmol) was *N*-deprotected using HCl 2M in Et_2O (3ml, 6 mmol) and was left overnight. After that the precipitate was formed, the supernatant was removed and 10 equiv of 2M of HCl in Et_2O were added and left for another 2h in order to complete the reaction. The supernatant was removed and the insoluble was washed with dietilether (4x10 ml) to afford the pure compound. Yield = 65 mg, 88%; R_f = 0.65 (EtOAc/nHep/AcOH 6/3.5/5); ^{1}H NMR (600 MHz, DMSO) δ 8.46 (s, 3H), 7.52 – 7.45 (m, 2H), 7.36 – 7.31 (m, 2H), 4.20 (bs, 1H), 3.92 (s, 2H), 2.97 (qd, *J* = 14.4, 5.7 Hz, 2H). ^{13}C NMR (151 MHz, DMSO) δ 169.59, 139.33, 133.65, 130.14, 128.88, 127.94, 127.15, 51.57, 34.48, 30.82.

(*R*)-*S*-(3-Chlorobenzyl)cysteine hydrochloride 6c

With a similar procedure, compound **6c** was prepared from **20c** (121 mg, 0.35 mmol) and HCl 2M in Et_2O (4 ml, 8 mmol). Yield = 72 mg, 73%; R_f = 0.56 (EtOAc/ nHep /AcOH 6/3.5/5); ^{1}H NMR (600 MHz, DMSO) δ 14.05 (s, 1H), 8.52 (s, 3H), 7.45 (s, 1H), 7.40 – 7.35 (m, 1H), 7.35 – 7.31 (m, 2H), 4.18 (t, *J* = 5.7 Hz, 1H), 3.84 (s, 2H), 2.92 (qd, *J* = 14.5, 5.7 Hz, 2H). ^{13}C NMR (151 MHz, DMSO) δ 169.58, 140.53, 132.97, 130.30, 128.79,

127.70, 127.05, 51.57, 34.53, 30.82. Anal. ($C_{10}H_{12}ClNO_2S$) C, H, N. calc.% C, 48.88; H, 4.92; N, 5.70; found. % , C, 49.18; H, 4.66; N, 5.96.

(*R*)-*S*-(4-Chlorobenzyl)cysteine hydrochloride 6d

With a similar procedure, compound **6d** was prepared from **20d** (139 mg, 0. 40 mmol) and HCl 2M in Et_2O (4,6 ml, 9 mmol). Yield = 94 mg, 83%; R_f = 0.56 (EtOAc/ nHep /AcOH 6/3.5/5); ^{1}H NMR (600 MHz, DMSO) δ 13.92 (s, 1H), 8.50 (s, 3H), 7.44 – 7.34 (m, 4H), 4.16 (t, *J* = 5.7 Hz, 1H), 3.83 (s, 2H), 2.90 (qd, *J* = 14.5, 5.7 Hz, 2H). ^{13}C NMR (151 MHz, DMSO) δ 169.59, 136.96, 131.66, 130.84, 128.40, 51.58, 34.43, 30.81. Anal. ($C_{10}H_{12}ClNO_2S$) C, H, N. calc.% C, 48.88; H, 4.92; N, 5.70; found. % , C, 49.13; H, 4.68; N, 6.03.

(*R*)-*S*-(2-Methoxybenzyl)cysteine hydrochloride 6e

With a similar procedure, compound **6e** was prepared from **20e** (136 mg, 0.40 mmol) and HCl 2M in Et_2O (4,6 ml, 9 mmol). Yield = 74 mg, 66%; R_f = 0.58 (EtOAc/ nHep /AcOH 6/3.5/5); ^{1}H NMR (600 MHz, DMSO) δ 13.92 (m, 1H) 8.47 (s, 3H), 7.32 – 7.24 (m, 2H), 7.01 (d, *J* = 8.1 Hz, 1H), 6.91 (t, *J* = 7.4 Hz, 1H), 4.15 (t, *J* = 5.8 Hz, 1H), 3.80 (s, 3H), 3.79 – 3.72 (m, 2H), 2.94 (dq, *J* = 14.4, 5.8 Hz, 2H). ^{13}C NMR (151 MHz, DMSO) δ 130.17, 128.67, 120.18, 111.03, 55.41, 51.68, 31.32, 29.91. Anal. ($C_{11}H_{15}NO_3S$) C, H, N. calc.% C, 54.75; H, 6.27; N, 5.80; found. % , C, 55.06; H, 5.98; N, 6.08.

(*R*)-*S*-(3-Methoxybenzyl)cysteine hydrochloride 6f

With a similar procedure, compound **6f** was prepared from **20f** (136 mg, 0. 40 mmol) and HCl 2M in Et_2O (4,6 ml, 9 mmol). Yield = 72 mg, 65%; R_f = 0.51 (EtOAc/ nHep /AcOH 6/3.5/5); ^{1}H NMR (600 MHz, DMSO) δ 13.92 (s, 1H), 8.52 (s, 3H), 7.25 (t, *J* = 7.8 Hz,

1H), 6.93 (m, 2H), 6.83 (dd, *J* = 8.2, 2.0 Hz, 1H), 4.16 (t, *J* = 5.8 Hz, 1H), 3.80 (s, 2H), 3.75 (s, 3H), 2.93 (qd, *J* = 14.5, 5.8 Hz, 2H). ^{13}C NMR (151 MHz, DMSO) δ 169.63, 159.25, 139.33, 129.48, 121.18, 114.55, 112.59, 55.01, 51.60, 35.26, 30.88. Anal. ($C_{11}H_{15}NO_3S$) C, H, N. calc.% C, 54.75; H, 6.27; N, 5.80; found. % , C, 55.03; H, 5.95; N, 6.14.

(*R*)-*S*-(4-Methoxybenzyl)cysteine hydrochloride 6g

With a similar procedure, compound **6g** was prepared from **20g** (134 mg, 0. 39 mmol) and HCl 2M in Et_2O (4,4 ml, 9 mmol). Yield = 100 mg, 92%; R_f = 0.49 (EtOAc/ nHep /AcOH 6/3.5/5); ^{1}H NMR (600 MHz, DMSO) δ 8.49 (s, 3H), 7.27 (d, *J* = 8.6 Hz, 2H), 6.89 (d, *J* = 8.6 Hz, 2H), 4.15 (t, *J* = 5.8 Hz, 1H), 3.77 (s, 2H), 3.74 (s, 3H), 2.90 (qd, *J* = 14.5, 5.8 Hz, 2H). ^{13}C NMR (151 MHz, DMSO) δ 169.66, 158.33, 130.13, 129.46, 113.84, 55.06, 51.62, 30.84. Anal. ($C_{11}H_{15}NO_3S$) C, H, N. calc.% C, 54.75; H, 6.27; N, 5.80; found. % , C, 54.91; H, 6.09; N, 5.94.

(*R*)-*S*-(Pyrid-4-ylmethyl)cysteine hydrochloride 6h

With a similar procedure, compound **6h** was prepared from **20h** (86 mg, 0. 28 mmol) and HCl 2M in Et_2O (3,1 ml, 6,3 mmol). Yield = 60 mg, 88%; R_f = 0.44 (EtOAc/ nHep /AcOH 6/3.5/5); ^{1}H NMR (400 MHz, DMSO) δ 8.83 (d, *J* = 6.0 Hz, 2H), 8.72 (s, 3H), 7.99 (d, *J* = 6.0 Hz, 2H), 4.20 (bs, 1H), 4.10 (q, *J* = 14.0 Hz, 2H), 3.00 (qd, *J* = 14.5, 5.7 Hz, 2H). ^{13}C NMR (151 MHz, DMSO) δ 169.33, 142.91, 139.56, 126.63, 51.58, 33.73, 30.64. Anal. ($C_9H_{12}N_2O_2S$) C, H, N. calc.% C,. 50.92; H, 5.70; N, 13.20; found. % , C, 50.65; H, 5.89; N, 13.44..

4.2 Pharmacology

4.2.1. Inhibition of the glutamate-evoked current

4.2.1.1. Cell Culture and Receptor Expression

HEK-293S cells were cultured in a 37 °C, 5% CO_2, humidified incubator, and in the Dulbecco's modified Eagle's medium (Invitrogen, Carlsbad, CA) supplemented with 10% fetal bovine serum (Invitrogen), 100 units of penicillin/mL and 0.1 mg streptomycin/mL (Sigma-Aldrich, St. Louis, MO). The DNA plasmids were prepared as previously described (Pei et al., 2009). The HEK-293S cells were transiently transfected to express the AMPA receptor by following a standard calcium phosphate method (Chen et al., 1987). The cells were also cotransfected with a plasmid encoding green fluorescent protein (GFP) as a transfection marker and a separate plasmid encoding large T-antigen to enhance the receptor expression at the single cell level (Huang et al., 2005). The weight ratio of the plasmid for GFP and the large T-antigen to that for AMPA receptor was 1:1:10, respectively. The plasmid used for transient transfection for AMPA receptors ranged from 5 to 15 μg per 35 mm dish. The cells were used for recording 48 h after transfection.

4.2.1.2. Compound preparation

A stock compound solution was prepared by dissolving the compound in powder form in pure DMSO solution at room temperature. The working stock of the compound solution was prepared by diluting the pure DMSO solution to the extracellular buffer. The external cellular solution contained (in mM) 145 NaCl, 3 KCl, 1 $CaCl_2$, 2 $MgCl_2$, and 10 HEPES (pH 7.4 adjusted by NaOH).

4.2.1.3. Whole-Cell Current Recording

The procedures for whole-cell current recording were previously described (Li et al., 2003). Briefly, an Axopatch-200B amplifier (Axon Instrument) was used in whole-cell recording at a cutoff frequency of 2-20 kHz by a built-in, 8-pole Bessel filter and digitized at a 5-50 kHz sampling frequency by a Digidata 1322A (Axon Instruments). An electrode for whole-cell recording had a resistance of ~3 MΩ when filled with the electrode solution containing (in mM) 110 CsF, 30 CsCl, 4 NaCl, 0.5 $CaCl_2$, 5 EGTA, and 10 HEPES (pH 7.4 adjusted by CsOH). All other reagents were dissolved in the extracellular buffer. A U-tube flow device (Li et al., 2003) was used to apply glutamate in the absence and presence of a compound to a cell expressing the receptor of interest. All whole-cell recordings were at -60 mV and 22 °C.

4.2.1.4. Data Analysis

Glutamate-induced current response of individual receptors expressed in HEK-293 cells was collected. Current amplitude was corrected for desensitization as described in earlier publications (Li et al., 2003, Wu et al., 2014). Unless noted otherwise, each data point in the plots represented an average of at least two measurements collected from at least three cells, and the standard deviation from the mean was reported. In our plots and estimate of the K_I value, we used A/A_I ratio. The A/A_I ratio can be expressed in eq 1a below:

$$\frac{A}{A_I} = 1 + I\frac{(\overline{AL_2})_O}{K_I} \qquad \text{eq 1a}$$

Again, A and A_I are the whole-cell current amplitude in the absence and presence of an inhibitor. $(\overline{AL_2})_0$ was defined in eq 1*b*. It should be pointed out that eq 1 is also applicable for assaying not only noncompetitive inhibitors but also competitive and uncompetitive inhibitors. For eq 1b, if we assume n = 2 (or two ligand molecules for binding and opening

the channel), as found before, (Li et al., 2003) we can define that $(\overline{AL_n})_0$ in eq 1*a* or $(\overline{AL_2})_0$ is expressed as a function of the fraction of all receptor forms. Φ is the equilibrium dissociation constant of channel opening.

$$(\overline{AL_2})_O = \frac{\overline{AL_2}}{A + AL + AL_2 + AL_2} = \frac{L^2}{L^2(1+\Phi) + 2K_1L\Phi + K_1^2\Phi} \quad \text{eq 1b}$$

Based on eq 1a and 1b, the apparent K_I value depends on ligand concentration. Therefore, using different glutamate concentration, we could measure and estimate the potency of an inhibition to the open and closed channel forms (Wu et al., 2014). Statistical differences in A/A_I values between the closed-channel and the open-channel states of $GluA2Q_{flip}$ channels were determined for various compounds using a two-sample, two-tailed, Student's *t* test. Statistical differences in A/A_I values for the closed-channel and the open-channel states among the four different AMPARs were determined using one-way ANOVA followed by Tukey's honestly significant difference (HSD) *post hoc* test.

4.2.2. Antitumor activity

4.2.2.1. Cell culture

PLC/PRF/5, HEP-G2, leukemia Jurkat T cells, U87MG, Caco-2, and HT-29 cell lines, were purchased from ATCC (LGC Standards srl, Milan, Italy). PLC/PRF/5 and HEP-G2 cells were grown in DMEM supplemented with 10% fetal bovine serum (FBS) 100 μg/ml streptomycin, 100 U/ml penicillin, 2 mM glutamine (Euroclone Spa, Milan, Italy). U87MG were grown in DMEM supplemented with 10% fetal bovine serum, 100 μg/ml streptomycin, 100 U/ml penicillin and 1% non-essential amino acids (Euroclone Spa, Milan, Italy). Caco-2 and HT-29 were maintained in DMEM supplemented with 10% fetal bovine serum, 100 μg/ml streptomycin, 100 U/ml penicillin, and 1% nonessential amino acids (Euroclone Spa, Milan, Italy). The cells were cultured in a humidified incubator at 37 °C with 95% atmospheric air/5% CO_2. Morphological analysis of transduced and differentiated cells was performed through May Grunwal-Giemsa staining of cytocentrifuged specimens.

4.2.2.2. Determination of cell growth inhibition

2,3-Benzodiazepine derivatives, GYKI 52466**,** and 5-fluoruracile (5-FU) (Sigma, Italy) were initially dissolved in DMSO at concentration of 100 mM, and serial dilutions were then prepared in culture medium, so that the final concentration of dimethyl sulfoxide (DMSO) was < 0.1%. Cell viability was assessed after 24–48–72 h of continuous exposure with different concentrations of the compounds (0,1–200 μM) using MTS assay (CellTiter 96® Aqueous One Solution Cell Proliferation Assay, Promega, Milan, Italy) and by counting cells with hemocytometer using the Trypan Blue exclusion method. Briefly, the different cell lines were plated on 96-well plates (Euroclone, Milan, Italy) at concentration of 2000 cells/cm^2. After exposure to desired concentrations of the different compounds,

20 µl MTS was added to each well and incubated for a period of 2.5 h. Finally, absorption was measured at 492 nm using a spectrophotometer Multiscan® MCC/340 (Labsystem, Finland). The percentage growth was calculated using the following calculation: % growth = 100 × [(T − T0) / (C − T0)] where (T) was the growth of the cells in presence of the compound at different concentrations and at a specific time point, (T0) represent the number of cells at the time 0 of the experiment and (C) the growth of the control at a specific time point. 5-fluoruracile (5-FU) was used as reference drug. The growth inhibition that reduces the cell population by 50% (GI_{50}) was calculated using GraphPad Prism 6 (Graph-Pad 6 Software Inc., San Diego, CA, USA).

4.2.2.3. Recovery of proliferation assay

Cells were plated at 20,000 cells/cm^2 and allow to growth overnight. Different concentrations of compound ***2c*** (2.5–5–7.5 µM) or vehicle containing DMSO (< 0.1%) were added to the cells for 72 h. After 72 h the media were replaced with fresh medium and cells were incubated and counted daily for other 72 h, by Trypan Blue exclusion method and also using MTS assay.

4.2.2.4. Cell cycle and BrdU/PI analysis

Human leukemia Jurkat T cells were seeded at a density of approximately 50,000 cells/cm^2 into 6-well plates, cultured overnight and different concentrations of ***2c*** compound (1.5, 2.5, 5 µM) or 0,1% DMSO (control) were added. Following 12–24–48 h of incubation, cells were harvested, washed with PBS. Cells were stained with Nicoletti solution (sodium citrate 0,1%, Triton X-100 0,1% and 20 µg/ml PI) for 15 min at 4 °C in the dark. Evaluation of the different phases of cell cycle was analyzed by BrdU/PI staining performed as described by Manfredini et al. (1997). Briefly, cells were pre-incubated with 10 µM BrdU (Sigma Aldrich, St Louise, MO, USA) and stained with a purified mouse

primary monoclonal antibody (MoAb) directed against BrdU (BD Biosciences, Erembodegem, Belgium) followed by a rabbit *anti*-mouse immunoglobulin IgG secondary antibody conjugated with fluorescein isothiocyanate (FITC) (Dako A/S, Glostrup, Denmark) Samples were then resuspended in a 50 µg/ml PI water solution. Both the assays were analyzed by Coulter Epics XL flow cytometer (Coulter Electronics Inc., Hialeah, FL, USA).

4.2.2.5. Analysis of cell death

The measurement of phosphatidylserine redistribution in a plasma membrane was conducted according to the manufacturer's instructions for the Annexin V-FITC/PI Apoptosis Detection kit (BD, Milan, Italy). Briefly, approximately 50,000 cells/cm^2 leukemia Jurkat T cells, following incubation for 12–24–48 h with 2.5, 5 µM of ***2c*** or 0,1% DMSO (control), were harvested, washed in cold PBS and re-suspended in 500 µl Annexin V binding buffer. Then, 5 µl Annexin V-FITC and 5 µl PI were added and incubated with the cells for 15 min at RT in the dark. The stained cells were analyzed directly by Coulter Epics XL flow cytometer (Coulter Electronics Inc., Hialeah, FL, USA).

4.2.2.6. LDH assay

The tested compound was directly added to leukemia Jurkat T to the desired concentrations. At the end of the exposure period (48 h), cell injury was quantified by measuring lactate dehydrogenase (LDH) release into the culture medium following the manufacturer's instructions (Cytotoxicity Detection kit Roche-Applied-Sciences, Milan, Italy). The absorbance of the reaction mixture at 492 nm was determined a multiscan MCC/340 microplate reader (Labsystem, Finland). The LDH signal that was associated with 100% cell death was determined by lysing cells with 0.2% Triton X-100.

4.2.2.7. Immunoblotting

Total and nuclear proteins were extracted from control and ***2c***-treated cells by lysing cells in RIPA buffer (50 mM Tris-HCl pH 7.4, 150 mM NaCl, 1% Na deoxycolate, 1% Triton X-100, 2 mM PMSF) (Sigma, Milan, Italy). Nuclei extraction from Jurkat T cells was performed using NE-PER nuclear and cytoplasmic extraction reagents (Pierce) according to the manufacturer's protocol. The obtained pellet was enriched in nuclei. Lysate protein concentrations were quantification using Bradford colorimetric method Comassie (Pierce, Rockford, USA) according to the manufacturer's protocol. Equal amount of proteins, 0.5 μg/μl for each sample was, loaded onto a pre-cast 12% SDS-PAGE (Invitrogen, Milan, Italy) and electrophoretically transferred to nitrocellulose membrane (Invitrogen, Milan, Italy). Membrane was blocked in TBST (20 mMTris- HCl, 0.5 M NaCl and 0.05% Tween 20) buffer containing 5% non-fat dried milk overnight at 4 °C and incubated with primary antibody *anti*-Cyclin B1 (1:1000), *anti*-cdc-2 (1:1000), *anti*-phospho-cdc2$^{(Tyr15)}$ (1:1000), *anti*-Wee-1 (1:1000), and *anti*-pospho-Wee-1$^{(Ser642)}$ (1:1000), *anti*-myelin transcription factor 1 (Myt-1) (1:1000), *anti*-phospho-histone *H3*$^{(Ser10)}$ (1:1000), *anti*-p21 Waf/Cip1 (1:1000), anti-bcl xl (1:500), anti-bax, (1:500), anti-p53 (1:500) at RT respectively for 3 h under gentle agitation (the primary antibodies were from Cell Signaling, USA). Membrane was then washed 3 times in TBST, incubated for 1 h with HRP-conjugated anti-rabbit or anti-mouse antibody (Cell Signaling, USA) and visualized using chemiluminescence method (Amersham, GE Healthcare Europe GmbH, Milan, Italy). The immune-complexes were analyzed using Densitometric analysis for determination of relative protein expression was done using a BioRad GS 690 Imaging densitometer with molecular analysis software (Life science, Milan, Italy) with β-actin or lamin B1 as loading control.

4.2.2.8. Protease assay

Caspase-3-related protease activity in cell lysates was determined using a commercially available kit (Promega, Milan, Italy). Briefly, Jurkat T cells were treated with 2,5 and 5 μM concentration of compound ***2c***, alone or in association with the pan-caspase inhibitor *Z*-VAD-FMK (50 μM) for 24 and 48 h. Cell lysate proteins (nuclei free), were mixed with assay buffer (containing 10 mM DTT) and with the colorimetric substrate DEVD-*p*NA (20 μmol) followed by incubation at 37 °C for 4 h. Absorbance was then red at 405 nm using a Multiskan MCC 340 system.

4.2.2.9. Statistical analysis

All data are presented as the mean ± SD of at least three different experiments done in quadruplicate. Unpaired *t*-test or one-way ANOVA analysis of variance with Dunnett's post-test, were performed to compare differences between the groups, as indicated in the figures (Graph-Pad 6 Software Inc., San Diego, CA, USA). *P* values < 0.05 were considered significant.

4.2.3. Electrophysiological studies

4.2.3.1. DNA Constructs and Expression in *Xenopus* Oocytes

cDNAs encoding GluN1-1a (Genbank accession number U11418 and U08261), GluN2A (D13211), GluN2B (U11419), GluN2C (M91563), and GluN2D (L31611) were generously provided by Dr. S. Heinemann (Salk Institute, La Jolla, CA), Dr. S. Nakanishi (Osaka Bioscience Institute, Osaka, Japan), and Dr. P. Seeburg (University of Heidelberg). Amino acid residues are numbered based on the full-length polypeptide sequence, including the signal peptide (initiating methionine is 1).For expression in *Xenopus laevis* oocytes, cDNAs were linearized using restriction enzymes and used as templates to synthesize cRNA using the mMessage mMachine kit (Ambion, Life Technologies, Paisley, UK). *Xenopus* oocytes were obtained from Rob Weymouth (*Xenopus* 1, Dexter, MI). The oocytes were injected with cRNAs encoding GluN1 and GluN2 in a 1:2 ratio, and maintained as previously described (Hansen et al., 2013).

4.2.3.2. Two-Electrode Voltage-Clamp Recordings

Two-electrode voltage-clamp (TEVC) recordings were performed on *Xenopus* oocytes essentially as previously described (Davies et al., 2006). Oocytes were perfused with extracellular recording solution comprised of 90 mM NaCl, 1 mM KCl, 10 mM HEPES, 0.5 mM $BaCl_2$, and 0.01 mM EDTA (pH 7.4 with NaOH). Current responses were recorded at a holding potential of −40 mV. Compounds were dissolved in extracellular recording solution. Data were analyzed using GraphPad Prism (GraphPad Software, La Jolla, CA). Agonist concentration–response data for individual oocytes were fitted to the Hill equation as previously described (Hansen et al., 2013).

5. References

Adesnik, H., Nicoll, R.A. (2007). Conservation of glutamate receptor 2-containing AMPA receptors during long-term potentiation. *J Neurosci. 27,* 4598-4602.

Armstrong, N., Gouaux, E. (2000). Mechanisms for activation and antagonism of an AMPA-sensitive glutamate receptor: crystal structures of the GluR2 ligand binding core. *Neuron*, *28*, 165-181.

Arundine, M.; Tymianski, M. (2003). Molecular mechanisms of calcium-dependentneurodegeneration in excitotoxicity. *Cell Calcium*, *34*, 325-337.

Balannik, V.; Menniti, F. S.; Paternain, A. V.; Lerma, J.; Stern-Bach, Y. (2005). Molecular mechanism of AMPA receptor noncompetitive antagonism. *Neuron*, *48*, 279-288.

Barria, A.; Malinow, R. (2005). NMDA receptor subunit composition controlssynaptic plasticity by regulating binding to CaMKII. *Neuron*, *48*, 289-301.

Beattie, E.C., Carroll, R.C., Yu, X., Morishita, W., Yasuda, H., von Zastrow, M. and Malenka, R.C. (2000). Regulation of AMPA receptor endocytosis by a signaling mechanism shared with LTD. *Nat Neurosci. 3*, 1291-1300.

Bräuner-Osborne, H.; Egebjerg, J.; Nielsen, E. Ø.; Madsen, U.; Krogsgaard-Larsen, P. (2000). Ligands for glutamate receptors: Design and therapeutic prospects. *J. Med. Chem*., *43*, 2609-2645.

Caporale N and Dan Y (2008). Spike timing-dependent plasticity: a Hebbian learning rule. *Annual review of neuroscience 31*, 25-46.

Castillo PE, Chiu CQ and Carroll RC (2011). Long-term plasticity at inhibitory synapses. *Current opinion in neurobiology 21*(2), 328-338.

Chaffey, H.; Chazot, P.L. (2008). NMDA receptor subtypes: structure, function and therapeutics. *Curr. Anaesth. Crit. Care 19*, 183-201.

Chen, B.S.; Braud, S.; Badger, J.D.2nd; Isaac, J.T.R.; Roche K.W. (2006). Regulation of NR1/NR2C N-methyl-D-aspartate (NMDA) receptors by phosphorylation. *J. Biol. Chem., 281*, 16583-16590.

Chen, B.S.; Roche K.W. (2009). Growth factor-dependent trafficking of cerebellar NMDA receptors via protein kinase B/Akt phosphorylation of NR2C. *Neuron*, *62*, 471-478.

Chen, C., Okayama, H. (1987). High-efficiency transformation of mammalian cells by plasmid DNA. *Mol. Cell. Biol*. *7*, 2745−2752.

Chen, P. E., Geballe, M. T., Katz, K., Erreger, K., Livesey, M. R., O'Toole, K. K., Le, P.,

Lee, J., Snyder, J., Traynelis, S. F., Wyllie, D. J. A. (2008). Modulation of glycine potency in rat recombinant NMDA receptors containing chimeric NR2A/2D subunits expressed in Xenopus laevis oocytes *J. Physiol*. *586*, 227– 245

Choi, Y.; Chen, H.V.; Lipton, S.A. (2001). Three pairs of cysteine residues mediateboth redox and Zn2+ modulation of the NMDA receptor. *J. Neurosci*., *21*, 392-400.

Choi, Y.B.; Tenneti, L.; Le, D.A.; Ortiz, J.; Bai, G.; Chen H.S.V.; Lipton S.A. (2000). Molecular basis of NMDA receptor-coupled ion channel modulation byS-nitrosylation. *Nat. Neurosci*., *3*, 15-21.

Chung, H.J.; Huang, Y.H.; Lau, L.F.; Huganir, R.L. (2004). Regulation of the NMDA receptor complex and trafficking by activity-dependent phosphorylation of the NR2B subunit PDZ ligand. *J. Neurosci*., *24*,10248-10259.

Cokić B, Stein V. (2008). Stargazin modulates AMPA receptor antagonism. *Neuropharmacology 54*:1062–1070.

Coleman SK, Moykkynen T, Cai C, von Ossowski L, Kuismanen E, Korpi ER and Keinanen K (2006). Isoform-specific early trafficking of AMPA receptor flip and flop variants. *J. Neurosci*., *26*, 11220-11229.

Collingridge, G. L., Olsen, R. W., Peters, J., Spedding, M. (2009). A nomenclature for ligand-gated ion channels. *Neuropharmacology 56*, 2-5

Cooke, S.F.; Bliss, T.V.P. (2006). Plasticity in the human central nervous system. *Brain*, *129*, 1659-1673.

Coyle, J.T.; Leski, M.L.; Morrison, J.H. The diverse roles of L-glutamic acid in brain signal transduction. In: Neuropsychopharmacology: The Fifth Generation of Progress, 5th Ed.; Lippincott Williams and Wilkins:Philadelphia,(2002); pp 71-90.§

Cull-Candy, S.; Brickley, S.; Farrant, M. (2001). NMDA receptor subunits: diversity, development and disease. *Curr. Opin. Neurobiol*., *11*, 327–335.

Cull-Candy, S.G.; Leszkiewics, D.N. (2004). Role of distinct NMDA receptorsubtypes at central synapses. *Sci STKE*, , *16*, 1-9.

Dan Y and Poo MM (2006). Spike timing-dependent plasticity: from synapse to perception. *Physiological reviews 86*(3): 1033-1048.

Davis, M., Ressler, K., Rothbaum, B. O., and Richardson, R. (2006). Effects of D-cycloserine on extinction: translation from preclinical to clinical work *Biol. Psychiatry 60*, 369– 375.

Diaz, E. (2010). Regulation of AMPA receptors by transmembrane accessory proteins. *Eur*

J Neurosci; *32*: 261–268.

Dingledine, R., Borges, K., Bowie, D., Traynelis, S. F. (1999). The glutamate receptor ion channels. *Pharmacol Rev*. *51*, 7-61

Dravid, S. M., Burger, P. B., Prakash, A., Geballe, M. T., Yadav, R., Le, P., Vellano, K., Snyder, J., and Traynelis, S. F. (2010). Structural Determinants of D-Cycloserine Efficacy at the NR1/NR2C NMDA Receptors *J. Neurosci. 30*, 2741– 2754.

Eriksson, M.; Nilsson, A.; Froelich-Fabre, S.; Akesson, E.; Dunker, J.; Seiger, A. (2002). Cloning and expression of the human N-methyl-D-aspartate receptor subunit NR3A. *Neurosci. Lett., 321*, 177-181.

Erreger, K.; Chen, P.E.; Wyllie, D.J.A. (2004), Traynelis, S.F. Glutamate receptor gating. *Crit. Rev. Neurobiol*., *16*, 187-224.

Espahbodinia, M.; Ettari, R.; Wen, W.; Wu,A.; Shen,Y.; Niu,L.; Grasso, S.; Zappalà, M. (2017) Development of novel N -3-bromoisoxazolin-5-yl substituted 2,3-benzodiazepines as noncompetitive AMPAR antagonists, *Biorg. Med. Chem., 25,* 3631-3637.

Fleming, J.J. and England, P.M. (2010). AMPA receptors and synaptic plasticity: a chemist's perspective. *Nat Chem Biol*. *6*: 89-97.

Furukawa, H. and Gouaux, E. (2003). Mechanisms of activation, inhibition and specificity: crystal structures of the NMDA receptor NR1 ligand-binding core *EMBO J. 22*, 2873–2885.

Gan, Q., Salussolia, C. L. and Wollmuth, L. P. (2015), Assembly of AMPA receptors: mechanisms and regulation. *J Physiol, 593*: 39–48

Ganor Y., I. Grinberg, A. Reis, I. Cooper, R.S. Goldstein, M. Levite (2009), Human T-leukemia and T-lymphoma express glutamate receptor AMPA GluR3, and the neurotransmitter glutamate elevates the cancer-related matrix-metalloproteinases inducer CD147/EMMPRIN, MMP-9 secretion and engraftment of T-leukemia in vivo. *Leuk. Lymphoma*, *5*, 985–997.

Ghasemi, M., Schachter S. C. (2011) The NMDA receptor complex as a therapeutic target in epilepsy: a review. *Epilepsy & Behavior 22* 617–640.

Geiger, J. R., Melcher, T., Koh, D. S., Sakmann, B., Seeburg, P. H., Jonas, P., Monyer, H. (1995). Relative abundance of subunit mRNAs determines gating and Ca2+ permeability of AMPA receptors in principal neurons and interneurons in rat CNS.

Neuron 15, 193-204

Gielen, M.; Retchless, BS.;Mony, L.; Johnson, J.W.; Paoletti. P. (2009). Mechanism of differential control of NMDA receptor activity by NR2 subunits. *Nature*, *459*, 703-707.

Gorter, J. A., Petrozzino, J. J., Aronica, E. M., Rosenbaum, D. M., Opitz, T., Bennett, M. V., Connor, J. A., Zukin, R. S. (1997). Global ischemia induces downregulation of Glur2 mRNA and increases AMPA receptor-mediated Ca2+ influx in hippocampal CA1 neurons of gerbil. *J. Neurosci*. *17*, 6179-6188

Grasso, S., De Sarro, G., De Sarro, A., Micale, N., Zappala, M., Puia, G., Baraldi, M., De Micheli, C. (1999). Synthesis and anticonvulsant activity of novel and potent 2,3-benzodiazepine AMPA/kainate receptor antagonists. *J. Med. Chem. 42*, 4414-4421

Grasso, S., Micale, N., Zappala, M., Galli, A., Costagli, C., Menniti, F. S., De Micheli, C. (2003). Characterization of the mechanism of anticonvulsant activity for a selected set of putative AMPA receptor antagonists. *Bioorg Med Chem Lett*. *13*, 443-446.

Hackos, D. H., Lupardus, P. J., Grand, T., Chen, Y., Wang, T.-M., Reynen, P., Gustafson, A., Wallweber, H. J. A., Volgraf, M., Sellers, B. D., Schwarz, J. B., Paoletti, P., Sheng, M., Zhou, Q., Hanson, J. E. (2016). Positive allosteric modulators of GluN2A-containing NMDARs with distinct modes of action and impacts on circuit function *Neuron 89*, 983– 999.

Hansen, K. B., Tajima, N., Risgaard, R., Perszyk, R. E., Jorgensen, L., Vance, K. M., Ogden, K. K., Clausen, R. P., Furukawa, H., and Traynelis, S. F. (2013). Structural determinants of agonist efficacy at the glutamate binding site of N-methyl-D-aspartate receptors *Mol. Pharmacol. 84*, 114– 127.

Hansen, K.B.; Clausen, R.P.; Bjerrum, E.J.; Bechmann, C.; Greenwood, J.R.;Christensen, C.; Kristensen, J.L.; Egebjerg, J.; Bräuner-Osborne H. (2005). Tweaking agonist efficacy at N-methyl-D-aspartate receptors by site-directed mutagenesis. *Mol. Pharmacol.*, *68*, 1510-1523.

Harvey CD, Yasuda R, Zhong H and Svoboda K (2008). The spread of Ras activity triggered by activation of a single dendritic spine. *Science 321*(5885), 136-140.

Hayashi, T., Rumbaugh, G., Huganir, R.L. (2005). Differential regulation of AMPA receptor subunit trafficking by palmitoylation of two distinct sites. *Neuron*. *47*,709-723.

Hayashi, T.; Thomas, G.; Huganir, R.L. (2009). Dual palmitoylation of NR2 subunits

regulates NMDA receptor trafficking. *Neuron*, *64*, 213-226.

Hayashi, Y., Shi, S.H., Esteban, J.A., Piccini, A., Poncer, J.C. and Malinow, R. (2000). Driving AMPA receptors into synapses by LTP and CaMKII: requirement for GluR1 and PDZ domain interaction. *Science*. *287*, 2262-2267.

Honore, T., Davies, S. N., Drejer, J., Fletcher, E. J., Jacobsen, P., Lodge, D., Nielsen, F. E. (1988). Quinoxalinediones: potent competitive non-NMDA glutamate receptor antagonists. *Science 241*, 701-703

Huang, Z., Li, G., Pei, W., Sosa, L. A., and Niu, L. (2005). Enhancing protein expression in single HEK 293 cells. *J. Neurosci. Methods* 142, 159−166.

Huggins, D.J.; Grant, G.H. (2005). The function of the amino terminal domain inNMDA receptor modulation. *J. Mol. Graph. Model*, *23*, 381-388.

Hume, R. I., Dingledine, R., Heinemann, S. F. (1991). Identification of a site in glutamate receptor subunits that controls calcium permeability. *Science 253*, 1028-1031.

Inanobe, A., Furukawa, H., Gouaux, E. (2005). Mechanism of partial agonist action at the NR1 subunit of NMDA receptors *Neuron 47*, 71– 84.

Isaac JT, Ashby M, McBain CJ. (2007). The role of the GluR2 subunit in AMPA receptor function and synaptic plasticity. *Neuron*; *54*,859–871.

Isaac, J.T., Nicoll, R.A. and Malenka, R.C. (1995). Evidence for silent synapses: implications for the expression of LTP. *Neuron*. *15*, 427-434.

Jespersen, A., Tajima, N., Fernandez-Cuervo, G., Garnier-Amblard, E. C., Furukawa, H. (2014). Structural insights into competitive antagonism in NMDA receptors *Neuron 81*, 366– 378.

Jiang, J., Suppiramaniam, V., Wooten, M.W. (2006). Posttranslational modifications and receptor-associated proteins in AMPA receptor trafficking and synaptic plasticity. *Neurosignals*. *15*, 266-282.

Karakas, E.; Simorowski, N.; Furukawa, H. (2011). Subunit arrangement and phenylethanolamine binding in GluN1/GluN2B NMDA receptors. *Nature*, *475*, 249-253.

Karakas, E.; Simorowski, N.; Furukawa. H. (2009). Structure of the zinc-boundamino-terminal domain of the NMDA receptor NR2B subunit. *EMBO J., 28*, 3910-3920.

Kew, J. N.; Kemp, J. A. (2005). Ionotropic and metabotropic glutamate receptor structure and pharmacology *Psychopharmacology* (Berl.), *179*, 4-29.

Lambolez, B., Ropert, N., Perrais, D., Rossier, J., Hestrin, S. (1996). Correlation between

kinetics and RNA splicing of alpha-amino-3-hydroxy-5-methylisoxazole-4-propionic acid receptors in neocortical neurons. *Proc Natl Acad Sci U S A*. *93*, 1797-1802.

Laube, B.; Kuhse, J.; Betz, H. (1998). Evidence for a tetrameric structure of recombinant NMDA receptors. *J. Neurosci., 18*, 2954-2961.

Lee, H.K., Barbarosie, M., Kameyama, K., Bear, M.F. and Huganir, R.L. (2000). Regulation of distinct AMPA receptor phosphorylation sites during bidirectional synaptic plasticity. *Nature*. *405,* 955-959.

Lee, H.K., Takamiya, K., He, K., Song, L., Huganir, R.L. (2010). Specific roles of AMPA receptor subunit GluR1 (GluA1) phosphorylation sites in regulating synaptic plasticity in the CA1 region of hippocampus. *J Neurophysiol*. *103*, 479-489.

Li, B.S.; Sun, M.K.; Zhang, L.; Takahashi, S.; Ma, W.; Vinade, L.; Kulkarni,A.B.; Brady, R.O.; Pant, H.C. (2001). Regulation of NMDA receptors by cyclindependentkinase-5. *Proc. Natl. Acad. Sci., 98*, 12742-12747.

Li, G.; Pei, W.; Niu, L. (2003). Channel-opening kinetics of GluR2Q(flip) AMPA receptor: a laser-pulse photolysis study. *Biochemistry 42*, 12358−12366.

Liu, S. J., Zukin, R. S. (2007). Ca2+-permeable AMPA receptors in synaptic plasticity and neuronal death. *Trends Neurosci*. *30*, 126-134

Liu, Y.; Wong, T.P.; Aarts, M.; Rooyakkers, A.; Liu, L.; Lai, T.W.; Wu, D.C.; Lu, J.; Tymianski, M.; Craig, A.M.; Wang, Y.T. (2007). NMDA receptor subunits have differential roles in mediating excitotoxic neuronal death both in vitro and in vivo. *J. Neurosci*., *27*, 2846-2857.

Liu, Y.; Zhang, J. Recent development in NMDA receptors. *Chinese Med. J. (*2000). *113*, 948-956.

Lodge D. (2009) The history of the pharmacology and cloning of ionotropic glutamate receptors and the development of idiosyncratic nomenclature. *Neuropharmacology 56*, 6–21.

Loftis, J.M.; Janowsky, A. *(*2003). The N-methyl-D-aspartate receptor subunit NR2B:localization, functional properties, regulation, and clinical implications. *Pharmacol. Ther. 97*, 55-85.

Low, C.M.; Zheng, F.; Lyuboslavsky, P.; Traynelis. S.F. (2000). Molecular determinants of coordinated proton and zinc inhibition of N-methyl-DaspartateNR1/NR2A receptors. *Proc. Acad. Natl. Sci., 97*, 11062-11067.

Luján R., R. Shigemoto, G. López-Bendito (2005). Glutamate and GABA receptor

signalling in the developing brain *Neuroscience*, *130*, 567–580.

Lynch, D.R.;Guttman, R.P. (2002). Excitotoxicity: Perspectives based on N-methyl-D-aspartate receptor subtypes. *J. Pharmacol. Exp. Ther*., *300*, 717-723.

Lynch, G. and Baudry, M. (1984). The biochemistry of memory: a new and specific hypothesis. *Science*. *224*, 1057-1063.

MacDermott AB, Mayer ML, Westbrook GL, Smith SJ and Barker JL (1986). NMDAreceptor activation increases cytoplasmic calcium concentration in cultured spinal cord neurones. *Nature 321*(6069): 519-522.

Madry, C.; Betz, H.; Geiger, J.R.P. (2008). Laube, B. Supralinear potentiation ofNR1/NR3A excitatory glycine receptors by Zn2+ and NR1 antagonist. Proc.N*atl. Acad. Sci., 105*, 12563-12568.

Malenka RC and Bear MF (2004). LTP and LTD: an embarrassment of riches. *Neuron 44(1)*, 5-21.

Malinow R and Miller JP (1986). Postsynaptic hyperpolarization during conditioning reversibly blocks induction of long-term potentiation. Nature *320*(6062), 529-530.

Malinow, R. (2003). AMPA receptor trafficking and long-term potentiation. Philos Trans R Soc Lond B Biol Sci. *358*, 707-714.

Man, H.Y., Lin, J.W., Ju, W.H., Ahmadian, G., Liu, L., Becker, L.E., Sheng, M. and Wang, Y.T. (2000). Regulation of AMPA receptor-mediated synaptic transmission by clathrin-dependent receptor internalization. *Neuron. 25,* 649-662.

Manfredini, R.; Balestri, R; Tagliafico E. (1997). Antisense inhibition of c-fes protooncogene blocks PMA-induced macrophage differentiation in HL60 and in FDC-*P*1/MAC-11 cells. *Blood*, *89*, 135–145

Maolanon, Alex R; Risgaard, Rune; Wang, Shuang-Yan; Snoep, Yoran; Papangelis, Athanasios; Yi, Feng; Holley, David; Barslund, Anne F; Svenstrup, Niels; B Hansen, Kasper; Clausen, Rasmus P. (2017). Subtype-Specific Agonists for NMDA Receptor Glycine Binding Sites. *ACS Chem. Neurosci*. 000.

Matsuda, K.; Kamiya, Y.; Matsuda, S.; Yuzaki, M. (2002). Cloning and characterization of a novel NMDA receptor subunit NR3B: a dominant subunit that reduces calcium permeability. *Brain Res. Mol*. Brain Res., *100*, 43-52.

Mayer, M. (2006). Glutamate receptors at atomic resolution. *Nature*, *440*, 456-462.

Mayer, M. L. (2005). Glutamate receptor ion channels. *Curr Opin Neurobiol. 15*, 282-288.

Micale, N., Colleoni, S., Postorino, G., Pellicano, A., Zappala, M., Lazzaro, J., Diana, V.,

Cagnotto, A., Mennini, T., Grasso, S. (2008). Structure-activity study of 2,3-benzodiazepin-4-ones noncompetitive AMPAR antagonists: identification of the 1-(4-amino-3-methylphenyl)-3,5-dihydro-7,8-ethylenedioxy-4H-2,3-benzodiazepin-4-one as neuroprotective agent. *Bioorg. Med. Chem*. *16*, 2200-2211.

Nishi, M.; Hinds, H.; Lu, H.P.; Kawata, M.; Hayashi, Y. (2001). Motoneuron specific expression of NR3B, a novel NMDA-type glutamate receptor subunit that works in a dominant-negative manner. *J. Neurosci. 21*, 1-6.

O'Leary, T.; Wyllie, D.J.A. (2009). Single-channel properties of N-methyl-D-aspartate receptors containing chimaeric GluN2A/GluN2D subunits. *Biochem. Soc. Trans*. *37*, 1347-1354.

Palmer, C. L., Cotton, L., Henley, J. M. (2005). The molecular pharmacology and cell biology of alpha-amino-3-hydroxy-5-methyl-4-isoxazolepropionic acid receptors. *Pharmacol Rev. 57*, 253-277.

Paoletti P.; Perin-Dureau F.; Fayyazuddin A.; Le Goff A.; Callebaut I.;Neyton J. (2000). Molecular organization of a zinc binding N-terminal modulatorydomain in a NMDA receptor subunit. *Neuron*, *28*, 911-925.

Paoletti, P.; Neyton, J. (2007). NMDA receptor subunits: function andpharmacology. *Curr. Opin. Pharmaco*l. *7*, 39-47.

Parenti, S.; G. Casagrande, M. Montanari, M. Espahbodinia, R. Ettari, A. Grande, L. Corsi, (2016). A novel 2,3-benzodiazepine-4-one derivative AMPA antagonist inhibits G2/M transition and induces apoptosis in human leukemia Jurkat T cell line, *Life Sciences*, *152*, 117-125.

Park, M., Penick, E.C., Edwards, J.G., Kauer, J.A. and Ehlers, M.D. (2004). Recycling endosomes supply AMPA receptors for LTP. *Science*. *305*, 1972-1975.

Parsons, G. C.; Danysz, W.; Quack, G. (1998). Glutamate in CNS disorders as a target for drug development: an update. *Drug News Perspect. 11*, 523-569.

Pei, W., Huang, Z., Wang, C., Han, Y., Park, J. S., and Niu, L. (2009). Flip and flop: a molecular determinant for AMPA receptor channel opening. *Biochemistry 48*, 3767−3777.

Perez, J.L., Khatri, L., Chang, C., Srivastava, S., Osten, P. and Ziff, E.B. (2001). PICK1 targets activated protein kinase Calpha to AMPA receptor clusters in spines of hippocampal neurons and reduces surface levels of the AMPA-type glutamate receptor subunit 2. *J Neurosci*. *21*, 5417-5428.

Petrenko, A.B.; Yamakura, T.; Baba, H.; Shimoji, K. (2003). The role of N-methyl-d-aspartate (NMDA) receptors in pain: a review. *Anesth. Analg., 97*, 1108-1116.

Plant, K., Pelkey, K.A., Bortolotto, Z.A., Morita, D., Terashima, A., McBain, C.J., Collingridge, G.L. and Isaac, J.T. (2006). Transient incorporation of native GluR2-lacking AMPA receptors during hippocampal long-term potentiation. *Nat Neurosci*. *9*, 602-604.

Popescu, G. (2005). Mechanism-based targeting of NMDA receptor functions. *Cell Mol. Life Sci. 62*, 2100-2111.

Prickett T.D., Y. Samuels (2012). Molecular pathway: dysregulated glutamatergic signaling pathway in cancer *Clin. Cancer Res*., *18*, 4240–4246

Qneibi, M. S., Micale, N., Grasso, S., Niu, L. (2012). Mechanism of inhibition of GluA2 AMPA receptor channel opening by 2,3-benzodiazepine derivatives: functional consequences of replacing a 7,8-methylenedioxy with a 7,8-ethylenedioxy moiety. *Biochemistry 51*, 1787-1795

Rachline, J.; Perin-Dureau, F.; Le Goff, A.; Neyton, J.; Paoletti, P. (2005). The micromolar zinc-binding domain on the NMDA receptor subunit NR2B. *J.Neurosci*. *25*, 308-317.

Rezessy B.; Sólyom S. (2004). Advanced pharmacophore model of non-competitive AMPA antagonist 2,3-benzodiazepines. *Lett. Drug Des. Discov*. *1*, 217-223.

Riedel, G.; Platt, B.; Micheau, J. (2003). Glutamate receptor function in learning and memory. *Behav. Brain Res*., *140*, 1-47.

Riou M, Stroebel D, Edwardson JM and Paoletti P (2012). An alternating GluN1-2-1-2 subunit arrangement in mature NMDA receptors. *PloS one* 7(4): e35134.

Ritz, M., Micale, N., Grasso, S., Niu, L. (2008). Mechanism of inhibition of the GluR2 AMPA receptor channel opening by 2,3-benzodiazepine derivatives. *Biochemistry 47*, 1061-1069

Ritz, M., Wang, C., Micale, N., Ettari, R., Niu, L. (2011). Mechanism of Inhibition of the GluA2 AMPA Receptor Channel Opening: the Role of 4-Methyl versus 4-Carbonyl Group on the Diazepine Ring of 2,3-Benzodiazepine Derivatives. *ACS Chem Neurosci*. *2*, 506-513

Rogawski, M. A., Hanada, T. (2013). Preclinical pharmacology of perampanel, a selective non-competitive AMPA receptor antagonist. *Acta Neurol Scand Suppl*, 19-24

Rzeski, W. L. Turski, C. Ikonomidou (2001). Glutamate antagonists limit tumor growth. *Proc. Natl. Acad. Sci. U. S. A., 98*, 6372–6377

Sacktor TC (2008). PKMzeta, LTP maintenance, and the dynamic molecular biology of memory storage. *Progress in brain research 169*, 27-40.

Safferling, M., Tichelaar, W., Kummerle, G., Jouppila, A., Kuusinen, A., Keinanen, K., Madden, D. R. (2001). First images of a glutamate receptor ion channel: oligomeric state and molecular dimensions of GluRB homomers. *Biochemistry 40*, 13948-13953.

Salter, M.W.; Kalia, L.V. (2004). Src kinases, a hub for NMDA receptor regulation. *Nat. Rev. Neurosci. 5*, 317-328.

Sanchez-Pérez, A.M.; Felipe, V. (2005). Serines 890 and 896 of the NMDA receptorsubunit NR1 are differentially phosphorylated by protein kinase C isoforms. *Neurochem. Int., 47*, 84-91.

Sans, N., Vissel, B., Petralia, R. S., Wang, Y. X., Chang, K., Royle, G. A., Wang, C. Y., O'Gorman, S., Heinemann, S. F., Wenthold, R. J. (2003). Aberrant formation of glutamate receptor complexes in hippocampal neurons of mice lacking the GluR2 AMPA receptor subunit. *J Neurosci*. *23*, 9367-9373.

Sasaki, Y.F.; Rothe, T.; Premkumar, L.S.; Das, S.; Cui, J.; Talantova,M.V.K.; Gong, X.; Chan, S.F.; Zhang, D.; Nakanishi, N.; Sucher, N.J.;Lipton, S.A. (2002). Characterization and comparison of the NR3A subunit of theNMDA receptor in recombinant systems and primary cortical neurons. *J.Neurophysiol*. *87*, 2052-2063.

Schiffer, H. H., Swanson, G. T., Heinemann, S. F. (1997). Rat GluR7 and a carboxy-terminal splice variant, GluR7b, are functional kainate receptor subunits with a low sensitivity to glutamate. *Neuron 19*, 1141-1146

Schorge, S.; Colquhoun, D. (2003). Studies of NMDA receptor function and stoichiometry with truncated and tandem subunits. *J. Neurosci*. *23*, 1151-1158.

Scott, D.B.; Blanpied, T.A.; Ehlers, M.D. (2003). Coordinated PKA and PKCphosphorylation suppresses RXR-mediated ER retention and regulates thesurface delivery of NMDA receptors. *Neuropharmacol*. *45*, 755-767.

Seeburg PH, Higuchi M and Sprengel R (1998). RNA editing of brain glutamate receptor channels: mechanism and physiology. *Brain Res. Brain Res. Rev. 26*, 217-229.

Seeburg, P. H. (1996). The role of RNA editing in controlling glutamate receptor channel properties. *J Neurochem*. *66*, 1-5

Seeburg, P. H., Hartner, J. (2003). Regulation of ion channel/neurotransmitter receptor function by RNA editing. *Curr Opin Neurobiol.13*, 279-283

Shepherd, J.D. and Huganir, R.L. (2007). The cell biology of synaptic plasticity: AMPA

receptor trafficking. *Annu Rev Cell Dev Biol. 23*, 613-643.

Shi, S.H., Hayashi, Y., Petralia, R.S., Zaman, S.H., Wenthold, R.J., Svoboda, K. and Malinow, R. (1999). Rapid spine delivery and redistribution of AMPA receptors after synaptic NMDA receptor activation. *Science*. *284*, 1811-1816.

Smits, V.A.; Medema. R.H. (2001). Checking out the G(2)/M transition *Biochem. Biophys. Acta*, *1519*, 1–12.

Snyder, E.M.; Nong, Y.; Almeida, C.G.; Paul, S.; Moran, T.; Choi, E.Y.;Nairn, A.C.; Salter, M.W.; Lombroso, P.J.; Gouras, G.K. (2005). Greengard, P. Regulation of NMDA receptor trafficking by amyloid-β. *Nat. Neurosci*. *8*, 1051-1058.

Sobolevsky, A. I., Rosconi, M. P., Gouaux, E. (2009). X-ray structure, symmetry and mechanism of an AMPA-subtype glutamate receptor. *Nature 462*, 745-756

Solyom, S., Tarnawa, I. (2002). Non-competitive AMPA antagonists of 2,3-benzodiazepine type. *Curr. Pharm. Des. 8*, 913-939.

Solyom, S.; Abraham, G.; Hamori, T.; Berzsenyl, P.; Andrasi, F.; Kurucz, I. (2007). Novel substituted 2,3-benzodiazepine derivatives U.S. Pat. Appl. 20070027143 A1 Feb 01

Sommer, B., Keinanen, K., Verdoorn, T. A., Wisden, W., Burnashev, N., Herb, A., Kohler, M., Takagi, T., Sakmann, B., Seeburg, P. H. (1990). Flip and flop: a cell-specific functional switch in glutamate-operated channels of the CNS. *Science 249*, 1580-1585

Sommer, B., Kohler, M., Sprengel, R., Seeburg, P. H. (1991). RNA editing in brain controls a determinant of ion flow in glutamate-gated channels. *Cell 67*, 11-19.

Standley, S.; Baudry, M. (2000). The role of glycosylation in ionotropicglutamatereceptor ligand binding, function, and trafficking.*CellMol Life Sci., 57*, 1508-1516.

Stepulak, A. H. Luksch, C. Gebhardt, O. Uckermann, J. Marzahn, M. Sifringer (2009). Expression of glutamate receptor subunits in human cancers. Histochem. *Cell Biol., 132*, 435–445

Stepulak, A. H. Luksch, O. Uckermann, M. Sifringer, W. Rzeski, K. Polberg (2011). Glutamate receptors in laryngeal cancer cells *Anticancer Res.*, *31*, 565–573

Szenasi G, Vegh M, Szabo G, Kertesz S, Kapus G, Albert M, Greff Z, LingI, Barkoczy J, Simig G, Spedding M, Harsing LG Jr. (2008). 2,3-benzodiazepinetypeAMPA receptor antagonists and their neuroprotective effects.NeurochemInt. *52*,166–183.

Talukder I, Borker P and Wollmuth LP (2010). Specific sites within the ligand-binding domain and ion channel linkers modulate NMDA receptor gating. *J. Neuroscience 30*, 11792- 11804.

Teh J.L., S. Chen (2012). Glutamatergic signaling in cellular transformation *Pigment Cell Melanoma Res, 25*, 331–342

Traynelis, S. F., Wollmuth, L. P., McBain, C. J., Menniti, F. S., Vance, K. M., Ogden, K. K., Hansen, K. B., Yuan, H., Myers, S. J., Dingledine, R. (2010). Glutamate receptor ion channels: structure, regulation, and function. *Pharmacol Rev 62*, 405-496

Urwyler, S., Floersheim, P., Roy, B. L., Koller, M. (2009). Drug design, in vitro pharmacology, and structure-activity relationships of 3-acylamino-2-aminopropionic acid derivatives, a novel class of partial agonists at the glycine site on the N-methyl-D-aspartate (NMDA) receptor complex *J. Med. Chem. 52*, 5093– 5107

Vance, K.M.; Somorowski, N.; Traynelis, S.F.; Furukawa, H. (2011). Ligand-specificdeactivation time course of GluN1/GluN2D NMDA receptors. *Nature Comm*. *2*, 294.

Vrajová, M.; Stastný, F.; Horácek, J.; Lochman, J.; Serý, O.; Peková, S.; Klaschka, J.; Höschl, C. (2010). Expression of the hippocampal NMDA receptor GluN1 subunit and its splicing isoforms in schizophrenia: postmortem study. *Neurochem. Res*. *35*, 994-1002.

Walczak K., S. Deneka-Hannemann, B. Jarosz, W. Zgrajka, F. Stoma, T. Trojanowski, W.A. Turski, W. Rzeski (2014). Kynurenic acid inhibits proliferation and migration of human glioblastoma T98G cells *Pharmacol.* Rep., *66*, 130–136

Wang, C., Wu, A., Shen, Y. C., Ettari, R., Grasso, S., Niu, L. (2015). Mechanism and Site of Inhibition of AMPA Receptors: Substitution of One and Two Methyl groups at the 4-Aminophenyl Ring of 2,3-Benzodiazepine and Implications in the "E" Site. *ACS Chem Neurosci*, *6*, 1371-1378.

Wang, C.; Han, Y.; Wu, A.; Solyom, S.; Niu, L. (2014). Mechanism and site of inhibition of AMPA receptors: pairing a thiadiazole with a 2,3-benzodiazepine scaffold. *ACS Chem Neurosci. 5*, 138-147.

Wang, J.; Liu, S.H.; Fu, Y.P.; Wang, J.H.; Lu, Y.M. (2003). Cdk5 activation induces hippocampal CA1 cell death by directly phosphorylating NMDA receptors. *Nat. Neurosci. 6*, 1039-1047.

Weiss, J.H. (2011). Ca2+ permeable AMPA channels in diseases of the nervous system. *Front. Mol. Neurosc*i. *4*, 42.

Wenthold RJ, Petralia RS, Blahos J II, Niedzielski AS. (1996). Evidence for multiple AMPA receptor complexes in hippocampal CA1/CA2 neurons. *J. Neurosci. 16*, 1982–

1989.

Wenzel, A.; Villa, M.; Mohler, H.; Benke, D. (1996). Developmental and Regional Expression of NMDA Receptor Subtypes Containing the NR2D Subunit in Rat Brain. *J. Neurochem. 66*, 1240-1248.

Wu, A.; Wang, C.Z.; Niu, L. (2014). Mechanism of inhibition of the GluA1 AMPA receptor channel opening by the 2,3-benzodiazepine compound GYKI52466 and a N-methyl-carbamoylderivative. *Biochemistry*, *53*, 3033–3041.

Yao, Y.; Mayer, M.L. (2006). Characterization of a soluble ligand binding domain ofthe NMDA receptor regulatory subunit NR3A. *J. Neurosci., 26*, 4559-4566.

Yelshanskaya, M.V., Singh A.K., Sampson J.M., Narangoda C., Kurnikova M. Sobolevsky A.I. (2016). Structural Bases of Noncompetitive Inhibition of AMPA-Subtype Ionotropic Glutamate Receptors by Antiepileptic Drugs. *Neuron* , *91*, 1305–1315.

Yi, F., Mou, T. C., Dorsett, K. N., Volkmann, R. A., Menniti, F. S., Sprang, S. R., Hansen, K. B. (2016). Structural Basis for Negative Allosteric Modulation of GluN2A-Containing NMDA Receptors *Neuron 91*, 1316– 1329.

Zamanillo, D., Sprengel, R., Hvalby, O., Jensen, V., Burnashev, N., Rozov, A., Kaiser, K.M., Koster, H.J., Borchardt, T., Worley, P., Lubke, J., Frotscher, M., Kelly, P.H., Sommer, B., Andersen, P., Seeburg, P.H. and Sakmann, B. (1999). Importance of AMPA receptors for hippocampal synaptic plasticity but not for spatial learning. *Science*. *284*, 1805-1811.

Zappalà, M.; Postorino, G.; Micale, N.; Caccamese, S.; Parrinello, N.; Roda, G.; Menniti, F. S.; Ferreri, G.; De Sarro, G.; Grasso, S. (2006). Synthesis, Chiral Resolution, and Enantiopharmacology of a Potent 2,3-Benzodiazepine Derivative as Noncompetitive AMPA Receptor Antagonist *J. Med. Chem., 49*, 575-581.

Zappala, M., Pellicano, A., Micale, N., Menniti, F. S., Ferreri, G., De Sarro, G., Grasso, S., De Micheli, C. (2006). New 7,8-ethylenedioxy-2,3-benzodiazepines as noncompetitive AMPA receptor antagonists. *Bioorg Med Chem Lett 16*, 167-170